SUPPLEMENTARY NOTE

A general method to improve fluorophores for live-cell and single-molecule microscopy

Jonathan B. Grimm, Brian P. English, Jiji Chen, Joel P. Slaughter, Zhengjian Zhang, Andrey Revyakin, Ronak Patel, John J. Macklin, Davide Normanno, Robert H. Singer, Timothée Lionnet, and Luke D. Lavis

Email: lavisl@janelia.hhmi.org; lionnett@janelia.hhmi.org

I. Quantum Mechanical Calculations and Synthetic Chemistry of Aza-Cyclic Rhodamines

The simplest rhodamine fluorophore, rhodamine 110 (**1**, **Fig. SN1a**), exhibits an absorption maximum in the blue (λ_{max} = 497 nm) with a high extinction coefficient (ε = 7.6 × 10^4 $M^{-1}cm^{-1}$), emission in the green (λ_{em} = 520 nm), and a high quantum yield (ϕ = 0.88).[1] Alkylation of the rhodamine elicits a bathochromic shift in absorption and fluorescence emission wavelengths. For example, tetramethylrhodamine (**2**) displays $\lambda_{max}/\lambda_{em}$ = 548 nm/572 nm and ε = 7.8 × 10^4 $M^{-1}cm^{-1}$ (**Fig. SN1a**). This shift in spectral properties is accompanied by a significant decrease in quantum yield, with TMR showing ϕ = 0.41. Both of these dyes are used in commercial self-labeling tag substrates and can be used to label intracellular and extracellular proteins in living cells.

The lower quantum efficiency of *N,N,N′,N′*-tetraalkylrhodamines such as **2** can be explained by an energetically favorable twisted internal charge transfer (TICT) state.[2-4] This process involves electron transfer from the nitrogen atom to the xanthene ring in the excited state with concomitant twisting of the C_{aryl}–N bond. This TICT state rapidly relaxes without emission of a photon and is a presumed major path of nonradiative decay in rhodamine dyes.[2-4] This diradical species may also undergo irreversible reactions leading to bleaching of the fluorophore.[4] Thus, rhodamine derivatives where TICT is disfavored should exhibit increased quantum efficiency, longer fluorescence lifetimes, and higher photostability.

Several structural parameters can promote the formation of this undesirable form. The TICT state is more energetically favorable in *N,N,N′,N′*-tetraalkylrhodamines due to a lower ionization potential (IP) of the dialkylanilino nitrogen atom relative to anilines with other substitution patterns.[5] Additionally, the homoallylic interactions between the *N*-alkyl groups and the xanthene system predispose twisting of the C_{aryl}–N bond, thereby promoting TICT and lowering fluorescence efficiency. Formation of the TICT state can be curtailed by incorporating the aniline into bicyclic or fused ring systems,[4,6] thus changing the ionization potential of the nitrogen substituent and propensity of the C–N bond to twist, thereby increasing quantum yield. Such structural modifications are undesirable, however, as they alter spectral properties and increase the size and hydrophobicity of the fluorophore.

We set out to develop an improved variant of TMR (**2**) with improved quantum yield and brightness. To minimize hydrophobic bulk and ensure facile syntheses, we considered rhodamine dyes bearing different azacyclic

groups ranging from aziridine to azepane (compounds **3**–**7**, **Fig. SN1a**). We reasoned that by incorporating the aniline nitrogens into a simple cyclic system we could control many of the structural parameters important in the formation of the TICT state. In previous work, we reported the pyrrolidine-containing rhodamine **5** showed 7-fold higher fluorescence brightness ($\varepsilon \times \phi$) than piperidino-rhodamine **6**;[7] dyes containing other azacycles have not been explored. It was not obvious how incorporation of different ring sizes would affect fluorescence properties. Smaller azacycles have higher IP values[5] and less steric bulk, making them potentially advantageous auxochromes for rhodamine dyes. Nonetheless, the higher ring strain in smaller azacycles such as the aziridine and azetidine-containing structures (**3** and **4**) might preclude the planar configuration required for the fluorescent xanthenium structure.

To investigate this effect of ring size on spectral properties, we first conducted a computational study of rhodamine 110 (**1**), TMR (**2**) and the azacyclic rhodamines **3**–**7** using standard *ab initio* Hartree–Fock methods to estimate equilibrium geometry. The *ortho*-carboxyl group was omitted from these structures to prevent cyclization to the closed lactone form during energy minimization, a common problem in computational chemistry studies of rhodamine dyes.[8] The calculated structures (**Fig. SN1b**) were analyzed for the length of the aryl carbon–nitrogen bond (C_{aryl}–N) and the minimum distance between hydrogen substituents *ortho* and alpha to the nitrogen (H_o–H_α; **Fig. SN1a**). These values are key parameters in the propensity of the molecule to undergo TICT. A shorter C_{aryl}–N value signifies increased double-bond character and lower tendency to adopt a twisted conformation. Likewise, a larger H_o–H_α value indicates less steric clash between substituents and lower predisposition for bond rotation.

The molecular modeling experiments suggested inclusion of different-sized azacycles could have large effects on rhodamine conformation. The calculated structure of aziridine derivative **3** contained puckered aziridine rings with the nitrogens out of the plane of the xanthene system (**Fig. SN1b**), consistent with the large ring strain (27 kcal mol^{-1}) present in the three-membered ring.[9] The other rhodamines (**1**, **2**, **4**–**7**), however, minimized to a largely planar structure encompassing the aniline nitrogens (**Fig. SN1b**), suggesting these dyes prefer the extended conjugation found in fluorescent rhodamines. The projected structure of rhodamine **4** was particularly surprising given the relatively large ring strain present in azetidine (estimated at 26 kcal mol^{-1}),[10] which would be expected to favor pyramidal nitrogen atoms. Rhodamine **4** also showed the shortest C_{aryl}–N bond length (1.349 Å) and longest H_o–H_α distance (2.56 Å) of the planar calculated structures (**Fig. SN1a**). Additionally, *N*-arylazetidines exhibit higher IP values compared to *N*,*N*-dialkylanilines (1-phenylazetidine IP = 7.61 eV; *N*,*N*-dimethylaniline IP = 7.37 eV)[5] suggesting a higher energetic penalty for the electron transfer from the aniline nitrogen to the xanthene ring system to form the TICT state. These results implied that rhodamine **4** would be less prone to undergo TICT and thus exhibit superior fluorescent properties to the TMR fluorophore (**2**).

We then tested our prediction by synthesizing compounds **3**–**7** and evaluating the fluorescence properties of these dyes. Our laboratory recently described a facile and efficient synthesis of rhodamines from fluorescein ditriflates using the Buchwald–Hartwig cross-coupling.[7] This divergent strategy allowed the preparation of compounds **3**–**7** from fluorescein (**8**; **Fig. SN1c**). As in previous work,[7] relatively high catalyst loading (10%) was required to minimize triflate hydrolysis and ensure high yields. Compounds **4**–**7** were highly colored, polar compounds that were purified by normal-phase flash chromatography with a strong solvent system

($CH_2Cl_2/CH_3OH/NH_3$). In contrast, rhodamine **3** was a colorless, nonpolar molecule and could be purified by normal-phase chromatography using weak solvent mixtures (EtOAc/hexanes).

We then evaluated the photophysical properties of compounds **3**–**7** in aqueous solution, comparing them to known rhodamines **1** and **2** (**Fig. SN1a**). Aziridine derivative **3** gave a colorless solution with no discernible fluorescence. This data, along with the computational results and chemical characteristics noted above, suggests the ring strain in the aziridine substituents forces the rhodamine molecule to adopt the closed lactone form. Compounds **4**–**7** showed λ_{max} and λ_{em} values similar to TMR (**2**) with increased ring size causing a slight bathochromic shift of up to 10 nm. Interestingly, compounds **4** and **7** showed a ~30% higher extinction coefficient than the other dyes; similar values have been observed with other tetralkylrhodamines such as rhodamine B ($\varepsilon = 1.06 \times 10^5\ M^{-1}cm^{-1}$).[7,11]

Although the λ_{max}, λ_{em}, and ε of the different rhodamine congeners show only modest dependence on ring size, the fluorescence lifetime (τ) and quantum yield (ϕ) varied widely as a function of molecular structure (**Fig. SN1a**). Rhodamine **4** exhibited a high quantum yield value (ϕ = 0.88) and long fluorescence lifetime (τ = 3.8 ns), significantly larger than the values for TMR (**2**; ϕ = 0.41, τ = 2.2 ns), and similar to the parent rhodamine 110 (**1**; ϕ = 0.88, τ = 3.3 ns). Pyrrolidine derivative **5** showed slightly lower values than rhodamine **4** with ϕ = 0.74 and τ = 3.6 ns. The piperidine derivative **6** showed a sharp decrease in fluorescence with ϕ = 0.10 and τ = 0.6 ns; the lifetime values for **5** and **6** are consistent with those measured for analogous esterified rhodamine dyes.[2] Compound **7** gave slightly higher values of ϕ = 0.25 and τ = 1.62 ns relative to **6**, suggesting that the increased flexibility of this larger ring can offset the other deleterious structural effects on rhodamine fluorescence.

Rhodamine **4** exhibits superior fluorescence brightness ($\varepsilon \times \phi$) to the parent rhodamine 110 (**1**) and the other tetraalkylrhodamines (**Fig. SN1d**). In particular, the brightness of azetidinyl-rhodamine **4** is nearly 3-fold higher than the established TMR fluorophore (**2**). This increase in brightness is independent of any change in λ_{max} or λ_{em}; the absorption and emission spectra of **2** and **4** are superimposable (**Fig. SN1e**). We note the experimental quantum yield values for dyes **2** and **4**–**7** are correlated with both the calculated C_{aryl}–N bond length (**Fig. SN1f**) and the minimum H_o–H_α distance (**Fig. SN1g**), demonstrating the predictive value of the computational modeling experiments and further supporting the hypothesis that TICT is an important nonradiative decay mechanism.[2-4] Based on its favorable brightness, improved photostability, and the λ_{max} = 549 nm, azetidinyl-rhodamine **4** was given the name "JF_{549}" (Janelia Fluor 549). The chemical stability of the azetidinyl groups in JF_{549} was verified by incubation with 10 mM β-mercaptoethanol where we observed no change in HPLC traces over 24 h (**Fig. SN1h**).

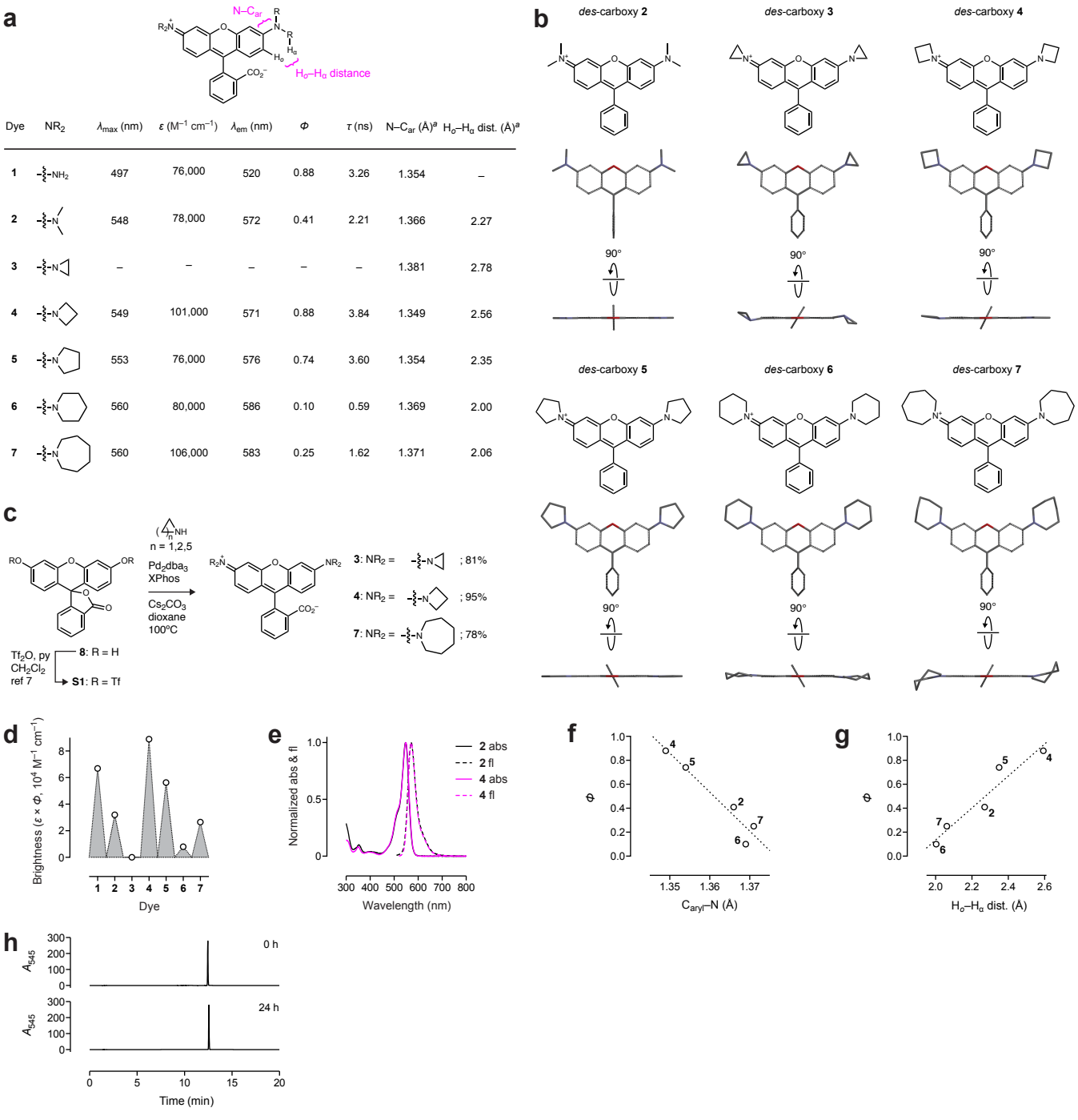

Figure SN1. Computational chemistry, organic synthesis, and spectroscopic properties of azacyclic rhodamine dyes. (**a**) Spectroscopic and computationally derived data for rhodamines **1**–**7**; [a]calculated values of nitrogen–carbon bond lengths (C_{aryl}–N) and *o*-hydrogen–α-hydrogen minimum distance (H_o–$H_α$ dist.) are from modeling of *des*-carboxy-rhodamine derivatives of **1**–**7**. (**b**) Chemical structures of *des*-carboxy-rhodamine derivatives of **1**–**7** and computationally derived, energy-minimized structures. (**c**) Synthesis of rhodamines **3, 4,** and **7** from fluorescein (**8**) using Pd-catalyzed cross-coupling. (**d**) Plot of brightness values ($ε × Φ$) for dyes **1**–**7**. (**e**) Normalized absorption (abs) and fluorescence emission (fl) spectra for tetramethylrhodamine (**2**) and JF_{549} (**4**). (**f**) Plot of experimental $Φ$ values *versus* calculated carbon–nitrogen bond lengths (C_{aryl}–N); linear regression R^2 = 0.93. (**g**) Plot of experimental $Φ$ values *versus* calculated minimum *o*-hydrogen–α-hydrogen distance (H_o–$H_α$ dist.); linear regression R^2 = 0.93. (**h**) HPLC traces of dye **4** incubated for 0 h and 24 h in PBS containing 10 mM β-mercaptoethanol.

II. Synthesis of JF_{549} HaloTag Ligand and SnapTag Ligand and Evaluation *In Vitro*

Rhodamine **4** (JF_{549}) constitutes a significant improvement in fluorescence properties compared to TMR (**2**). This enhancement is brought about by a negligible structural change—the addition of two carbon atoms. We expected that this minor modification would preserve the excellent labeling efficiency observed with TMR in self-labeling tag strategies. The HaloTag protein was optimized using a tetramethylrhodamine ligand, and exhibits rapid labeling kinetics with ligands based on this particular dye.[12,13] Additionally, rhodamine dyes exist in equilibrium between an "open," zwitterionic, quinoid form and a "closed," lipophilic, lactone form.[14] This dynamic amphipathicity makes net neutral rhodamines such as dyes **1**, **2**, and **4** excellent ligands for live-cell labeling technologies; the dye efficiently traverses the cellular membrane without detergents or chemical masking groups and excess ligand can be rapidly washed away.[15]

We therefore prepared the HaloTag ligand and SnapTag ligand conjugates of rhodamine **4** (**Fig. SN2a**). The diacetate derivative of 6-carboxyfluorescein (**S2**) was first protected as a *tert*-butyl ester to yield compound **S3**. The acetate groups were saponified with NaOH and this intermediate was triflated to give 6-carboxyfluorescein ditriflate **S4** in 69% yield over two steps. Cross-coupling of **S4** with azetidine gave rhodamine **S5**, which was deprotected to yield carboxylic acid **S6**. Treatment of **S6** with DSC followed by reaction with SnapTag ligand amine **S7**[16] yielded JF_{549}–HaloTag ligand **9**. Likewise, the SnapTag ligand of JF_{549} (**29**) could be prepared by activation of carboxylic acid **S6** with DSC, followed by reaction with **S8**. Molecules **9** and **29** are direct analogs of the commercial TMR-based HaloTag (**10**) and SnapTag ligands, respectively.

We then set out to compare the binding kinetics of the ligands **9** and **10** upon reaction with their cognate HaloTag protein moiety *in vitro*, using a purified fusion protein consisting of the HaloTag enzyme and the T7 RNA polymerase[17] (HaloTag–RNAP) as a model. After mixing each ligand with the HaloTag–RNAP protein, we quantified the fluorescence of HaloTag–RNAP protein bands by SDS-PAGE at different time points. Reaction of HaloTag–RNAP with ligands **9** or **10** was nearly complete in <1 min (**Fig. SN2b**) showing the similarity in structure of JF_{549} (**4**) to TMR (**2**) preserves the rapid labeling kinetics observed with TMR-based ligand **10** ($\sim 10^7$ $M^{-1}s^{-1}$).[13] In contrast, the labeling reaction for a Cy3-based HaloTag ligand[17] (**S9**, **Fig. SN2c**) showed slower reaction kinetics, requiring >40 min for complete labeling (**Fig. SN2b**). To compare the brightness of JF_{549}, TMR, and Cy3 ligands (**9**, **10**, and **S9**), we generated a fusion protein of the HaloTag and bacteriophage MS2 coat protein[18] (HaloTag–MS2) and prepared conjugates with the three dyes. We then imaged single molecules of the labeled HaloTag–MS2 conjugate bound to immobilized cognate RNA using TIRF microscopy.[17,19] Analysis of the traces for each dye (n >200) showed the JF_{549} ligand exhibited nearly 2-fold greater mean photon counts/s relative to both TMR and Cy3 under the same imaging conditions and gave an overall 1.6-fold larger average photon yield (**Fig. SN2d**). This result demonstrates that direct replacement of TMR or Cy3 with JF_{549} can further improve an optimized single-molecule biochemical assay.

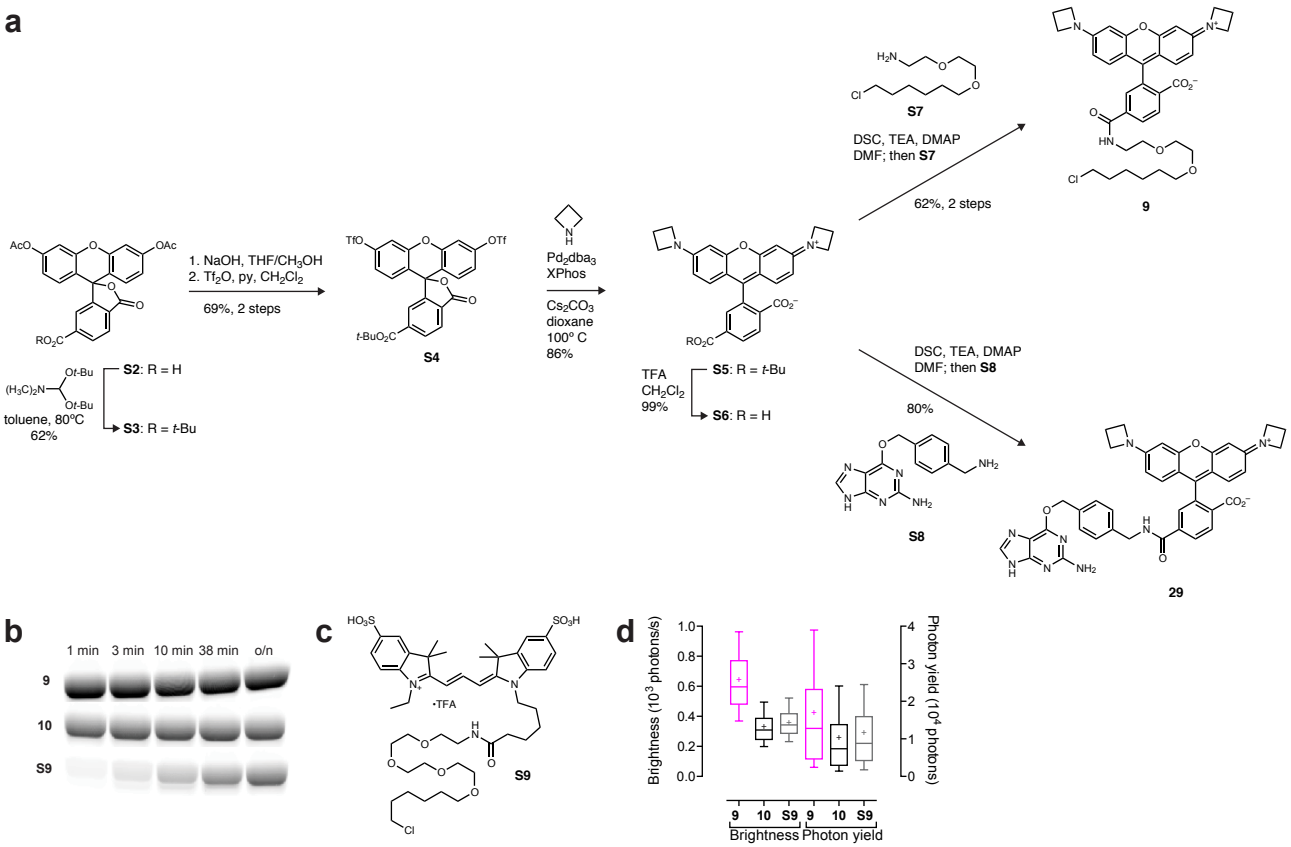

Figure SN2. Synthesis and Evaluation of JF_{549} ligands. (**a**) Synthesis of JF_{549}–HaloTag ligand (**9**) and JF_{549}–SnapTag ligand (**29**). (**b**) Fluorescence scan of HaloTag–RNAP fusion protein (35 μM) after incubation with 100 μM ligands **9**, **10**, and **S9** for indicated time and run on SDS-PAGE gel. (**c**) Structure of Cy3–HaloTag ligand **S9**. (**d**) Whisker plot comparing brightness and photon yield of HaloTag–MS2 labeled with ligand **9** (n = 258), **10** (n = 270), or **S9** (n = 224); cross indicates mean; whiskers span 10–90 percentile.

III. Synthesis and Properties of Silarhodamines and Preparation of HaloTag Ligands

We then sought to extend this chemistry to the silarhodamine dyes. The silicon-containing analogs of TMR (**2**) were previously reported by Johnsson and coworkers to be efficient labels for the SnapTag and HaloTag proteins inside cells.[20] We first prepared the novel silafluorescein (**S13**, **Fig. SN3a**). Reaction of known silaanthrone **S10**[21] with the Grignard reagent prepared from *tert*-butyl 2-bromobenzoate (**S11**) gave bis(silyl ether) **S12**. Deprotection of this material with TBAF afforded silafluorescein (**S13**) which shows $\lambda_{max}/\lambda_{em}$ = 579/599 nm, $\varepsilon = 9.3 \times 10^4$ $M^{-1}cm^{-1}$, and ϕ = 0.53 at high pH (**Fig. SN3b,c**). Compound **S13** is pH sensitive and undergoes a cooperative transition to a colorless form upon acidification (pK_a = 8.27, Hill coefficient = 1.69; **Fig. SN3b,d**). Compared to either fluorescein (**8**) or carbofluorescein (**S15**),[1] silafluorescein exhibits longer $\lambda_{max}/\lambda_{em}$ values, a higher pK_a, and a higher degree of cooperativity upon protonation. We then converted silafluorescein to compounds **25** and **26** using a palladium-catalyzed cross-coupling strategy (**Fig. SN3a**). Triflation of silafluorescein **S13** afforded compound **S14**. Cross-coupling of **S14** with dimethylamine or azetidine yielded tetraalkylrhodamine analogs **25** (SiTMR) and **26** (JF_{646}), respectively, both in high yield.

Given the success of the palladium-catalyzed cross-coupling reaction with the unsubstituted silafluorescein ditriflate **S14**, we then pursued the synthesis of HaloTag ligands based on JF_{646} (**26**) and SiTMR (**25**) from a 6-carboxy-silafluorescein derivative (**Fig. SN3e**). Addition of metalated diester **S16** to silaanthrone **S10** using the "turbo Grignard" reagent afforded the protected 6-carboxy-silafluorescein derivative **S17** in modest yield. This material was deprotected with TBAF and triflated to yield coupling partner **S18**. Pd-catalyzed amination of **S18** with azetidine or dimethylamine gave compounds **S19** and **S20**. Deprotection with TFA produced the 6-carboxy-azetidinyl-silarhodamine (**S21**) and the known 6-carboxy-SiTMR (**S22**).[20] Coupling of these acids with amine **S7** then afforded JF_{646}–HaloTag ligand **27** and the previously reported SiTMR–HaloTag ligand **28**.[20]

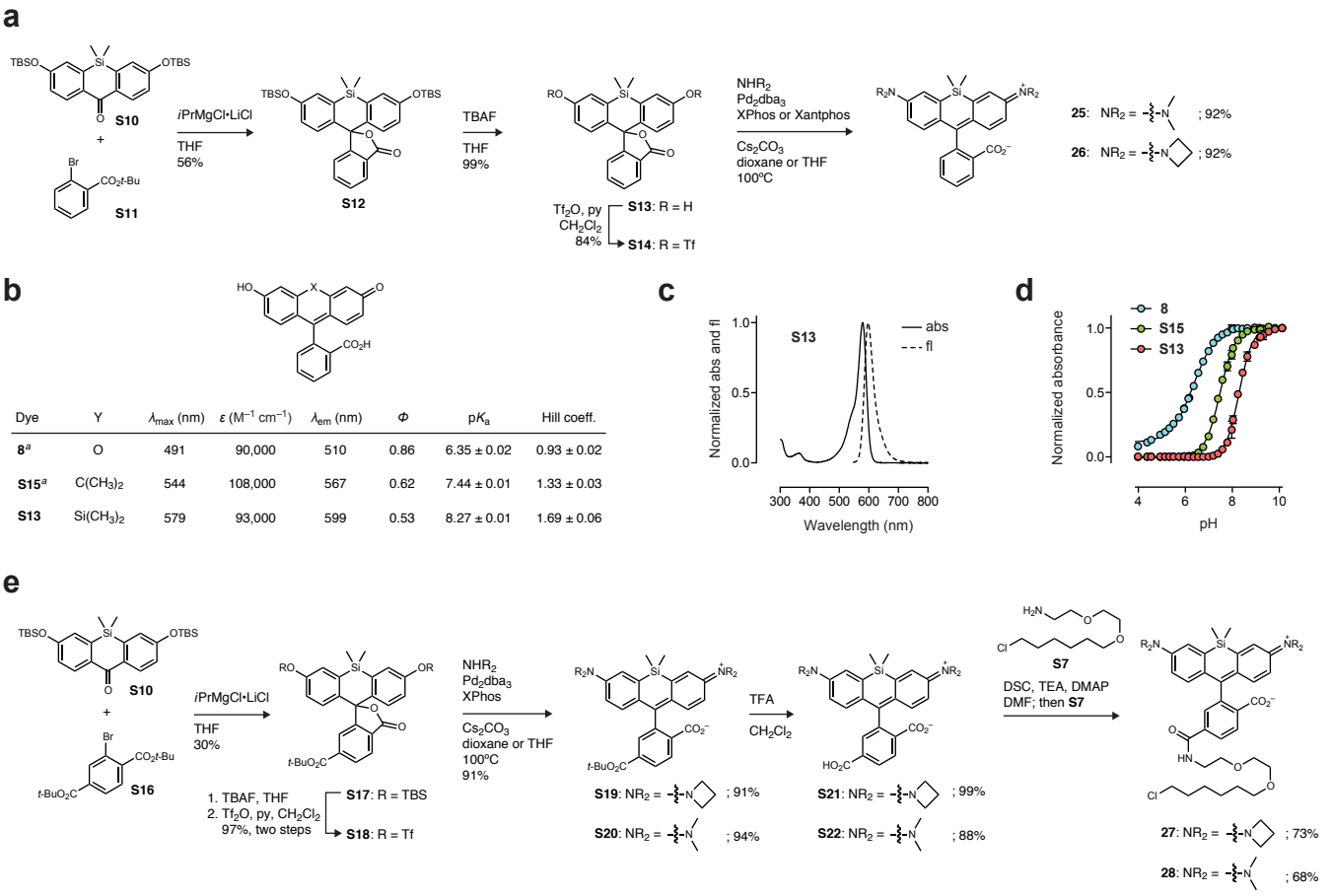

Dye	Y	λ_{max} (nm)	ε (M^{-1} cm^{-1})	λ_{em} (nm)	Φ	pK_a	Hill coeff.
8[a]	O	491	90,000	510	0.86	6.35 ± 0.02	0.93 ± 0.02
S15[a]	$C(CH_3)_2$	544	108,000	567	0.62	7.44 ± 0.01	1.33 ± 0.03
S13	$Si(CH_3)_2$	579	93,000	599	0.53	8.27 ± 0.01	1.69 ± 0.06

Figure SN3. Synthesis and properties of silarhodamine dyes. (**a**) Synthesis of silarhodamines **25** and **26** from silafluorescein (**S13**) via Pd-catalyzed cross-coupling. (**b**) Spectroscopic data for fluorescein (**8**), carbofluorescein (**S15**), and silafluorescein (**S13**) in 0.1 M NaOH; pK_a and Hill coefficients values are ± s.e.m; [a]Data taken from ref 1. (c) Normalized absorption (abs) and fluorescence emission (fl) spectra for silafluorescein (**S13**) in 0.1 M NaOH. (d) Normalized, absorbance-based pH titrations of fluorescein (**8**), carbofluorescein (**S15**), and silafluorescein (**S13**). (**e**) Synthesis of JF_{646}–HaloTag ligand **27** and SiTMR–HaloTag ligand **28**.

IV. Synthesis of Other Azetidinyl Dyes

The *N*,*N*-dialkylamino group is a common structural motif found across the disparate classes of chemical fluorophores. Based on the improvements in fluorescence properties observed in the rhodamine (**2** *versus* **4**) and silarhodamine (**25** *versus* **26**) cases, we set out to replace the *N*,*N*-dialkylamino groups with azetidines in other dyes. In all cases, the azetidine motif was installed using Pd-catalyzed cross-coupling on an aryl halide or aryl triflate (**Fig. SN4**). We also synthesized *N*,*N*-dialkylamino-containing analogs for comparison when not commercially available.

Preparation of the 7-azetidinyl-4-methylcoumarin (**12**) was accomplished by cross-coupling of azetidine with known triflate **S23** (**Fig. SN4a**).[22] The use of the commercially available third-generation palladacycle RuPhos-Pd-G3 enabled the desired reaction in 91% yield. Synthesis of 7-azetidinyl-3-carboxycoumarin (**Fig. SN4b**) began with the preparation of 3-azetidinyl-phenol (**S25**) from 3-bromophenol (**S24**) via the amination protocol developed by Verkade.[23] Vilsmeier formylation of **S25** provided aldehyde **S26**, which was subjected to Knoevenagel condensation with diethyl malonate to yield the coumarin ester **S27**. Hydrolysis of this material afforded coumarin **14**. This carboxylic acid was activated *in situ* using TSTU and reacted with amine **S8** to yield SnapTag ligand **31**. This compound is the direct azetidinyl analog of the commercial "Snap Cell 430" ligand (**30**).

Naphthalimide fluorophore **15** was prepared starting from known 4-(*N*,*N*-dimethylamino)-1,8-naphthalic anhydride **S28** (**Fig. SN4c**).[24] Condensation with glycine *tert*-butyl ester afforded naphthalimide **S29**; deprotection with TFA gave fluorophore **15**. The preparation of azetidine **16** followed a different sequence (**Fig. SN4d**). Reaction of commercial 4-bromo-1,8-naphthalic anhydride **S30** with glycine *tert*-butyl ester gave 4-bromo-naphthalimide **S31**. Cross-coupling of azetidine using RuPhos/RuPhos-Pd-G3 produced *tert*-butyl ester **S32**. Deprotection of the ester with TFA gave the desired azetidinyl fluorophore **16**. We note that attempts to cross-couple **S30** with azetidine afforded only poor isolated yields of the azetidinyl naphthalic anhydride.

To prepare azetidinyl acridine **18**, proflavine (**S33**) was hydrolyzed under microwave irradiation in concentrated H_2SO_4 to yield 3,6-dihydroxyacridine (**S34**). This crude intermediate was triflated to yield the ditriflate **S35** in 63% over two steps. Cross-coupling with azetidine using $Pd(OAc)_2$ and BINAP afforded the desired acridine **18** (**Fig. SN4e**). Known rhodol **19** was prepared from tetramethylrhodamine (**2**) by saponification (**Fig. SN4f**).[25-27] The azetidinyl analog **20** was synthesized by reaction of fluorescein ditriflate (**S1**) with limiting amounts of azetidine using cross-coupling conditions described earlier for compound **4** (**Fig. SN1c**). This gave monoazetidine **S36** in 30% isolated yield. Hydrolysis of the remaining triflate group provided the desired rhodol **20** (**Fig. SN4g**).

Preparation of the carborhodamines **21** and **22** began with carbofluorescein **S15**, which could be triflated to yield ditriflate **S37**.[1] Cross-coupling of this intermediate with dimethylamine or azetidine yielded tetramethylrhodamine analog **21** or the azetidinyl derivative **22** in high yield (**Fig. SN4h**). Synthesis of oxazine **24** started with the *N*-acyl-dihydroresorufin (**S38**; *i.e.*, Amplex Red or Amplite Red). This material was easily triflated to give compound **S39**. Pd-catalyzed cross-coupling with azetidine afforded the reduced oxazine **S40**, which was oxidized to the fluorescent **24** using DDQ in wet CH_2Cl_2 (**Fig. SN4i**).

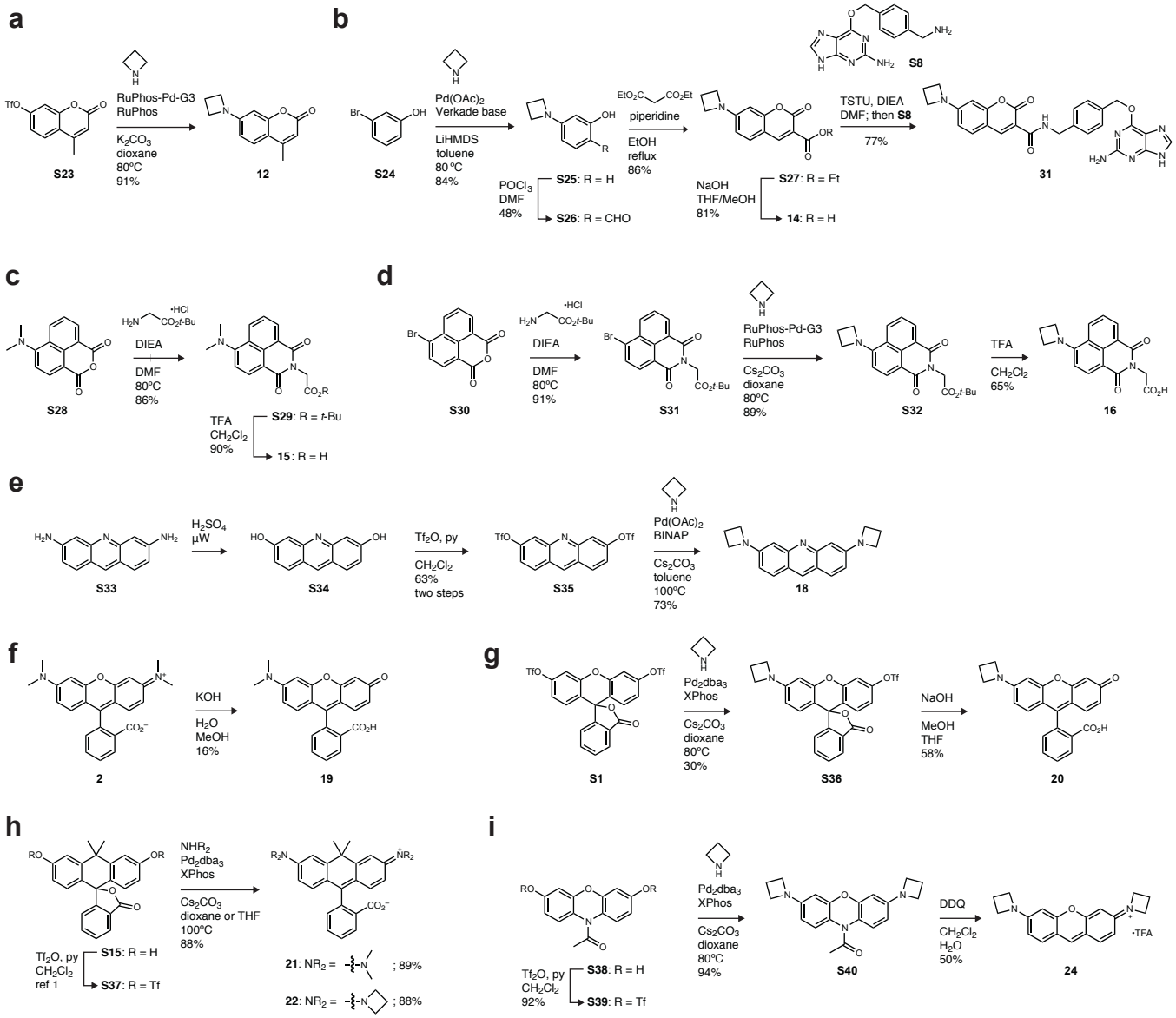

Figure SN4. Synthesis of other *N,N*-dialkylamino-containing fluorophores and their azetidinyl congeners. (**a**) Synthesis of coumarin 461 analog **12**. (**b**) Synthesis of coumarin **14** and SnapTag ligand **31**. (**c**) Synthesis of naphthalimide **15**. (**d**) Synthesis of naphthalimide **16**. (**e**) Synthesis of Acridine Orange analog **18**. (**f**) Synthesis of *N,N*-dimethylamino-rhodol **19**. (**g**) Synthesis of azetidinyl-rhodol **20**. (**h**) Synthesis of tetramethyl-carborhodamine (**21**) and azetidinyl-carborhodamine (**22**). (**i**) Synthesis of Oxazine 1 analog **24**.

V. Methods for Molecular Modeling and *in Vitro* Evaluation

Molecular modeling. Computational experiments were performed using the commercial software package Spartan'10 (version 1.1.0, Wavefunction). Restricted Hartree–Fock minimizations were performed on *des*-carboxy analogs of rhodamines **1**–**7** (**Fig. SN1b**) using the 6-31+G* basis set. Density functional theory (DFT; B3LYP) gave similar results (not shown).

pK_a Determination. The pK_a of compound fluorescein derivatives (**Fig. SN3b,d**) was performed in buffers containing 150 mM NaCl and 10 mM buffer as previously described.[1] The following buffer systems were used: citrate (pH 4.0–6.2); phosphate (pH 5.8–8.0); tris (pH 7.8–9.0); carbonate (pH 9.2–10.0). Absorbance values at λ_{max} were read on 5 μM samples (n = 3) and fitted to a sigmoidal dose response curve (variable slope) using GraphPad Prism software.[28]

Purification and Labeling of MS2 Protein. The single-chain tandem-dimer of bacteriophage MS2 coat protein (tdMS2, which specifically binds to one MS2 RNA stem-loop target)[18] was recombinantly expressed in *E. coli* strain BL21 (DE3), with a $(His)_6$-HaloTag at the *N*-terminus (*i.e.*, HaloTag–MS2). This protein was purified using standard Ni·NTA chromatography per recommendations of the Ni·NTA resin manufacturer (Qiagen). Labeling of the HaloTag–MS2 fusion was carried out in PBS supplemented with 5 mM HEPES pH 7.4, 2.5 mM $MgCl_2$, 1 mM DTT, 0.002% v/v NP40, 2% v/v glycerol, and 1–2% v/v DMSO. The HaloTag–MS2 protein (35 μM) and HaloTag ligands **9**, **10**, or **S9** (100 μM) were incubated at ambient temperature for 38 min, after which the samples were incubated at 4° C overnight (o/n, additional 17 h) to ensure complete labeling. An aliquot of the labeling reaction (2 μL) was removed at 1 min, 3 min, 10 min, 38 min, and after the o/n incubation at 4° C. These samples were loaded directly on a 12% prepacked SDS-PAGE gel (Bio-Rad) for analysis. After electrophoresis, the gel was imaged using a Typhoon Trio+ scanner (GE Healthcare) with standard fluorescence detection settings for Cy3/TMR. Coomassie staining confirmed consistent protein loading in the gel (not shown). For single-molecule imaging, the labeled proteins were purified from excess ligand using Zeba spin desalting columns (Thermo Scientific) following the manufacturer's instructions.

***In Vitro* Single-Molecule Imaging and Photon Counting.** *In vitro* single-molecule measurements were performed on a custom-built actively stabilized total internal reflection fluorescence microscope (TIRFM) as described previously.[17,19] RNA and DNA oligonucleotides were from Integrated DNA Technologies. 3Bio indicates a 3'-biotin modification; 5ATTO633N indicates a 5'-Atto633 dye modification; 3IAbRQSp indicates a 3'-Iowa Black red quencher–spacer modification. RNA oligonucleotides with the sequence:

GCACGAGCATCAGCCGTGCCCACCCCTATCCCTTATCTTAAC/3Bio

containing the cognate MS2 hairpin target sequence (underscored) were annealed to the Atto633-labeled DNA oligonucleotides with the sequence:

/5ATTO633N/GTTAAGATAAGGGATAGGG/3IAbRQSp/

This was immobilized on passivated surface through streptavidin–biotin interactions at a density of ~1000 molecules per 100 μm × 100 μm field of view. The fluorescently-labeled HaloTag–MS2 protein (5 nM) was then introduced into the imaging chamber sample in a PBS buffer supplemented with 0.1% v/v Tween 20, 1 mM Trolox, 2.5 mM protocatechuic acid, 10 μg/mL protocatechuate dehydrogenase, and 0.3 U/μL RNasin (Promega) to bind the target

RNA. After binding, the excess HaloTag–MS2 protein was removed by washing the imaging chamber with a low ionic strength imaging buffer (50 mM HEPES, pH 7.6, 0.1% v/v Tween 20, 1 mM Trolox, 2.5 mM protocatechuic acid, 10 μg/mL protocatechuate dehydrogenase, and 0.3 U/μl RNasin) in which no dissociation of the RNA-bound HaloTag–MS2 was observed for the time period of subsequent photon counting measurements (not shown). After washing with imaging buffer, the position of the sample with respect to the microscope was stabilized by tracking surface-immobilized beads.[17,19] The positions of each RNA target were mapped using the Atto633 label excited with a 640 nm laser (Coherent Cube 100, intensity 100 W/cm^2). In parallel, RNA-bound, labeled HaloTag–MS2 proteins were excited with a 532 nm laser (Coherent Verdi G2, intensity 100–300 W/cm^2) until >95% of fluorophores on HaloTag–MS2 were bleached. Imaging was carried out using two separate Electron-Multiplication CCD cameras (Andor iXon+, exposure of 0.2 s, conventional acquisition). Locations of RNA and protein molecules were identified and colocalized as previously described.[17,19] Typically, >50% of RNA molecules non-randomly colocalized with a labeled HaloTag–MS2 molecule within 80 nm. Time traces of camera counts from RNA-bound HaloTag–MS2 molecules were calculated as the total signal from a 5 pixel × 5 pixel region of interest (25-pixel ROI) centered to within 1 pixel at well-isolated molecules (>1 micron from nearest molecule), minus the total signal from a 7 pixel × 7 pixel perimeter around the ROI (corrected by a factor of 24/25). Photobleaching events were picked manually by examination of traces. Photon counts were obtained from camera counts by correction for pre-amplification gain (= 4.9).

Stability Study of Compound 4. To a solution of PBS containing 10 mM β-mercaptoethanol was added rhodamine **4** (20 μM). This sample was analysed immediately (0 h) and after 24 h at ambient temperature using an Agilent 1200 analytical HPLC system equipped with an autosampler and photodiode array detector. Using the HPLC autosampler, 10 μL of this solution was injected onto a 4.6 × 150 mm C-18 column (Phenomenex) eluting with a gradient of 10–95% v/v CH_3CN:H_2O containing 0.1% TFA over 20 min.

VI. General Experimental Information for Synthesis

Commercial reagents were obtained from reputable suppliers and used as received. All solvents were purchased in septum-sealed bottles stored under an inert atmosphere. All reactions were sealed with septa through which a nitrogen atmosphere was introduced unless otherwise noted. Reactions were conducted in round-bottomed flasks or septum-capped crimp-top vials containing Teflon-coated magnetic stir bars. Heating of reactions was accomplished with a silicon oil bath or an aluminum reaction block on top of a stirring hotplate equipped with an electronic contact thermometer to maintain the indicated temperatures.

Reactions were monitored by thin layer chromatography (TLC) on precoated TLC glass plates (silica gel 60 F_{254}, 250 μm thickness) or by LC/MS (4.6 mm × 150 mm 5 μm C18 column; 5 μL injection; 10–95% or 50–95% CH_3CN/H_2O, linear gradient, with constant 0.1% v/v TFA additive; 20 min run; 1 mL/min flow; ESI; positive ion mode; UV detection at 254 nm). TLC chromatograms were visualized by UV illumination or developed with *p*-anisaldehyde, ceric ammonium molybdate, or $KMnO_4$ stain. Flash chromatography was performed on an automated purification system using pre-packed silica gel columns. High-resolution mass spectrometry was

performed by the Mass Spectrometry Center in the Department of Medicinal Chemistry at the University of Washington and the High Resolution Mass Spectrometry Facility at the University of Iowa.

NMR spectra were recorded on a 400 MHz spectrometer. ^{1}H and ^{13}C chemical shifts (δ) were referenced to TMS or residual solvent peaks, and ^{19}F chemical shifts (δ) were referenced to $CFCl_3$. Data for ^{1}H NMR spectra are reported as follows: chemical shift (δ ppm), multiplicity (s = singlet, d = doublet, t = triplet, q = quartet, dd = doublet of doublets, m = multiplet), coupling constant (Hz), integration. Data for ^{13}C NMR spectra are reported by chemical shift (δ ppm) with hydrogen multiplicity (C, CH, CH_2, CH_3) information obtained from DEPT spectra.

VII. Synthesis of Aza-Cyclic Rhodamines

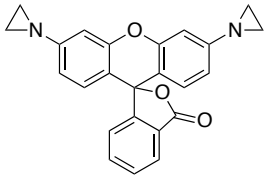

3',6'-Di(aziridin-1-yl)-3*H*-spiro[isobenzofuran-1,9'-xanthen]-3-one (3): A vial was charged with fluorescein ditriflate **S1**[7] (200 mg, 0.335 mmol), Pd_2dba_3 (31 mg, 0.034 mmol, 0.1 eq), XPhos (48 mg, 0.101 mmol, 0.3 eq), and Cs_2CO_3 (306 mg, 0.939 mmol, 2.8 eq). The vial was sealed and evacuated/backfilled with nitrogen (3×). Dioxane (2 mL) was added, and the reaction was flushed again with nitrogen (3×). Following the addition of aziridine (87 μL, 1.68 mmol, 5 eq), the reaction was stirred at 100 °C for 90 min. It was then cooled to room temperature, filtered through Celite with CH_2Cl_2, and concentrated to dryness. Purification by silica gel chromatography (0–50% EtOAc/CH_2Cl_2, linear gradient) afforded **3** (104 mg, 81%) as an off-white foam. ^{1}H NMR ($CDCl_3$, 400 MHz) δ 8.04 – 7.99 (m, 1H), 7.67 (td, *J* = 7.4, 1.3 Hz, 1H), 7.61 (td, *J* = 7.4, 1.1 Hz, 1H), 7.17 (dt, *J* = 7.6, 0.9 Hz, 1H), 6.88 (d, *J* = 2.1 Hz, 2H), 6.71 (dd, *J* = 8.5, 2.2 Hz, 2H), 6.62 (d, *J* = 8.5 Hz, 2H), 2.15 (s, 8H); ^{13}C NMR ($CDCl_3$, 101 MHz) δ 169.5 (C), 157.6 (C), 153.2 (C), 152.0 (C), 135.1 (CH), 129.8 (CH), 128.8 (CH), 126.9 (C), 125.1 (CH), 124.1 (CH), 117.5 (CH), 113.0 (C), 108.7 (CH), 83.3 (C), 28.0 (CH_2); HRMS (ESI) calcd for $C_{24}H_{19}N_2O_3$ $[M+H]^+$ 383.1390, found 383.1393.

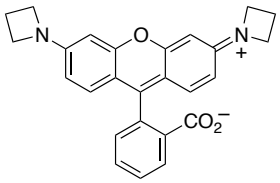

JF_{549} (4): A vial was charged with fluorescein ditriflate **S1**[7] (75 mg, 126 μmol), Pd_2dba_3 (11.5 mg, 12.6 μmol, 0.1 eq), XPhos (18.0 mg, 37.7 μmol, 0.3 eq), and Cs_2CO_3 (115 mg, 352 μmol, 2.8 eq). The vial was sealed and evacuated/backfilled with nitrogen (3×). Dioxane (1 mL) was added, and the reaction was flushed again with nitrogen (3×). Following the addition of azetidine (20.3 μL, 302 μmol, 2.4 eq), the reaction was stirred at 100 °C for 18 h. It was then cooled to room temperature, diluted with MeOH, deposited onto Celite, and concentrated to

dryness. Purification by silica gel chromatography (0–10% MeOH (2 M NH_3)/CH_2Cl_2, linear gradient; dry load with Celite) afforded **4** (49 mg, 95%) as a purple solid. ^{1}H NMR ($CDCl_3$, 400 MHz) δ 8.03 – 7.96 (m, 1H), 7.63 (td, *J* = 7.4, 1.3 Hz, 1H), 7.58 (td, *J* = 7.4, 1.1 Hz, 1H), 7.20 – 7.13 (m, 1H), 6.56 (d, *J* = 8.6 Hz, 2H), 6.20 (d, *J* = 2.3 Hz, 2H), 6.09 (dd, *J* = 8.6, 2.3 Hz, 2H), 3.91 (t, *J* = 7.3 Hz, 8H), 2.37 (p, *J* = 7.2 Hz, 4H); ^{13}C NMR ($CDCl_3$, 101 MHz) δ 169.9 (C), 153.7 (C), 153.1 (C), 152.9 (C), 134.6 (CH), 129.4 (CH), 129.0 (CH), 127.8 (C), 125.0 (CH), 124.3 (CH), 107.9 (C), 107.8 (CH), 97.7 (CH), 52.2 (CH_2), 16.8 (CH_2); Analytical HPLC: >99% purity (4.6 mm × 150 mm 5 µm C18 column; 5 µL injection; 10–95% CH_3CN/H_2O, linear gradient, with constant 0.1% v/v TFA additive; 20 min run; 1 mL/min flow; ESI; positive ion mode; detection at 550 nm); HRMS (ESI) calcd for $C_{26}H_{23}N_2O_3$ $[M+H]^+$ 411.1703, found 411.1714.

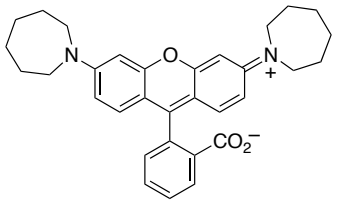

2-(3,6-Di(azepan-1-yl)xanthylium-9-yl)benzoate (7): A vial was charged with fluorescein ditriflate **S1**[7] (200 mg, 0.335 mmol), Pd_2dba_3 (31 mg, 0.034 mmol, 0.1 eq), XPhos (48 mg, 0.101 mmol, 0.3 eq), and Cs_2CO_3 (306 mg, 0.939 mmol, 2.8 eq). The vial was sealed and evacuated/backfilled with nitrogen (3×). Dioxane (2 mL) was added, and the reaction was flushed again with nitrogen (3×). Following the addition of hexamethyleneimine (91 µL, 0.805 mmol, 2.4 eq), the reaction was stirred at 100 °C for 18 h. It was then cooled to room temperature, diluted with MeOH, deposited onto Celite, and concentrated to dryness. Purification by silica gel chromatography (0–10% MeOH (2 M NH_3)/CH_2Cl_2, linear gradient; dry load with Celite) afforded **7** (130 mg, 78%) as a purple solid. ^{1}H NMR (MeOD, 400 MHz) δ 8.12 – 8.07 (m, 1H), 7.65 (td, *J* = 7.5, 1.6 Hz, 1H), 7.61 (td, *J* = 7.4, 1.6 Hz, 1H), 7.27 (d, *J* = 9.5 Hz, 2H), 7.25 – 7.22 (m, 1H), 7.02 (dd, *J* = 9.5, 2.5 Hz, 2H), 6.93 (d, *J* = 2.5 Hz, 2H), 3.81 – 3.71 (m, 8H), 1.93 – 1.82 (m, 8H), 1.66 – 1.55 (m, 8H); ^{13}C NMR (MeOD, 101 MHz) δ 173.3 (C), 163.0 (C), 159.4 (C), 157.7 (C), 141.6 (C), 133.9 (C), 133.2 (CH), 131.0 (CH), 130.7 (CH), 130.5 (CH), 130.4 (CH), 115.1 (C), 114.7 (CH), 97.1 (CH), 51.8 (CH_2), 28.0 (CH_2), 27.4 (CH_2); Analytical HPLC: 98.9% purity (4.6 mm × 150 mm 5 µm C18 column; 5 µL injection; 10–95% CH_3CN/H_2O, linear gradient, with constant 0.1% v/v TFA additive; 20 min run; 1 mL/min flow; ESI; positive ion mode; detection at 550 nm); HRMS (ESI) calcd for $C_{32}H_{35}N_2O_3$ $[M+H]^+$ 495.2642, found 495.2642.

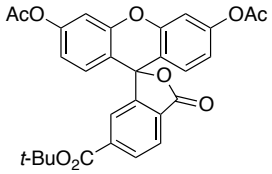

6-(*tert*-Butoxycarbonyl)-3-oxo-3*H*-spiro[isobenzofuran-1,9'-xanthene]-3',6'-diyl diacetate (S3): A suspension of 6-carboxyfluorescein diacetate (**S2**, 1.39 g, 3.02 mmol) in toluene (6 mL) was heated to 80 °C, and *N*,*N*-

dimethylformamide di-*tert*-butyl acetal (4.34 mL, 18.1 mmol, 6 eq) was added dropwise over 5 min. The reaction was stirred at 80 °C for 15 min. After cooling the mixture to room temperature, it was diluted with saturated $NaHCO_3$ and extracted with CH_2Cl_2 (2×). The combined organic extracts were dried ($MgSO_4$), filtered, and evaporated. Flash chromatography (0–20% EtOAc/hexanes, linear gradient, with constant 40% v/v CH_2Cl_2) provided **S3** as a colorless solid (971 mg, 62%). ^{1}H NMR ($CDCl_3$, 400 MHz) δ 8.26 (dd, *J* = 8.0, 1.3 Hz, 1H), 8.07 (dd, *J* = 8.0, 0.7 Hz, 1H), 7.73 (dd, *J* = 1.2, 0.8 Hz, 1H), 7.12 (dd, *J* = 2.1, 0.4 Hz, 2H), 6.84 (dd, *J* = 8.7, 2.1 Hz, 2H), 6.80 (dd, *J* = 8.7, 0.5 Hz, 2H), 2.32 (s, 6H), 1.56 (s, 9H); ^{13}C NMR ($CDCl_3$, 101 MHz) δ 168.9 (C), 168.3 (C), 164.0 (C), 152.8 (C), 152.3 (C), 151.7 (C), 138.8 (C), 131.4 (CH), 129.4 (C), 129.1 (CH), 125.2 (CH), 125.1 (CH), 118.0 (CH), 116.0 (C), 110.6 (CH), 83.0 (C), 82.1 (C), 28.2 (CH_3), 21.3 (CH_3); HRMS (ESI) calcd for $C_{29}H_{25}O_9$ $[M+H]^+$ 517.1493, found 517.1495.

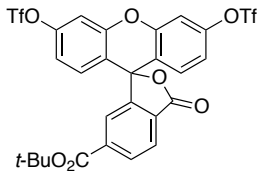

6-*tert*-Butoxycarbonylfluorescein ditriflate (S4): To a solution of **S3** (910 mg, 1.76 mmol) in 1:1 THF/MeOH (20 mL) was added 1 M NaOH (4.23 mL, 4.23 mmol, 2.4 eq). The reaction was stirred at room temperature for 1 h. The resulting red-orange solution was acidified with 1 N HCl (5 mL), diluted with water, and extracted with EtOAc (2×). The organics were washed with brine, dried ($MgSO_4$), filtered, and concentrated *in vacuo* to provide a red solid. The crude solid was suspended in CH_2Cl_2 (15 mL) and cooled to 0 °C. Pyridine (1.14 mL, 14.1 mmol, 8 eq) and trifluoromethanesulfonic anhydride (1.19 mL, 7.05 mmol, 4 eq) were added, and the ice bath was removed. The reaction was stirred at room temperature for 1 h. It was subsequently diluted with water and extracted with CH_2Cl_2 (2×). The combined organic extracts were dried ($MgSO_4$), filtered, and evaporated. Silica gel chromatography (0–25% EtOAc/hexanes, linear gradient) yielded 841 mg (69%) of **S4** as a colorless solid. ^{1}H NMR ($CDCl_3$, 400 MHz) δ 8.28 (dd, *J* = 8.0, 1.3 Hz, 1H), 8.11 (dd, *J* = 8.0, 0.7 Hz, 1H), 7.75 (dd, *J* = 1.2, 0.7 Hz, 1H), 7.32 (d, *J* = 2.4 Hz, 2H), 7.04 (dd, *J* = 8.8, 2.5 Hz, 2H), 6.94 (d, *J* = 8.8 Hz, 2H), 1.57 (s, 9H); ^{19}F NMR ($CDCl_3$, 376 MHz) δ -73.12 (s); ^{13}C NMR ($CDCl_3$, 101 MHz) δ 167.7 (C), 163.8 (C), 152.2 (C), 151.5 (C), 150.5 (C), 139.3 (C), 131.9 (CH), 130.1 (CH), 128.8 (C), 125.8 (CH), 124.9 (CH), 118.9 (C), 118.8 (q, $^1J_{CF}$ = 320.9 Hz, CF_3), 118.0 (CH), 111.0 (CH), 83.3 (C), 80.5 (C), 28.2 (CH_3); HRMS (ESI) calcd for $C_{27}H_{19}F_6O_{11}S_2$ $[M+H]^+$ 697.0267, found 697.0255.

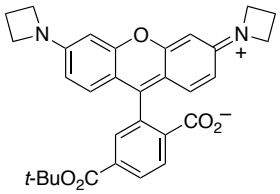

6-*tert*-Butoxycarbonyl-JF$_{549}$ (S5): A vial was charged with ditriflate **S4** (150 mg, 0.215 mmol), Pd_2dba_3 (20 mg, 0.022 mmol, 0.1 eq), XPhos (31 mg, 0.065 mmol, 0.3 eq), and Cs_2CO_3 (196 mg, 0.603 mmol, 2.8 eq). The vial was

sealed and evacuated/backfilled with nitrogen (3×). Dioxane (1.5 mL) was added, and the reaction was flushed again with nitrogen (3×). Following the addition of azetidine (35 µL, 0.517 mmol, 2.4 eq), the reaction was stirred at 100 °C for 18 h. It was then cooled to room temperature, diluted with MeOH, deposited onto Celite, and concentrated to dryness. Purification by silica gel chromatography (0–10% MeOH (2 M NH_3)/CH_2Cl_2, linear gradient; dry load with Celite) afforded **S5** (95 mg, 86%) as a dark purple solid. ^{1}H NMR ($CDCl_3$, 400 MHz) δ 8.19 (dd, *J* = 8.0, 1.4 Hz, 1H), 8.02 (dd, *J* = 8.0, 0.7 Hz, 1H), 7.73 (dd, *J* = 1.3, 0.7 Hz, 1H), 6.55 (d, *J* = 8.6 Hz, 2H), 6.21 (d, *J* = 2.3 Hz, 2H), 6.09 (dd, *J* = 8.6, 2.3 Hz, 2H), 3.92 (t, *J* = 7.3 Hz, 8H), 2.38 (p, *J* = 7.2 Hz, 4H), 1.54 (s, 9H); ^{13}C NMR ($CDCl_3$, 101 MHz) δ 169.1 (C), 164.5 (C), 153.8 (C), 153.0 (C), 152.6 (C), 137.9 (C), 131.1 (C), 130.6 (CH), 129.0 (CH), 125.4 (CH), 125.0 (CH), 107.9 (CH), 107.4 (C), 97.6 (CH), 82.4 (C), 52.2 (CH_2), 28.2 (CH_3), 16.8 (CH_2); HRMS (ESI) calcd for $C_{31}H_{31}N_2O_5$ $[M+H]^+$ 511.2227, found 511.2253.

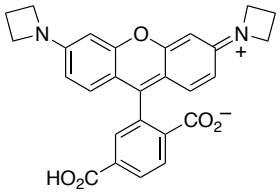

6-Carboxy-JF$_{549}$ (S6): Ester **S5** (70 mg, 0.137 mmol) was taken up in CH_2Cl_2 (2.5 mL), and trifluoroacetic acid (0.5 mL) was added. The reaction was stirred at room temperature for 6 h. Toluene (3 mL) was added; the reaction mixture was concentrated to dryness and then azeotroped with MeOH three times to provide **S6** as a dark red powder (77 mg, 99%, TFA salt). Analytical HPLC and NMR indicated that the material was >95% pure and did not require further purification prior to amide coupling. ^{1}H NMR (MeOD, 400 MHz) δ 8.40 (dd, *J* = 8.2, 0.6 Hz, 1H), 8.37 (dd, *J* = 8.2, 1.5 Hz, 1H), 7.94 (dd, *J* = 1.5, 0.6 Hz, 1H), 7.06 (d, *J* = 9.2 Hz, 2H), 6.61 (dd, *J* = 9.2, 2.2 Hz, 2H), 6.55 (d, *J* = 2.2 Hz, 2H), 4.31 (t, *J* = 7.6 Hz, 8H), 2.56 (p, *J* = 7.6 Hz, 4H); ^{19}F NMR (MeOD, 376 MHz) δ -75.32 (s); ^{13}C NMR (MeOD, 101 MHz) δ 167.7 (C), 167.5 (C), 160.1 (C), 158.7 (C), 158.0 (C), 136.2 (C), 135.9 (C), 135.4 (C), 132.8 (CH), 132.25 (CH), 132.24 (CH), 132.19 (CH), 114.8 (C), 113.6 (CH), 95.2 (CH), 52.9 (CH_2), 16.8 (CH_2); Analytical HPLC: >99% purity (4.6 mm × 150 mm 5 µm C18 column; 5 µL injection; 10–95% CH_3CN/H_2O, linear gradient, with constant 0.1% v/v TFA additive; 20 min run; 1 mL/min flow; ESI; positive ion mode; detection at 550 nm); HRMS (ESI) calcd for $C_{27}H_{23}N_2O_5$ $[M+H]^+$ 455.1601, found 455.1610.

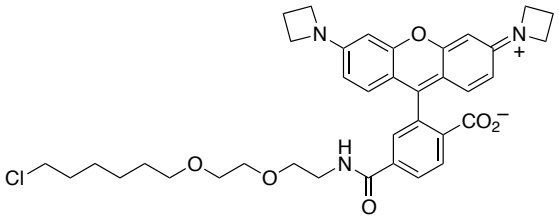

JF$_{549}$–HaloTag ligand (9): Acid **S6** (10 mg, 17.6 µmol) was combined with DSC (9.9 mg, 38.7 µmol, 2.2 eq) in DMF (1 mL). After adding Et_3N (14.7 µL, 106 µmol, 6 eq) and DMAP (0.2 mg, 1.76 µmol, 0.1 eq), the reaction was stirred at room temperature for 1 h while shielded from light. A solution of HaloTag(O2)amine **S7** (9.8 mg, 44.0

μmol, 2.5 eq) in DMF (100 μL) was then added. The reaction was stirred an additional 4 h at room temperature. It was subsequently diluted with saturated $NaHCO_3$ and extracted with CH_2Cl_2 (2×). The combined organic extracts were dried ($MgSO_4$), filtered, deposited onto Celite, and concentrated *in vacuo*. Silica gel chromatography (0–10% MeOH/CH_2Cl_2, linear gradient, with constant 1% v/v AcOH additive; dry load with Celite) followed by reverse phase HPLC (10–95% MeCN/H_2O, linear gradient, with constant 0.1% v/v TFA additive) afforded 8.5 mg (62%, TFA salt) of **9** as a dark red solid. ^{1}H NMR (MeOD, 400 MHz) δ 8.79 (t, *J* = 5.4 Hz, 1H), 8.39 (d, *J* = 8.2 Hz, 1H), 8.20 (dd, *J* = 8.2, 1.8 Hz, 1H), 7.80 (d, *J* = 1.6 Hz, 1H), 7.07 (d, *J* = 9.2 Hz, 2H), 6.61 (dd, *J* = 9.2, 2.2 Hz, 2H), 6.56 (d, *J* = 2.2 Hz, 2H), 4.31 (t, *J* = 7.6 Hz, 8H), 3.68 – 3.55 (m, 8H), 3.53 (t, *J* = 6.6 Hz, 2H), 3.43 (t, *J* = 6.5 Hz, 2H), 2.56 (p, *J* = 7.6 Hz, 4H), 1.77 – 1.66 (m, 2H), 1.56 – 1.27 (m, 6H); ^{19}F NMR (MeOD, 376 MHz) δ -75.33 (s); Analytical HPLC: >99% purity (4.6 mm × 150 mm 5 μm C18 column; 5 μL injection; 10–95% CH_3CN/H_2O, linear gradient, with constant 0.1% v/v TFA additive; 20 min run; 1 mL/min flow; ESI; positive ion mode; detection at 550 nm); HRMS (ESI) calcd for $C_{37}H_{43}ClN_3O_6$ $[M+H]^+$ 660.2835, found 660.2844.

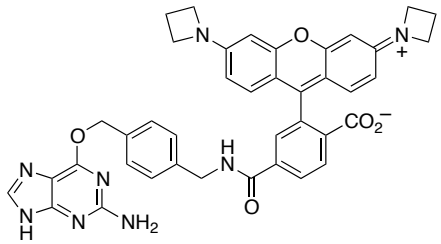

JF_{549}–SnapTag ligand (29): Acid **S6** (10 mg, 17.6 μmol) was combined with DSC (9.9 mg, 38.7 μmol, 2.2 eq) in DMF (1 mL). After adding Et_3N (14.7 μL, 106 μmol, 6 eq) and DMAP (0.2 mg, 1.76 μmol, 0.1 eq), the reaction was stirred at room temperature for 1 h while shielded from light. Benzylguanine **S8** ("BG-NH_2," 11.9 mg, 44.0 μmol, 2.5 eq) was then added. The reaction was stirred an additional 2 h at room temperature. Purification of the crude reaction mixture by reverse phase HPLC (10–95% MeCN/H_2O, linear gradient, with constant 0.1% v/v TFA additive) afforded 11.5 mg (80%, TFA salt) of **29** as a dark red solid. ^{1}H NMR (MeOD, 400 MHz) δ 9.28 (t, *J* = 5.8 Hz, 1H), 8.39 (d, *J* = 8.3 Hz, 1H), 8.20 (dd, *J* = 8.2, 1.8 Hz, 1H), 8.17 (s, 1H), 7.81 (d, *J* = 1.7 Hz, 1H), 7.50 (d, *J* = 8.1 Hz, 2H), 7.40 (d, *J* = 8.2 Hz, 2H), 7.04 (d, *J* = 9.2 Hz, 2H), 6.58 (dd, *J* = 9.1, 2.2 Hz, 2H), 6.54 (d, *J* = 2.1 Hz, 2H), 5.60 (s, 2H), 4.63 – 4.55 (m, 2H), 4.30 (t, *J* = 7.6 Hz, 8H), 2.56 (p, *J* = 7.7 Hz, 4H); ^{19}F NMR (MeOD, 376 MHz) δ -75.44 (s); Analytical HPLC: 98.3% purity (4.6 mm × 150 mm 5 μm C18 column; 5 μL injection; 10–95% CH_3CN/H_2O, linear gradient, with constant 0.1% v/v TFA additive; 20 min run; 1 mL/min flow; ESI; positive ion mode; UV detection at 550 nm); HRMS (ESI) calcd for $C_{40}H_{35}N_8O_5$ $[M+H]^+$ 707.2725, found 707.2723.

VIII. Synthesis of Silarhodamines

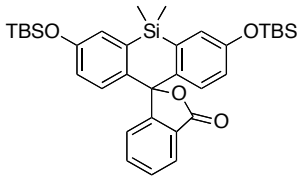

3,7-Bis((*tert*-butyldimethylsilyl)oxy)-5,5-dimethyl-3'*H*,5*H*-spiro[dibenzo[*b*,*e*]siline-10,1'-isobenzofuran]-3'-one (S12): A vial was charged with *tert*-butyl 2-bromobenzoate (**S11**, 309 mg, 1.20 mmol, 1.5 eq), sealed, and flushed with nitrogen. After dissolving the bromide in THF (2 mL) and cooling the reaction to −15 °C, *i*PrMgCl·LiCl (1.3 M in THF, 924 µL, 1.20 mmol, 1.5 eq) was added. The reaction was warmed to −5 °C and stirred for 5 h. Ketone **S10**[21] (400 mg, 0.802 mmol) in THF (2 mL) was then added dropwise. After stirring for 10 min at −5 °C, the reaction mixture was warmed to room temperature and stirred for 30 min. It was subsequently quenched with saturated NH_4Cl, diluted with water, and extracted with EtOAc (2×). The combined organics were washed with brine, dried ($MgSO_4$), filtered, and evaporated. Silica gel chromatography (0–20% Et_2O/hexanes, linear gradient) provided 271 mg (56%) of **S12** as a colorless gum. ^{1}H NMR ($CDCl_3$, 400 MHz) δ 7.97 (dt, *J* = 7.5, 0.9 Hz, 1H), 7.66 (td, *J* = 7.5, 1.2 Hz, 1H), 7.56 (td, *J* = 7.5, 0.9 Hz, 1H), 7.35 – 7.29 (m, 1H), 7.12 (d, *J* = 2.7 Hz, 2H), 6.85 (d, *J* = 8.7 Hz, 2H), 6.67 (dd, *J* = 8.7, 2.7 Hz, 2H), 0.97 (s, 18H), 0.62 (s, 3H), 0.60 (s, 3H), 0.19 (s, 12H); ^{13}C NMR ($CDCl_3$, 101 MHz) δ 170.5 (C), 155.3 (C), 154.0 (C), 137.8 (C), 137.2 (C), 134.0 (CH), 129.1 (CH), 128.6 (CH), 126.6 (C), 126.1 (CH), 125.1 (CH), 124.7 (CH), 121.2 (CH), 90.8 (C), 25.8 (CH_3), 18.4 (C), 0.2 (CH_3), -1.5 (CH_3), -4.21 (CH_3), -4.23 (CH_3); HRMS (ESI) calcd for $C_{34}H_{47}O_4Si_3$ $[M+H]^+$ 603.2777, found 603.2771.

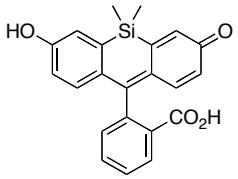

Silafluorescein (S13): To a solution of silyl ether **S12** (194 mg, 0.322 mmol) in THF (5 mL) at 0 °C was added TBAF (1.0 M in THF, 965 µL, 0.965 mmol, 3 eq). The reaction was stirred at 0 °C for 10 min. It was subsequently diluted at 0 °C with saturated NH_4Cl and extracted with EtOAc (2×). The organic extracts were dried ($MgSO_4$), filtered, evaporated, and deposited onto silica gel. Flash chromatography (20–100% EtOAc/hexanes, linear gradient, with constant 1% v/v AcOH additive; dry load with silica gel) yielded **S13** (120 mg, 99%) as an off-white solid. ^{1}H NMR (MeOD, 400 MHz) δ 7.95 (d, *J* = 7.7 Hz, 1H), 7.77 (td, *J* = 7.6, 1.1 Hz, 1H), 7.65 (td, *J* = 7.6, 0.7 Hz, 1H), 7.32 (d, *J* = 7.7 Hz, 1H), 7.13 (d, *J* = 2.7 Hz, 2H), 6.74 (d, *J* = 8.7 Hz, 2H), 6.65 (dd, *J* = 8.7, 2.7 Hz, 2H), 0.61 (s, 3H), 0.55 (s, 3H); ^{13}C NMR (MeOD, 101 MHz) δ 172.6 (C), 158.3 (C), 155.8 (C), 138.8 (C), 136.3 (C), 135.6 (CH), 130.4 (CH), 129.6 (CH), 127.4 (C), 126.6 (CH), 125.8 (CH), 121.1 (CH), 117.7 (CH), 92.9 (C), 0.2 (CH_3), -1.6 (CH_3); Analytical HPLC: >99% purity (4.6 mm × 150 mm 5 µm C18 column; 5 µL injection; 10–95% CH_3CN/H_2O, linear gradient, with constant 0.1% v/v TFA additive; 20 min run; 1 mL/min flow; ESI; positive ion mode; UV detection at 254 nm); HRMS (ESI) calcd for $C_{22}H_{19}O_4Si$ $[M+H]^+$ 375.1047, found 375.1047.

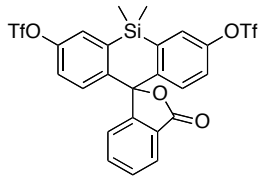

Silafluorescein ditriflate (S14): Silafluorescein **S13** (120 mg, 0.320 mmol) was taken up in CH_2Cl_2 (5 mL) and cooled to 0 °C. Pyridine (207 µL, 2.56 mmol, 8.0 eq) and trifluoromethanesulfonic anhydride (216 µL, 1.28 mmol, 4.0 eq) were added, and the ice bath was removed. The reaction was stirred at room temperature for 2 h. It was subsequently diluted with water and extracted with CH_2Cl_2 (2×). The combined organic extracts were washed with brine, dried ($MgSO_4$), filtered, and concentrated *in vacuo*. Flash chromatography on silica gel (0–30% EtOAc/hexanes, linear gradient) afforded 172 mg (84%) of **S14** as a colorless foam. ^{1}H NMR ($CDCl_3$, 400 MHz) δ 8.04 (dt, J = 7.7, 0.9 Hz, 1H), 7.77 (td, J = 7.5, 1.2 Hz, 1H), 7.66 (td, J = 7.5, 0.8 Hz, 1H), 7.57 (dd, J = 2.4, 0.5 Hz, 2H), 7.38 (dt, J = 7.6, 0.7 Hz, 1H), 7.185 (AB of ABX, n_A = 2878.9, J_{AX} = 0.3, n_B = 2871.0, J_{BX} = 2.8, J_{AB} = 8.9 Hz, 4H), 0.75 (s, 3H), 0.72 (s, 3H); ^{19}F NMR ($CDCl_3$, 376 MHz) δ -73.30; ^{13}C NMR ($CDCl_3$, 101 MHz) δ 169.2 (C), 151.8 (C), 149.5 (C), 144.3 (C), 139.3 (C), 134.8 (CH), 130.3 (CH), 129.2 (CH), 127.0 (CH), 126.5 (CH), 126.0 (C), 124.6 (CH), 122.8 (CH), 118.9 (CF_3, $^1J_{CF}$ = 320.8 Hz), 88.7 (C), 0.1 (CH_3), -1.7 (CH_3); HRMS (ESI) calcd for $C_{24}H_{17}F_6O_8S_2Si$ $[M+H]^+$ 639.0033, found 639.0030.

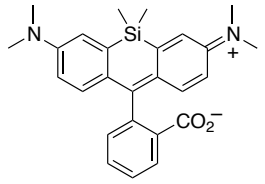

Tetramethylsilarhodamine (SiTMR, 25): A vial was charged with ditriflate **S14** (60 mg, 94.0 µmol), Pd_2dba_3 (8.6 mg, 9.4 µmol, 0.1 eq), XPhos (13.4 mg, 28.2 µmol, 0.3 eq), and Cs_2CO_3 (86 mg, 263 µmol, 2.8 eq). The vial was sealed and evacuated/backfilled with nitrogen (3×). Dimethylamine (2 M in THF, 0.94 mL, 1.88 mmol, 20 eq) was added, and the reaction was stirred at 100 °C for 2 h. It was then cooled to room temperature, diluted with CH_2Cl_2, deposited onto Celite, and concentrated to dryness. Purification by silica gel chromatography (0–40% EtOAc/hexanes, linear gradient; dry load with Celite) afforded **25** (37 mg, 92%) as a pale blue-green solid. ^{1}H NMR ($CDCl_3$, 400 MHz) δ 7.96 (dt, J = 7.6, 0.9 Hz, 1H), 7.63 (td, J = 7.5, 1.2 Hz, 1H), 7.53 (td, J = 7.5, 0.9 Hz, 1H), 7.29 (dt, J = 7.7, 0.8 Hz, 1H), 6.97 (d, J = 2.9 Hz, 2H), 6.78 (d, J = 8.9 Hz, 2H), 6.55 (dd, J = 8.9, 2.9 Hz, 2H), 2.96 (s, 12H), 0.64 (s, 3H), 0.61 (s, 3H); ^{13}C NMR ($CDCl_3$, 101 MHz) δ 170.8 (C), 154.6 (C), 149.4 (C), 137.1 (C), 133.8 (CH), 132.1 (C), 128.8 (CH), 128.3 (CH), 127.2 (C), 125.7 (CH), 124.7 (CH), 116.7 (CH), 113.4 (CH), 92.0 (C), 40.4 (CH_3), 0.6 (CH_3), -1.4 (CH_3); Analytical HPLC: >99% purity (4.6 mm × 150 mm 5 µm C18 column; 5 µL injection; 10–95% CH_3CN/H_2O, linear gradient, with constant 0.1% v/v TFA additive; 20 min run; 1 mL/min flow; ESI; positive ion mode; detection at 650 nm); HRMS (ESI) calcd for $C_{26}H_{29}N_2O_2Si$ $[M+H]^+$ 429.1993, found 429.1991.

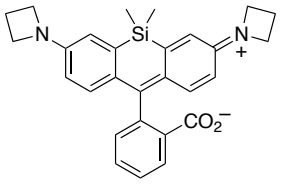

JF_{646} (26): A vial was charged with ditriflate **S14** (75 mg, 117 μmol), Pd_2dba_3 (10.8 mg, 11.7 μmol, 0.1 eq), XPhos (16.8 mg, 35.2 μmol, 0.3 eq), and Cs_2CO_3 (107 mg, 329 μmol, 2.8 eq). The vial was sealed and evacuated/backfilled with nitrogen (3×). Dioxane (1 mL) was added, and the reaction was flushed again with nitrogen (3×). Following the addition of azetidine (19.0 μL, 282 μmol, 2.4 eq), the reaction was stirred at 100 °C for 3 h. It was then cooled to room temperature, diluted with CH_2Cl_2, deposited onto Celite, and concentrated to dryness. Purification by silica gel chromatography (0–50% EtOAc/hexanes, linear gradient; dry load with Celite) afforded **26** (49 mg, 92%) as an off-white solid. ^{1}H NMR ($CDCl_3$, 400 MHz) δ 7.98 – 7.93 (m, 1H), 7.63 (td, J = 7.5, 1.2 Hz, 1H), 7.53 (td, J = 7.5, 0.9 Hz, 1H), 7.32 – 7.28 (m, 1H), 6.75 (d, J = 8.7 Hz, 2H), 6.66 (d, J = 2.6 Hz, 2H), 6.25 (dd, J = 8.7, 2.7 Hz, 2H), 3.89 (t, J = 7.2 Hz, 8H), 2.36 (p, J = 7.2 Hz, 4H), 0.60 (s, 3H), 0.58 (s, 3H); ^{13}C NMR ($CDCl_3$, 101 MHz) δ 170.7 (C), 154.3 (C), 151.0 (C), 137.1 (C), 133.7 (CH), 132.9 (C), 128.8 (CH), 128.0 (CH), 127.2 (C), 125.8 (CH), 124.8 (CH), 115.7 (CH), 112.3 (CH), 92.1 (C), 52.4 (CH_2), 17.1 (CH_2), 0.5 (CH_3), -1.5 (CH_3); Analytical HPLC: 98.7% purity (4.6 mm × 150 mm 5 μm C18 column; 5 μL injection; 10–95% CH_3CN/H_2O, linear gradient, with constant 0.1% v/v TFA additive; 20 min run; 1 mL/min flow; ESI; positive ion mode; detection at 650 nm); HRMS (ESI) calcd for $C_{28}H_{29}N_2O_2Si$ $[M+H]^+$ 453.1993, found 453.1998.

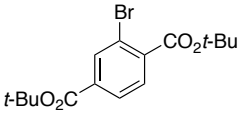

Di-*tert*-butyl 2-bromoterephthalate (S16): A suspension of 2-bromoterephthalic acid (2.50 g, 10.2 mmol) in toluene (25 mL) was heated to 80 °C, and *N*,*N*-dimethylformamide di-*tert*-butyl acetal (24.5 mL, 102 mmol, 10 eq) was added dropwise over 15 min. The reaction was stirred at 80 °C for 30 min. After cooling the mixture to room temperature, it was diluted with saturated $NaHCO_3$ and extracted with EtOAc (2×). The combined organic extracts were washed with water and brine, dried ($MgSO_4$), filtered, and evaporated. Flash chromatography (0–10% Et_2O/hexanes, linear gradient) provided **S16** as a colorless gum (3.29 g, 90%). ^{1}H NMR ($CDCl_3$, 400 MHz) δ 8.19 (d, J = 1.4 Hz, 1H), 7.92 (dd, J = 8.0, 1.6 Hz, 1H), 7.67 (d, J = 8.0 Hz, 1H), 1.62 (s, 9H), 1.60 (s, 9H); ^{13}C NMR ($CDCl_3$, 101 MHz) δ 165.4 (C), 163.8 (C), 138.0 (C), 135.1 (C), 134.9 (CH), 130.4 (CH), 128.1 (CH), 120.7 (C), 83.3 (C), 82.3 (C), 28.26 (CH_3), 28.25 (CH_3); HRMS (ESI) calcd for $C_{16}H_{21}BrO_4Na$ $[M+Na]^+$ 379.0515, found 379.0531.

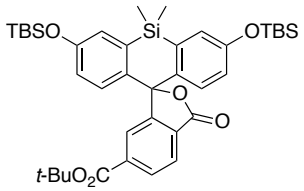

***tert*-Butyl 3,7-bis((tert-butyldimethylsilyl)oxy)-5,5-dimethyl-3'-oxo-3'*H*,5*H*-spiro[dibenzo[*b*,*e*]siline-10,1'-isobenzofuran]-6'-carboxylate (S17):** A vial was charged with bromide **S16** (537 mg, 1.50 mmol, 1.5 eq), sealed, and flushed with nitrogen. After dissolving the bromide in THF (2.5 mL) and cooling the reaction to −50 °C, *i*PrMgCl·LiCl (1.3 M in THF, 1.16 mL, 1.50 mmol, 1.5 eq) was added. The reaction was warmed to −40 °C and stirred for 2 h. A solution of **S10**[21] (500 mg, 1.00 mmol) in THF (2.5 mL) was then added dropwise. The reaction mixture was warmed to room temperature and stirred for 2 h. It was subsequently quenched with saturated NH_4Cl, diluted with water, and extracted with EtOAc (2×). The combined organics were washed with brine, dried ($MgSO_4$), filtered, and evaporated. Silica gel chromatography (0–10% Et_2O/hexanes, linear gradient) provided 213 mg (30%) of **S17** as a colorless solid. ^{1}H NMR ($CDCl_3$, 400 MHz) δ 8.13 (dd, *J* = 8.0, 1.3 Hz, 1H), 7.98 (dd, *J* = 8.0, 0.7 Hz, 1H), 7.84 (dd, *J* = 1.2, 0.8 Hz, 1H), 7.13 (d, *J* = 2.7 Hz, 2H), 6.93 (d, *J* = 8.7 Hz, 2H), 6.72 (dd, *J* = 8.7, 2.7 Hz, 2H), 1.56 (s, 9H), 0.98 (s, 18H), 0.67 (s, 3H), 0.59 (s, 3H), 0.196 (s, 6H), 0.194 (s, 6H); ^{13}C NMR ($CDCl_3$, 101 MHz) δ 170.1 (C), 164.3 (C), 155.4 (C), 155.0 (C), 137.5 (C), 136.9 (C), 136.8 (C), 130.2 (CH), 128.7 (C), 128.3 (CH), 125.9 (CH), 125.2 (CH), 125.1 (CH), 121.6 (CH), 90.6 (C), 82.5 (C), 28.2 (CH_3), 25.8 (CH_3), 18.4 (C), -0.1 (CH_3), -0.7 (CH_3), -4.21 (CH_3), -4.23 (CH_3); HRMS (ESI) calcd for $C_{39}H_{55}O_6Si_3$ $[M+H]^+$ 703.3301, found 703.3311.

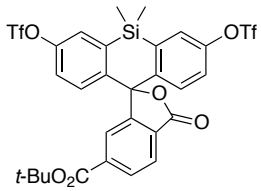

6-*tert*-Butoxycarbonylsilafluorescein ditriflate (S18): To a solution of silyl ether **S17** (205 mg, 0.292 mmol) in THF (5 mL) at 0 °C was added TBAF (1.0 M in THF, 1.17 mL, 1.17 mmol, 4 eq). The reaction was stirred at 0 °C for 10 min. It was subsequently diluted with saturated NH_4Cl and extracted with EtOAc (2×). The organic extracts were washed with brine, dried ($MgSO_4$), filtered, and evaporated to provide an orange residue. The crude intermediate was taken up in CH_2Cl_2 (5 mL) and cooled to 0 °C. Pyridine (189 µL, 2.33 mmol, 8 eq) and trifluoromethanesulfonic anhydride (196 µL, 1.17 mmol, 4 eq) were added, and the ice bath was removed. The reaction was stirred at room temperature for 2 h. It was then diluted with water and extracted with CH_2Cl_2 (2×). The combined organics were washed with brine, dried ($MgSO_4$), filtered, and concentrated *in vacuo*. Flash chromatography on silica gel (0–20% EtOAc/hexanes, linear gradient) afforded 209 mg (97%) of **S18** as a colorless solid. ^{1}H NMR ($CDCl_3$, 400 MHz) δ 8.21 (dd, *J* = 8.0, 1.3 Hz, 1H), 8.05 (dd, *J* = 8.0, 0.7 Hz, 1H), 7.93 – 7.90 (m, 1H), 7.58 (d, *J* = 2.6 Hz, 2H), 7.28 (d, *J* = 8.9 Hz, 2H), 7.22 (dd, *J* = 8.9, 2.7 Hz, 2H), 1.58 (s, 9H), 0.81 (s, 3H), 0.71 (s, 3H); ^{19}F NMR ($CDCl_3$, 376 MHz) δ -73.28 (s); ^{13}C NMR ($CDCl_3$, 101 MHz) δ 168.9 (C), 163.8 (C), 152.8 (C), 149.5 (C), 144.1 (C), 138.3 (C), 138.2 (C), 131.2 (CH), 128.8 (CH), 128.0 (C), 126.8 (CH), 126.6 (CH), 124.8 (CH),

123.2 (CH), 118.9 (q, $^1J_{CF}$ = 320.8 Hz, CF_3), 88.6 (C), 83.1 (C), 28.2 (CH_3), -0.1 (CH_3), -0.9 (CH_3); HRMS (ESI) calcd for $C_{29}H_{25}F_6O_{10}S_2Si$ $[M+H]^+$ 739.0557, found 739.0555.

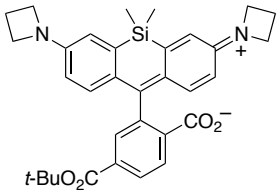

6-*tert*-Butoxycarbonyl-JF$_{646}$ (S19): A vial was charged with ditriflate **S18** (100 mg, 135 μmol), Pd_2dba_3 (12.4 mg, 13.5 μmol, 0.1 eq), XPhos (19.4 mg, 40.6 μmol, 0.3 eq), and Cs_2CO_3 (124 mg, 379 μmol, 2.8 eq). The vial was sealed and evacuated/backfilled with nitrogen (3×). Dioxane (1 mL) was added, and the reaction was flushed again with nitrogen (3×). Following the addition of azetidine (21.9 μL, 325 μmol, 2.4 eq), the reaction was stirred at 100 °C for 4 h. It was then cooled to room temperature, diluted with CH_2Cl_2, deposited onto Celite, and concentrated to dryness. Purification by silica gel chromatography (0–50% EtOAc/hexanes, linear gradient; dry load with Celite) afforded **S19** (68 mg, 91%) as an off-white foam. ^{1}H NMR ($CDCl_3$, 400 MHz) δ 8.11 (dd, *J* = 8.0, 1.3 Hz, 1H), 7.95 (dd, *J* = 8.0, 0.7 Hz, 1H), 7.82 (dd, *J* = 1.2, 0.8 Hz, 1H), 6.82 (d, *J* = 8.7 Hz, 2H), 6.66 (d, *J* = 2.6 Hz, 2H), 6.29 (dd, *J* = 8.7, 2.7 Hz, 2H), 3.90 (t, *J* = 7.3 Hz, 8H), 2.36 (p, *J* = 7.2 Hz, 4H), 1.54 (s, 9H), 0.64 (s, 3H), 0.58 (s, 3H); ^{13}C NMR ($CDCl_3$, 101 MHz) δ 170.3 (C), 164.5 (C), 155.4 (C), 151.0 (C), 137.2 (C), 136.2 (C), 132.4 (C), 129.9 (CH), 129.2 (C), 127.7 (CH), 125.6 (CH), 125.2 (CH), 115.6 (CH), 112.6 (CH), 91.9 (C), 82.3 (C), 52.3 (CH_2), 28.2 (CH_3), 17.0 (CH_2), 0.2 (CH_3), -0.7 (CH_3); HRMS (ESI) calcd for $C_{33}H_{37}N_2O_4Si$ $[M+H]^+$ 553.2517, found 553.2529.

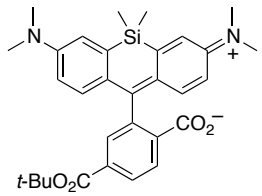

6-*tert*-Butoxycarbonyl-SiTMR (S20): A vial was charged with ditriflate **S18** (70 mg, 94.8 μmol), Pd_2dba_3 (8.7 mg, 9.5 μmol, 0.1 eq), XPhos (13.6 mg, 28.4 μmol, 0.3 eq), and Cs_2CO_3 (86 mg, 265 μmol, 2.8 eq). The vial was sealed and evacuated/backfilled with nitrogen (3×). Dimethylamine (2 M in THF, 0.95 mL, 1.90 mmol, 20 eq) was added, and the reaction was stirred at 100 °C for 2 h. It was then cooled to room temperature, diluted with CH_2Cl_2, deposited onto Celite, and concentrated to dryness. Purification by silica gel chromatography (0–40% EtOAc/hexanes, linear gradient; dry load with Celite) afforded **S20** (47 mg, 94%) as an off-white foam. ^{1}H NMR ($CDCl_3$, 400 MHz) δ 8.11 (dd, *J* = 8.0, 1.3 Hz, 1H), 7.96 (dd, *J* = 8.0, 0.7 Hz, 1H), 7.83 (dd, *J* = 1.2, 0.8 Hz, 1H), 6.96 (d, *J* = 2.9 Hz, 2H), 6.86 (d, *J* = 8.9 Hz, 2H), 6.59 (dd, *J* = 9.0, 2.9 Hz, 2H), 2.97 (s, 12H), 1.54 (s, 9H), 0.68 (s, 3H), 0.60 (s, 3H); ^{13}C NMR ($CDCl_3$, 101 MHz) δ 170.4 (C), 164.5 (C), 155.5 (C), 149.4 (C), 137.3 (C), 136.3 (C), 131.5 (C), 129.9 (CH), 129.3 (C), 127.9 (CH), 125.6 (CH), 125.1 (CH), 116.7 (CH), 113.8 (CH), 91.8 (C), 82.3 (C), 40.4 (CH_3), 28.2 (CH_3), 0.2 (CH_3), -0.6 (CH_3); HRMS (ESI) calcd for $C_{31}H_{37}N_2O_4Si$ $[M+H]^+$ 529.2517, found 529.2532.

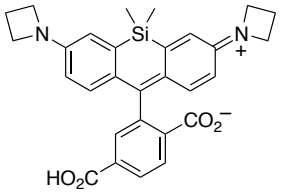

6-Carboxy-JF$_{646}$ (S21): Ester **S19** (68 mg, 0.123 mmol) was taken up in CH_2Cl_2 (2.5 mL), and trifluoroacetic acid (0.5 mL) was added. The reaction was stirred at room temperature for 6 h. Toluene (3 mL) was added; the reaction mixture was concentrated to dryness and then azeotroped with MeOH three times to provide **S21** as a dark blue-green solid (75 mg, 99%, TFA salt). Analytical HPLC and NMR indicated that the material was >95% pure and did not require further purification prior to amide coupling. ^{1}H NMR (MeOD, 400 MHz) δ 8.30 – 8.23 (m, 2H), 7.82 – 7.78 (m, 1H), 6.90 (d, *J* = 2.5 Hz, 2H), 6.86 (d, *J* = 9.2 Hz, 2H), 6.33 (dd, *J* = 9.2, 2.5 Hz, 2H), 4.27 (t, *J* = 7.4 Hz, 8H), 2.51 (p, *J* = 7.6 Hz, 4H), 0.60 (s, 3H), 0.53 (s, 3H); ^{19}F NMR (MeOD, 376 MHz) δ -75.45 (s); Analytical HPLC: 98.7% purity (4.6 mm × 150 mm 5 μm C18 column; 5 μL injection; 10–95% CH_3CN/H_2O, linear gradient, with constant 0.1% v/v TFA additive; 20 min run; 1 mL/min flow; ESI; positive ion mode; detection at 650 nm); HRMS (ESI) calcd for $C_{29}H_{29}N_2O_4Si$ $[M+H]^+$ 497.1891, found 497.1890.

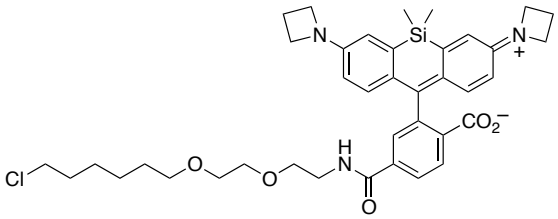

JF$_{646}$–HaloTag ligand (27): Acid **S21** (30 mg, 49.1 μmol) was combined with DSC (28 mg, 108 μmol, 2.2 eq) in DMF (2 mL). After adding Et_3N (41 μL, 295 μmol, 6 eq) and DMAP (0.6 mg, 4.91 μmol, 0.1 eq), the reaction was stirred at room temperature for 1 h while shielded from light. A solution of HaloTag(O2)amine **S7** (27 mg, 123 μmol, 2.5 eq) in DMF (250 μL) was then added. The reaction was stirred an additional 2 h at room temperature. It was subsequently diluted with saturated $NaHCO_3$ and extracted with EtOAc (2×). The combined organic extracts were washed with water and brine, dried ($MgSO_4$), filtered, and concentrated *in vacuo*. Silica gel chromatography (10–100% EtOAc/toluene, linear gradient) afforded 25 mg (73%) of **27** as a blue foam. ^{1}H NMR ($CDCl_3$, 400 MHz) δ 7.98 (dd, *J* = 8.0, 0.7 Hz, 1H), 7.90 (dd, *J* = 8.0, 1.4 Hz, 1H), 7.68 (dd, *J* = 1.2, 0.7 Hz, 1H), 6.75 (d, *J* = 8.7 Hz, 2H), 6.74 – 6.68 (m, 1H), 6.66 (d, *J* = 2.6 Hz, 2H), 6.26 (dd, *J* = 8.7, 2.7 Hz, 2H), 3.89 (t, *J* = 7.3 Hz, 8H), 3.67 – 3.60 (m, 6H), 3.56 – 3.53 (m, 2H), 3.50 (t, *J* = 6.7 Hz, 2H), 3.39 (t, *J* = 6.7 Hz, 2H), 2.36 (p, *J* = 7.2 Hz, 4H), 1.78 – 1.68 (m, 2H), 1.56 – 1.47 (m, 2H), 1.44 – 1.35 (m, 2H), 1.35 – 1.25 (m, 2H), 0.63 (s, 3H), 0.57 (s, 3H); Analytical HPLC: >99% purity (4.6 mm × 150 mm 5 μm C18 column; 5 μL injection; 10–95% CH_3CN/H_2O, linear gradient, with constant 0.1% v/v TFA additive; 20 min run; 1 mL/min flow; ESI; positive ion mode; UV detection at 650 nm); HRMS (ESI) calcd for $C_{39}H_{49}ClN_3O_5Si$ $[M+H]^+$ 702.3125, found 702.3137.

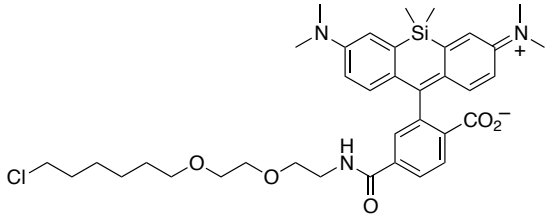

SiTMR–HaloTag ligand (28): Ester **S20** (45 mg, 85.1 μmol) was taken up in CH_2Cl_2 (2.5 mL), and trifluoroacetic acid (0.5 mL) was added. The reaction was stirred at room temperature for 6 h. Toluene (3 mL) was added; the reaction mixture was concentrated to dryness and then azeotroped with MeOH three times to provide the known 6-carboxy-SiTMR[20] **S22** as a dark blue-green solid (44 mg, 88%, TFA salt). Acid **S22** (20 mg, 34.1 μmol) was then combined with DSC (19.2 mg, 75.0 μmol, 2.2 eq) in DMF (1.5 mL). After adding Et_3N (28.5 μL, 205 μmol, 6 eq) and DMAP (0.4 mg, 3.41 μmol, 0.1 eq), the reaction was stirred at room temperature for 1 h while shielded from light. A solution of HaloTag(O2)amine **S7** (19.1 mg, 85.2 μmol, 2.5 eq) in DMF (250 μL) was then added. The reaction was stirred an additional 4 h at room temperature. It was subsequently diluted with saturated $NaHCO_3$ and extracted with EtOAc (2×). The combined organic extracts were washed with water and brine, dried ($MgSO_4$), filtered, and concentrated *in vacuo*. Silica gel chromatography (10–100% EtOAc/toluene, linear gradient) afforded 15.8 mg (68%) of **28** as a pale blue foam. Characterization data for this preparation matched that previously reported[20] for **28**. ^{1}H NMR (DMSO-d_6, 400 MHz) δ 8.77 (t, *J* = 5.5 Hz, 1H), 8.08 (dd, *J* = 8.0, 1.3 Hz, 1H), 8.02 (dd, *J* = 8.0, 0.4 Hz, 1H), 7.69 – 7.65 (m, 1H), 7.02 (d, *J* = 2.4 Hz, 2H), 6.65 (dd, *J* = 9.0, 2.6 Hz, 2H), 6.61 (d, *J* = 8.9 Hz, 2H), 3.57 (t, *J* = 6.6 Hz, 2H), 3.53 – 3.46 (m, 4H), 3.46 – 3.40 (m, 2H), 3.40 – 3.34 (m, 2H), 3.31 (t, *J* = 6.5 Hz, 2H), 2.92 (s, 12H), 1.70 – 1.60 (m, 2H), 1.46 – 1.36 (m, 2H), 1.36 – 1.19 (m, 4H), 0.64 (s, 3H), 0.52 (s, 3H); Analytical HPLC: >99% purity (4.6 mm × 150 mm 5 μm C18 column; 5 μL injection; 30–95% CH_3CN/H_2O, linear gradient, with constant 0.1% v/v TFA additive; 20 min run; 1 mL/min flow; ESI; positive ion mode; detection at 650 nm); HRMS (ESI) calcd for $C_{37}H_{49}ClN_3O_5Si$ $[M+H]^+$ 678.3130, found 678.3139.

IX. Synthesis of Other Azetidinyl Dyes

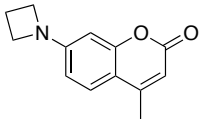

7-(Azetidin-1-yl)-4-methyl-2*H*-chromen-2-one (12): A vial was charged with 4-methylumbelliferone triflate[22] (**S23**, 300 mg, 0.973 mmol), RuPhos-G3-palladacycle (41 mg, 0.049 mmol, 0.05 eq), RuPhos (23 mg, 0.049 mmol, 0.05 eq), and K_2CO_3 (188 mg, 1.36 mmol, 1.4 eq). The vial was sealed and evacuated/backfilled with nitrogen (3×). Dioxane (8 mL) was added, and the reaction was flushed again with nitrogen (3×). Following the addition of azetidine (72 μL, 1.07 mmol, 1.1 eq), the reaction was stirred at 80 °C for 6.5 h. It was then cooled to room temperature, deposited onto Celite, and concentrated to dryness. Purification by silica gel chromatography (0–30% EtOAc/hexanes, linear gradient; dry load with Celite) afforded **12** (190 mg, 91%) as a yellow solid. ^{1}H NMR ($CDCl_3$, 400 MHz) δ 7.38 (d, *J* = 8.6 Hz, 1H), 6.30 (dd, *J* = 8.6, 2.3 Hz, 1H), 6.22 (d, *J* = 2.3 Hz, 1H), 5.97 (q, *J* =

1.1 Hz, 1H), 4.03 – 3.95 (m, 4H), 2.44 (p, J = 7.3 Hz, 2H), 2.34 (d, J = 1.1 Hz, 3H); ^{13}C NMR ($CDCl_3$, 101 MHz) δ 162.0 (C), 155.7 (C), 154.0 (C), 153.1 (C), 125.5 (CH), 110.4 (C), 109.5 (CH), 107.8 (CH), 97.2 (CH), 51.9 (CH_2), 18.7 (CH_3), 16.6 (CH_2); Analytical HPLC: >99% purity (4.6 mm × 150 mm 5 μm C18 column; 5 μL injection; 10–95% CH_3CN/H_2O, linear gradient, with constant 0.1% v/v TFA additive; 20 min run; 1 mL/min flow; ESI; positive ion mode; detection at 350 nm); HRMS (ESI) calcd for $C_{13}H_{14}NO_2$ $[M+H]^+$ 216.1019, found 216.1014.

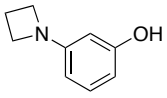

3-(Azetidin-1-yl)phenol (S25): A flask was charged with $Pd(OAc)_2$ (130 mg, 0.578 mmol, 0.05 eq), sealed, and evacuated/backfilled with nitrogen (3×). Toluene (40 mL) was added; separate solutions of 3-bromophenol (**S24**, 2.00 g, 11.6 mmol) in toluene (8 mL), 2,8,9-triisobutyl-2,5,8,9-tetraaza-1-phosphabicyclo[3.3.3]undecane ("Verkade base," 396 mg, 1.16 mmol, 0.1 eq) in toluene (8 mL), and LiHMDS (1.0 M in THF, 26.6 mL, 26.6 mmol, 2.3 eq) were then added sequentially. Following the addition of azetidine (935 μL, 13.9 mmol, 1.2 eq), the reaction was stirred at 80 °C for 18 h. It was then cooled to room temperature, deposited onto Celite, and concentrated to dryness. Purification by silica gel chromatography (0–35% EtOAc/hexanes, linear gradient; dry load with Celite) afforded **S25** (1.44 g, 84%) as an off-white solid. ^{1}H NMR ($CDCl_3$, 400 MHz) δ 7.05 (t, J = 8.0 Hz, 1H), 6.19 (ddd, J = 8.0, 2.4, 0.8 Hz, 1H), 6.04 (ddd, J = 8.1, 2.1, 0.8 Hz, 1H), 5.92 (t, J = 2.3 Hz, 1H), 4.77 (s, 1H), 3.89 – 3.81 (m, 4H), 2.34 (p, J = 7.2 Hz, 2H); ^{13}C NMR ($CDCl_3$, 101 MHz) δ 156.7 (C), 153.9 (C), 130.1 (CH), 105.1 (CH), 104.5 (CH), 99.0 (CH), 52.7 (CH_2), 17.0 (CH_2); HRMS (ESI) calcd for $C_9H_{12}NO$ $[M+H]^+$ 150.0913, found 150.0915.

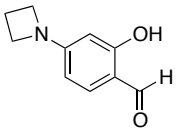

4-(Azetidin-1-yl)-2-hydroxybenzaldehyde (S26): DMF (2 mL) was cooled to 0 °C under nitrogen, and $POCl_3$ (500 μL, 5.36 mmol, 2 eq) was added dropwise. The ice bath was then removed, and the reaction was stirred at room temperature for 1 h. Phenol **S25** (400 mg, 2.68 mmol) in DMF (4 mL) was then added. After stirring the reaction at room temperature for 1 h, it was carefully diluted with saturated $NaHCO_3$ (~20 mL) and EtOAc (~20 mL) and vigorously stirred for 10 min. The mixture was diluted with additional water and extracted with EtOAc (2×). The combined organic extracts were washed with water and brine, dried ($MgSO_4$), filtered, and concentrated *in vacuo*. The residue was purified by flash chromatography on silica gel (0–40% EtOAc/hexanes, linear gradient) to yield 230 mg (48%) of **S26** as a white solid. ^{1}H NMR ($CDCl_3$, 400 MHz) δ 11.69 (s, 1H), 9.50 (s, 1H), 7.25 (d, J = 8.5 Hz, 1H), 5.94 (dd, J = 8.5, 2.1 Hz, 1H), 5.75 (d, J = 2.1 Hz, 1H), 4.08 – 3.98 (m, 4H), 2.43 (p, J = 7.4 Hz, 2H); ^{13}C NMR ($CDCl_3$, 101 MHz) δ 192.6 (CH), 164.4 (C), 156.6 (C), 135.5 (CH), 112.2 (C), 103.2 (CH), 95.6 (CH), 51.2 (CH_2), 16.3 (CH_2); HRMS (ESI) calcd for $C_{10}H_{12}NO_2$ $[M+H]^+$ 178.0863, found 178.0866.

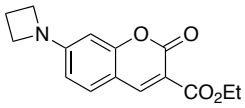

Ethyl 7-(azetidin-1-yl)-2-oxo-2*H*-chromene-3-carboxylate (S27): Aldehyde **S26** (175 mg, 0.988 mmol) was suspended in EtOH (10 mL). Diethyl malonate (301 μL, 1.98 mmol, 2 eq) and piperidine (29 μL, 0.296 mmol, 0.3 eq) were added, and the reaction was stirred at reflux for 12 h. It was then cooled to room temperature and allowed to stand for 12 h, during which time a yellow solid crystallized out of the solution. The mixture were filtered; the filter cake was washed with EtOH and dried to afford 232 mg (86%) of **S27** as a bright yellow crystalline solid. ^{1}H NMR ($CDCl_3$, 400 MHz) δ 8.39 (s, 1H), 7.31 (d, *J* = 8.6 Hz, 1H), 6.26 (dd, *J* = 8.6, 2.2 Hz, 1H), 6.09 (d, *J* = 2.1 Hz, 1H), 4.37 (q, *J* = 7.1 Hz, 2H), 4.10 – 4.02 (m, 4H), 2.48 (p, *J* = 7.4 Hz, 2H), 1.38 (t, *J* = 7.1 Hz, 3H); ^{13}C NMR ($CDCl_3$, 101 MHz) δ 164.2 (C), 158.13 (C), 158.12 (C), 155.2 (C), 149.5 (CH), 131.0 (CH), 109.4 (C), 108.39 (C), 108.36 (CH), 95.4 (CH), 61.2 (CH_2), 51.4 (CH_2), 16.3 (CH_2), 14.5 (CH_3); HRMS (ESI) calcd for $C_{15}H_{15}NO_4Na$ $[M+Na]^+$ 296.0893, found 296.0900.

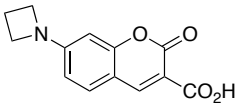

7-(Azetidin-1-yl)-2-oxo-2*H*-chromene-3-carboxylic acid (14): Ester **S27** (65 mg, 0.238 mmol) was taken up in 1:1 THF/MeOH (8 mL), and 1 M NaOH (476 μL, 0.476 mmol, 2 eq) was added. The reaction was stirred at room temperature for 3 h. It was then acidified with 1 M HCl (500 μL), and the resulting yellow suspension was filtered. The filter cake was washed (water, EtOAc) and dried to provide **14** (47 mg, 81%) as a bright yellow solid. ^{1}H NMR (DMSO-d_6, 400 MHz) δ 12.52 (s, 1H), 8.59 (s, 1H), 7.64 (d, *J* = 8.7 Hz, 1H), 6.42 (dd, *J* = 8.7, 2.2 Hz, 1H), 6.23 (d, *J* = 1.9 Hz, 1H), 4.10 – 4.01 (m, 4H), 2.39 (p, *J* = 7.4 Hz, 2H); ^{13}C NMR (DMSO-d_6, 101 MHz) δ 164.4 (C), 159.1 (C), 157.4 (C), 155.1 (C), 149.7 (CH), 131.7 (CH), 108.7 (CH), 108.0 (C), 107.6 (C), 94.7 (CH), 51.2 (CH_2), 15.6 (CH_2); Analytical HPLC: >99% purity (4.6 mm × 150 mm 5 μm C18 column; 5 μL injection; 10–95% CH_3CN/H_2O, linear gradient, with constant 0.1% v/v TFA additive; 20 min run; 1 mL/min flow; ESI; positive ion mode; detection at 400 nm); HRMS (ESI) calcd for $C_{13}H_{12}NO_4$ $[M+H]^+$ 246.0761, found 246.0770.

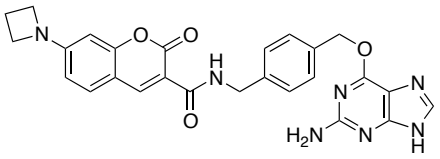

7-Azetidinylcoumarin–SnapTag ligand (31): Acid **14** (6.0 mg, 24.5 μmol) was combined with TSTU (11.0 mg, 36.7 μmol, 1.5 eq) in DMF (1 mL). After adding DIEA (21.3 μL, 122 μmol, 5 eq), the reaction was stirred at room temperature for 1 h while shielded from light. Benzylguanine **S8** ("BG-NH_2," 9.9 mg, 36.7 μmol, 1.5 eq) was then added. The reaction was stirred an additional 2 h at room temperature. Purification of the crude reaction mixture by reverse phase HPLC (10–75% $MeCN/H_2O$, linear gradient, with constant 0.1% v/v TFA additive) afforded 11.5 mg (77%, TFA salt) of **31** as a yellow solid. ^{1}H NMR (MeOD, 400 MHz) δ 8.65 (s, 1H), 8.31 (s, 1H), 7.57 – 7.50 (m,

3H), 7.41 (d, J = 8.1 Hz, 2H), 6.45 (dd, J = 8.7, 2.1 Hz, 1H), 6.22 (d, J = 2.0 Hz, 1H), 5.64 (s, 2H), 4.62 (s, 2H), 4.15 – 4.06 (m, 4H), 2.48 (p, J = 7.4 Hz, 2H); ^{19}F NMR (MeOD, 376 MHz) δ -75.44 (s); Analytical HPLC: >99% purity (4.6 mm × 150 mm 5 μm C18 column; 5 μL injection; 10–95% CH_3CN/H_2O, linear gradient, with constant 0.1% v/v TFA additive; 20 min run; 1 mL/min flow; ESI; positive ion mode; detection at 400 nm); HRMS (ESI) calcd for $C_{26}H_{24}N_7O_4$ $[M+H]^+$ 498.1884, found 498.1891.

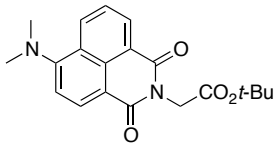

***tert*-Butyl 2-(6-(dimethylamino)-1,3-dioxo-1*H*-benzo[*de*]isoquinolin-2(3*H*)-yl)acetate (S29):** To a solution of 4-dimethylamino-1,8-naphthalic anhydride[24] (**S28**, 200 mg, 0.829 mmol) and glycine *tert*-butyl ester hydrochloride (153 mg, 0.912 mmol, 1.1 eq) in DMF (5 mL) was added DIEA (318 mL, 1.82 mmol, 2.2 eq), and the reaction was stirred at 80 °C for 18 h. It was then diluted with water and extracted with EtOAc (2×). The combined organics were washed with water and brine, dried ($MgSO_4$), filtered, and evaporated. Flash chromatography on silica gel (5–50% EtOAc/hexanes, linear gradient) yielded 254 mg (86%) of **S29** as a yellow solid. ^{1}H NMR ($CDCl_3$, 400 MHz) δ 8.58 (dd, J = 7.3, 1.2 Hz, 1H), 8.49 (d, J = 8.2 Hz, 1H), 8.45 (dd, J = 8.5, 1.2 Hz, 1H), 7.65 (dd, J = 8.5, 7.3 Hz, 1H), 7.11 (d, J = 8.2 Hz, 1H), 4.83 (s, 2H), 3.11 (s, 6H), 1.48 (s, 9H); ^{13}C NMR ($CDCl_3$, 101 MHz) δ 167.5 (C), 164.4 (C), 163.8 (C), 157.3 (C), 133.1 (CH), 131.6 (CH), 131.4 (CH), 130.6 (C), 125.4 (C), 124.9 (CH), 122.8 (C), 114.6 (C), 113.4 (CH), 82.1 (C), 44.9 (CH_3), 42.1 (CH_2), 28.2 (CH_3); HRMS (ESI) calcd for $C_{20}H_{22}N_2O_4Na$ $[M+Na]^+$ 377.1472, found 377.1476.

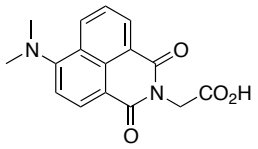

2-(6-(Dimethylamino)-1,3-dioxo-1*H*-benzo[*de*]isoquinolin-2(3*H*)-yl)acetic acid (15): Ester **S29** (75 mg, 0.212 mmol) was taken up in CH_2Cl_2 (4 mL), and trifluoroacetic acid (0.8 mL) was added. The reaction was stirred at room temperature for 8 h. Toluene (5 mL) was added; the reaction mixture was concentrated to dryness and then azeotroped with MeOH three times. The resulting residue was triturated with CH_2Cl_2/hexanes, filtered, and dried to provide **15** as a yellow solid (57 mg, 90%). ^{1}H NMR (DMSO-d_6, 400 MHz) δ 12.96 (s, 1H), 8.56 (dd, J = 8.5, 1.2 Hz, 1H), 8.48 (dd, J = 7.3, 1.1 Hz, 1H), 8.36 (d, J = 8.3 Hz, 1H), 7.78 (dd, J = 8.5, 7.3 Hz, 1H), 7.23 (d, J = 8.4 Hz, 1H), 4.71 (s, 2H), 3.12 (s, 6H); ^{13}C NMR (DMSO-d_6, 101 MHz) δ 169.5 (C), 163.3 (C), 162.6 (C), 156.8 (C), 132.6 (CH), 132.0 (CH), 130.8 (CH), 129.7 (C), 124.9 (CH), 124.1 (C), 121.8 (C), 112.9 (CH), 112.4 (C), 44.3 (CH_3), 40.9 (CH_2); Analytical HPLC: >99% purity (4.6 mm × 150 mm 5 μm C18 column; 5 μL injection; 10–95% CH_3CN/H_2O, linear gradient, with constant 0.1% v/v TFA additive; 20 min run; 1 mL/min flow; ESI; positive ion mode; detection at 450 nm); HRMS (ESI) calcd for $C_{16}H_{14}N_2O_4Na$ $[M+Na]^+$ 321.0846, found 321.0851.

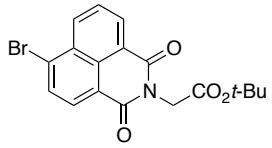

***tert*-Butyl 2-(6-bromo-1,3-dioxo-1*H*-benzo[*de*]isoquinolin-2(3*H*)-yl)acetate (S31):** To a solution of 4-bromo-1,8-naphthalic anhydride (**S30**, 960 mg, 3.46 mmol) and glycine *tert*-butyl ester hydrochloride (639 mg, 3.81 mmol, 1.1 eq) in DMF (15 mL) was added DIEA (1.33 mL, 7.62 mmol, 2.2 eq), and the reaction was stirred at 80 °C for 18 h. It was then diluted with water and extracted with EtOAc (2×). The combined organics were washed with water and brine, dried ($MgSO_4$), filtered, and evaporated. Flash chromatography on silica gel (0–30% EtOAc/hexanes, linear gradient) yielded 1.23 g (91%) of **S31** as an off-white solid. ^{1}H NMR ($CDCl_3$, 400 MHz) δ 8.68 (dd, *J* = 7.3, 1.1 Hz, 1H), 8.60 (dd, *J* = 8.5, 1.1 Hz, 1H), 8.43 (d, *J* = 7.9 Hz, 1H), 8.05 (d, *J* = 7.9 Hz, 1H), 7.86 (dd, *J* = 8.5, 7.3 Hz, 1H), 4.84 (s, 2H), 1.49 (s, 9H); ^{13}C NMR ($CDCl_3$, 101 MHz) δ 167.0 (C), 163.38 (C), 163.35 (C), 133.7 (CH), 132.5 (CH), 131.6 (CH), 131.2 (CH), 130.78 (C), 130.75 (C), 129.3 (C), 128.2 (CH), 122.8 (C), 122.0 (C), 82.5 (C), 42.3 (CH_2), 28.2 (CH_3); HRMS (ESI) calcd for $C_{18}H_{16}BrNO_4Na$ $[M+Na]^+$ 412.0155, found 412.0154.

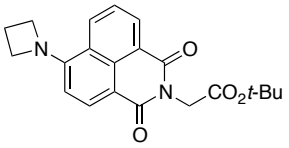

***tert*-Butyl 2-(6-(azetidin-1-yl)-1,3-dioxo-1*H*-benzo[*de*]isoquinolin-2(3*H*)-yl)acetate (S32):** A vial was charged with bromide **S31** (150 mg, 0.384 mmol), RuPhos-G3-palladacycle (16 mg, 0.019 mmol, 0.05 eq), RuPhos (9.0 mg, 0.019 mmol, 0.05 eq), and Cs_2CO_3 (188 mg, 0.577 mmol, 1.5 eq). The vial was sealed and evacuated/backfilled with nitrogen (3×). Dioxane (2 mL) was added, and the reaction was flushed again with nitrogen (3×). Following the addition of azetidine (36 μL, 0.538 mmol, 1.4 eq), the reaction was stirred at 100 °C for 2 h. It was then cooled to room temperature, diluted with CH_2Cl_2, deposited onto Celite, and concentrated to dryness. Purification by silica gel chromatography (10–75% EtOAc/hexanes, linear gradient; dry load with Celite) afforded **S32** (125 mg, 89%) as an orange solid. ^{1}H NMR ($CDCl_3$, 400 MHz) δ 8.56 (dd, *J* = 7.3, 1.1 Hz, 1H), 8.41 (d, *J* = 8.5 Hz, 1H), 8.27 (dd, *J* = 8.5, 1.1 Hz, 1H), 7.52 (dd, *J* = 8.5, 7.3 Hz, 1H), 6.41 (d, *J* = 8.5 Hz, 1H), 4.83 (s, 2H), 4.56 – 4.47 (m, 4H), 2.58 (p, *J* = 7.5 Hz, 2H), 1.48 (s, 9H); ^{13}C NMR ($CDCl_3$, 101 MHz) δ 167.7 (C), 164.5 (C), 163.7 (C), 152.7 (C), 133.7 (CH), 131.5 (CH), 130.9 (C), 130.5 (CH), 123.7 (CH), 122.3 (C), 121.0 (C), 109.6 (C), 106.2 (CH), 81.9 (C), 55.4 (CH_2), 42.1 (CH_2), 28.2 (CH_3), 17.1 (CH_2); HRMS (ESI) calcd for $C_{21}H_{22}N_2O_4Na$ $[M+Na]^+$ 389.1472, found 389.1472.

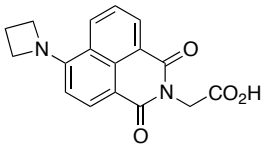

2-(6-(Azetidin-1-yl)-1,3-dioxo-1*H*-benzo[*de*]isoquinolin-2(3*H*)-yl)acetic acid (16): Ester **S32** (75 mg, 0.205 mmol) was taken up in CH_2Cl_2 (4 mL), and trifluoroacetic acid (0.8 mL) was added. The reaction was stirred at room temperature for 4 h. Toluene (5 mL) was added; the reaction mixture was concentrated to dryness and then azeotroped with MeOH three times. The resulting residue was purified by reverse phase HPLC (10–95% MeCN/H_2O, linear gradient, with constant 0.1% v/v TFA additive) to provide **16** as an orange solid (41 mg, 65%). ^{1}H NMR (DMSO-d_6, 400 MHz) δ 12.89 (s, 1H), 8.45 (s, 1H), 8.44 – 8.42 (m, 1H), 8.24 (d, J = 8.5 Hz, 1H), 7.64 (dd, J = 8.3, 7.5 Hz, 1H), 6.51 (d, J = 8.6 Hz, 1H), 4.68 (s, 2H), 4.53 (t, J = 7.6 Hz, 4H), 2.50 (p, J = 7.6 Hz, 2H); ^{13}C NMR (DMSO-d_6, 101 MHz) δ 169.6 (C), 163.4 (C), 162.4 (C), 152.2 (C), 132.9 (CH), 131.1 (CH), 130.8 (CH), 130.0 (C), 123.8 (CH), 121.1 (C), 120.0 (C), 107.4 (C), 105.9 (CH), 55.1 (CH_2), 40.9 (CH_2), 16.4 (CH_2); Analytical HPLC: >99% purity (4.6 mm × 150 mm 5 μm C18 column; 5 μL injection; 10–95% CH_3CN/H_2O, linear gradient, with constant 0.1% v/v TFA additive; 20 min run; 1 mL/min flow; ESI; positive ion mode; detection at 450 nm); HRMS (ESI) calcd for $C_{17}H_{14}N_2O_4Na$ $[M+Na]^+$ 333.0846, found 333.0858.

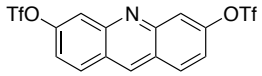

Acridine-3,6-diyl bis(trifluoromethanesulfonate) (S35): Proflavine hydrochloride (**S33**, 250 mg, 1.02 mmol) was suspended in water (1 mL) in a microwave vial, and concentrated H_2SO_4 (450 μL) was added. The sealed mixture was heated in a microwave at 195 °C for 8 h. The brown suspension was diluted with water and filtered; the resulting filter cake was washed with water and dried to provide crude 3,6-dihydroxyacridine **S34** as a red-brown solid (260 mg). The 3,6-dihydroxyacridine (**S34**, 260 mg, 1.23 mmol) was then suspended in CH_2Cl_2 (5 mL). Pyridine (796 μL, 9.85 mmol, 8 eq) and trifluoromethanesulfonic anhydride (828 μL, 4.92 mmol, 4 eq) were added, and the reaction was stirred at room temperature for 2 h. It was subsequently diluted with water and extracted with CH_2Cl_2 (2×). The combined organic extracts were dried ($MgSO_4$), filtered, and concentrated *in vacuo*. Purification by flash chromatography on silica gel (0–30% EtOAc/hexanes, linear gradient) afforded 303 mg (63%, 2 steps) of **S35** as an off-white solid. ^{1}H NMR ($CDCl_3$, 400 MHz) δ 8.93 (s, 1H), 8.19 – 8.13 (m, 4H), 7.54 (dd, J = 9.2, 2.4 Hz, 2H); ^{19}F NMR ($CDCl_3$, 376 MHz) δ -73.10 (s); ^{13}C NMR ($CDCl_3$, 101 MHz) δ 151.1 (C), 149.5 (C), 137.0 (CH), 131.2 (CH), 125.7 (C), 121.4 (CH), 120.8 (CH), 119.0 (q, $^1J_{CF}$ = 321.0 Hz, CF_3); HRMS (ESI) calcd for $C_{15}H_8F_6NO_6S_2$ $[M+H]^+$ 475.9692, found 475.9689.

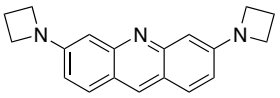

3,6-Di(azetidin-1-yl)acridine (18): A vial was charged with ditriflate **S35** (200 mg, 0.421 mmol), $Pd(OAc)_2$ (19 mg, 0.084 mmol, 0.2 eq), BINAP (79 mg, 0.126 mmol, 0.3 eq), and Cs_2CO_3 (384 mg, 1.18 mmol, 2.8 eq). The vial was sealed and evacuated/backfilled with nitrogen (3×). Toluene (2.5 mL) was added, and the reaction was flushed again with nitrogen (3×). Following the addition of azetidine (68 μL, 1.01 mmol, 2.4 eq), the reaction was stirred at 100 °C for 18 h. It was then cooled to room temperature, diluted with MeOH, deposited onto Celite, and

concentrated to dryness. Purification by silica gel chromatography (0–10% MeOH (2 M NH_3)/CH_2Cl_2, linear gradient; dry load with Celite) afforded acridine **18** (89 mg, 73%) as a red-orange solid. ^{1}H NMR (MeOD, 400 MHz) δ 8.44 (s, 1H), 7.74 (d, *J* = 9.0 Hz, 2H), 6.78 (dd, *J* = 9.0, 2.2 Hz, 2H), 6.57 (d, *J* = 2.0 Hz, 2H), 4.08 (t, *J* = 7.3 Hz, 8H), 2.47 (p, *J* = 7.3 Hz, 4H); ^{13}C NMR (MeOD, 101 MHz) δ 156.0 (C), 144.2 (CH), 143.1 (C), 132.6 (CH), 118.1 (C), 114.1 (CH), 91.4 (CH), 52.3 (CH_2), 17.0 (CH_2); Analytical HPLC: >99% purity (4.6 mm × 150 mm 5 µm C18 column; 5 µL injection; 10–95% CH_3CN/H_2O, linear gradient, with constant 0.1% v/v TFA additive; 20 min run; 1 mL/min flow; ESI; positive ion mode; detection at 500 nm); HRMS (ESI) calcd for $C_{19}H_{20}N_3$ $[M+H]^+$ 290.1652, found 290.1650.

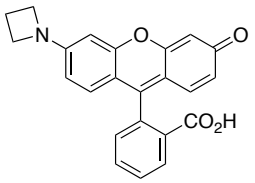

2-(6-(Azetidin-1-yl)-3-oxo-3*H*-xanthen-9-yl)benzoic acid (20): A vial was charged with fluorescein ditriflate **S1**[7] (500 mg, 0.838 mmol), Pd_2dba_3 (38 mg, 0.042 mmol, 0.05 eq), XPhos (60 mg, 0.126 mmol, 0.15 eq), and Cs_2CO_3 (382 mg, 1.17 mmol, 1.4 eq). The vial was sealed and evacuated/backfilled with nitrogen (3×). Dioxane (4 mL) was added, and the reaction was flushed again with nitrogen (3×). Following the addition of azetidine (57 µL, 0.838 mmol, 1 eq), the reaction was stirred at 80 °C for 2 h. It was then cooled to room temperature, deposited onto Celite, and concentrated to dryness. Purification by silica gel chromatography (0–35% EtOAc/hexanes, linear gradient; dry load with Celite) afforded the azetidinyl rhodol monotriflate **S36** (125 mg, 30%) as an off-white solid. The intermediate rhodol triflate **S36** (72 mg, 0.143 mmol) was taken up in 1:1 THF/MeOH (5 mL), and 1 M NaOH (286 µL, 0.286 mmol, 2 eq) was added. After stirring the reaction at room temperature for 6 h, the reaction was concentrated to dryness. The residue was purified by reverse phase HPLC (10–95% $MeCN/H_2O$, linear gradient, with constant 0.1% v/v TFA additive) to yield 40 mg (58%) of **20** as a bright orange solid. ^{1}H NMR (MeOD, 400 MHz) δ 8.36 – 8.30 (m, 1H), 7.85 (td, *J* = 7.5, 1.5 Hz, 1H), 7.81 (td, *J* = 7.6, 1.5 Hz, 1H), 7.43 – 7.38 (m, 1H), 7.16 (d, *J* = 9.3 Hz, 1H), 7.15 (d, *J* = 9.0 Hz, 1H), 7.08 (d, *J* = 2.3 Hz, 1H), 6.93 (dd, *J* = 9.0, 2.3 Hz, 1H), 6.74 (dd, *J* = 9.3, 2.2 Hz, 1H), 6.64 (d, *J* = 2.2 Hz, 1H), 4.44 – 4.35 (m, 4H), 2.58 (p, *J* = 7.7 Hz, 2H); ^{13}C NMR (MeOD, 101 MHz) δ 168.4 (C), 168.0 (C), 161.0 (C), 159.9 (C), 159.1 (C), 157.9 (C), 135.7 (C), 134.0 (CH), 133.1 (CH), 132.42 (CH), 132.40 (CH), 132.1 (C), 131.7 (CH), 131.2 (CH), 118.0 (CH), 117.1 (C), 116.4 (C), 115.9 (CH), 103.3 (CH), 95.1 (CH), 53.4 (CH_2), 16.7 (CH_2); Analytical HPLC: >99% purity (4.6 mm × 150 mm 5 µm C18 column; 5 µL injection; 10–95% CH_3CN/H_2O, linear gradient, with constant 0.1% v/v TFA additive; 20 min run; 1 mL/min flow; ESI; positive ion mode; detection at 500 nm); HRMS (ESI) calcd for $C_{23}H_{18}NO_4$ $[M+H]^+$ 372.1230, found 372.1230.

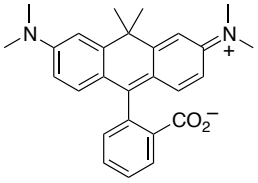

Tetramethylcarborhodamine (CTMR, 21): A vial was charged with carbofluorescein ditriflate **S37**[1] (64 mg, 103 μmol), Pd_2dba_3 (9.4 mg, 10.3 μmol, 0.1 eq), XPhos (14.7 mg, 30.8 μmol, 0.3 eq), and Cs_2CO_3 (94 mg, 288 μmol, 2.8 eq). The vial was sealed and evacuated/backfilled with nitrogen (3×). Dimethylamine (2 M in THF, 1.03 mL, 2.06 mmol, 20 eq) was added, and the reaction was stirred at 100 °C for 2 h. It was then cooled to room temperature, diluted with CH_2Cl_2, deposited onto Celite, and concentrated to dryness. Purification by silica gel chromatography (10–100% EtOAc/hexanes, linear gradient; dry load with Celite) afforded **21** (38 mg, 89%) as a light blue solid. ^{1}H NMR ($CDCl_3$, 400 MHz) δ 8.01 – 7.96 (m, 1H), 7.58 (td, *J* = 7.4, 1.5 Hz, 1H), 7.53 (td, *J* = 7.4, 1.3 Hz, 1H), 7.09 – 7.05 (m, 1H), 6.89 (d, *J* = 2.6 Hz, 2H), 6.60 (d, *J* = 8.8 Hz, 2H), 6.51 (dd, *J* = 8.8, 2.6 Hz, 2H), 2.98 (s, 12H), 1.88 (s, 3H), 1.77 (s, 3H); ^{13}C NMR ($CDCl_3$, 101 MHz) δ 171.0 (C), 155.6 (C), 150.8 (C), 146.9 (C), 134.5 (CH), 129.0 (CH), 128.8 (CH), 127.4 (C), 124.9 (CH), 124.0 (CH), 119.8 (C), 111.7 (CH), 109.2 (CH), 88.3 (C), 40.6 (CH_3), 38.7 (C), 35.8 (CH_3), 32.6 (CH_3); Analytical HPLC: >99% purity (4.6 mm × 150 mm 5 μm C18 column; 5 μL injection; 10–95% CH_3CN/H_2O, linear gradient, with constant 0.1% v/v TFA additive; 20 min run; 1 mL/min flow; ESI; positive ion mode; detection at 600 nm); HRMS (ESI) calcd for $C_{27}H_{29}N_2O_2$ $[M+H]^+$ 413.2224, found 413.2232.

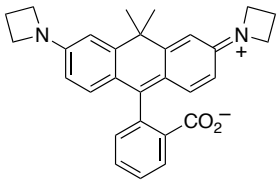

2-(3,6-Di(azetidin-1-yl)-10,10-dimethylanthracen-9-ylium-9(10*H*)-yl)benzoate (22): A vial was charged with carbofluorescein ditriflate **S37**[1] (60 mg, 96.4 μmol), Pd_2dba_3 (8.8 mg, 9.64 μmol, 0.1 eq), XPhos (13.8 mg, 28.9 μmol, 0.3 eq), and Cs_2CO_3 (88 mg, 270 μmol, 2.8 eq). The vial was sealed and evacuated/backfilled with nitrogen (3×). Dioxane (1 mL) was added, and the reaction was flushed again with nitrogen (3×). Following the addition of azetidine (15.6 μL, 231 μmol, 2.4 eq), the reaction was stirred at 100 °C for 3 h. It was then cooled to room temperature, diluted with CH_2Cl_2, deposited onto Celite, and concentrated to dryness. Purification by silica gel chromatography (10–100% EtOAc/hexanes, linear gradient; dry load with Celite) afforded **22** (37 mg, 88%) as a pale blue solid. ^{1}H NMR ($CDCl_3$, 400 MHz) δ 8.00 – 7.95 (m, 1H), 7.58 (td, *J* = 7.4, 1.4 Hz, 1H), 7.53 (td, *J* = 7.4, 1.2 Hz, 1H), 7.08 – 7.03 (m, 1H), 6.58 (d, *J* = 2.4 Hz, 2H), 6.55 (d, *J* = 8.5 Hz, 2H), 6.20 (dd, *J* = 8.6, 2.4 Hz, 2H), 3.90 (t, *J* = 7.2 Hz, 8H), 2.37 (p, *J* = 7.2 Hz, 4H), 1.82 (s, 3H), 1.72 (s, 3H); ^{13}C NMR ($CDCl_3$, 101 MHz) δ 170.9 (C), 155.6 (C), 152.4 (C), 146.9 (C), 134.5 (CH), 128.94 (CH), 128.89 (CH), 127.4 (C), 125.0 (CH), 124.1 (CH), 120.6 (C), 110.4 (CH), 107.9 (CH), 88.4 (C), 52.4 (CH_2), 38.6 (C), 35.7 (CH_3), 32.3 (CH_3), 17.0 (CH_2); Analytical HPLC: >99% purity (4.6 mm × 150 mm 5 μm C18 column; 5 μL injection; 10–95% CH_3CN/H_2O, linear gradient,

with constant 0.1% v/v TFA additive; 20 min run; 1 mL/min flow; ESI; positive ion mode; detection at 600 nm); HRMS (ESI) calcd for $C_{29}H_{29}N_2O_2$ $[M+H]^+$ 437.2224, found 437.2236.

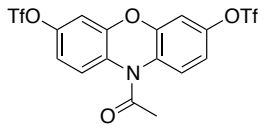

10-Acetyl-10*H*-phenoxazine-3,7-diyl bis(trifluoromethanesulfonate) (S39): Amplex Red (**S38**, 449 mg, 1.75 mmol) was taken up in CH_2Cl_2 (45 mL) and cooled to 0 °C. Pyridine (1.14 mL, 14.0 mmol, 8.0 eq) and trifluoromethanesulfonic anhydride (1.17 mL, 6.98 mmol, 4.0 eq) were added, and the ice bath was removed. The reaction was stirred at room temperature for 3 h. It was subsequently diluted with water and extracted with CH_2Cl_2 (2×). The combined organic extracts were washed with brine, dried ($MgSO_4$), filtered, and concentrated *in vacuo*. Flash chromatography on silica gel (0–35% EtOAc/hexanes, linear gradient) afforded 836 mg (92%) of **S39** as an off-white solid. ^{1}H NMR ($CDCl_3$, 400 MHz) δ 7.58 – 7.54 (m, 2H), 7.14 – 7.09 (m, 4H), 2.35 (s, 3H); ^{19}F NMR ($CDCl_3$, 376 MHz) δ -73.15 (s); ^{13}C NMR ($CDCl_3$, 101 MHz) δ 168.9 (C), 151.0 (C), 147.4 (C), 129.1 (C), 126.3 (CH), 118.8 (q, $^1J_{CF}$ = 320.9 Hz, CF_3), 117.2 (CH), 111.1 (CH), 23.0 (CH_3); HRMS (ESI) calcd for $C_{16}H_{10}F_6NO_8S_2$ $[M+H]^+$ 521.9747, found 521.9748.

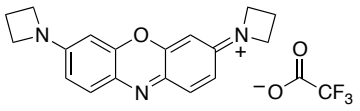

3,7-Di(azetidin-1-yl)phenoxazin-5-ium trifluoroacetate (24): A vial was charged with ditriflate **S39** (150 mg, 0.288 mmol), Pd_2dba_3 (26 mg, 0.029 mmol, 0.1 eq), XPhos (41 mg, 0.086 mmol, 0.3 eq), and Cs_2CO_3 (262 mg, 0.806 mmol, 2.8 eq). The vial was sealed and evacuated/backfilled with nitrogen (3×). Dioxane (4 mL) was added, and the reaction was flushed again with nitrogen (3×). Following the addition of azetidine (47 µL, 0.691 mmol, 2.4 eq), the reaction was stirred at 80 °C for 4 h. It was then cooled to room temperature, deposited onto Celite, and concentrated to dryness. Purification by silica gel chromatography (5–50% EtOAc/hexanes, linear gradient; dry load with Celite) afforded the *N*-acetyl leuco-dye **S40** (91 mg, 94%) as a colorless solid. The intermediate leuco-dye **S40** (63 mg, 0.189 mmol) was taken up in a mixture of CH_2Cl_2 (11.7 mL) and water (1.3 mL) and cooled to 0 °C. DDQ (47 mg, 0.207 mmol, 1.1 eq) was added, and the reaction was stirred at room temperature for 2.5 h. A second portion of DDQ (21 mg, 0.094 mmol, 0.5 eq) was added, and the reaction was stirred for an additional 30 min. The mixture was evaporated, redissolved in MeCN, deposited onto Celite, and concentrated to dryness. Silica gel chromatography (0–15% MeOH/CH_2Cl_2, linear gradient, with constant 1% v/v AcOH additive; dry load with Celite) followed by reverse phase HPLC (10–95% MeCN/H_2O, linear gradient, with constant 0.1% v/v TFA additive) afforded 38 mg (50%) of **24** as a deep blue solid. ^{1}H NMR (MeOD, 400 MHz) δ 7.72 (d, J = 9.3 Hz, 2H), 6.92 (dd, J = 9.3, 2.4 Hz, 2H), 6.50 (d, J = 2.4 Hz, 2H), 4.43 (t, J = 7.7 Hz, 8H), 2.60 (p, J = 7.7 Hz, 4H); ^{19}F NMR (MeOD, 376 MHz) δ -75.45 (s); ^{13}C NMR (MeOD, 101 MHz) δ 158.0 (C), 150.3 (C), 135.4 (CH), 135.3 (C), 116.4 (CH), 95.1 (CH), 53.7 (CH_2), 16.6 (CH_2); Analytical HPLC: >99% purity (4.6 mm × 150 mm 5 µm C18 column; 5 µL

injection; 10–95% CH_3CN/H_2O, linear gradient, with constant 0.1% v/v TFA additive; 20 min run; 1 mL/min flow; ESI; positive ion mode; detection at 650 nm); HRMS (ESI) calcd for $C_{18}H_{18}N_3O$ $[M]^+$ 292.1444, found 292.1439.

X. References

1 Grimm, J.B. *et al.* Carbofluoresceins and carborhodamines as scaffolds for high-contrast fluorogenic probes. *ACS Chem. Biol.* **8**, 1303–1310 (2013).

2 Vogel, M., Rettig, W., Sens, R. & Drexhage, K.H. Structural relaxation of rhodamine dyes with different *N*-substitution patterns—a study of fluorescence decay times and quantum yields. *Chem. Phys. Lett.* **147**, 452–460 (1988).

3 Grabowski, Z.R., Rotkiewicz, K. & Rettig, W. Structural changes accompanying intramolecular electron transfer: Focus on twisted intramolecular charge-transfer states and structures. *Chem. Rev.* **103**, 3899–4032 (2003).

4 Song, X., Johnson, A. & Foley, J. 7-Azabicyclo[2.2.1]heptane as a unique and effective dialkylamino auxochrome moiety: Demonstration in a fluorescent rhodamine dye. *J. Am. Chem. Soc.* **130**, 17652-17653 (2008).

5 Rozeboom, M.D., Houk, K., Searles, S. & Seyedrezai, S.E. Photoelectron spectroscopy of *N*-aryl cyclic amines. Variable conformations and relationships to gas-and solution-phase basicities. *J. Am. Chem. Soc.* **104**, 3448–3453 (1982).

6 Karstens, T. & Kobs, K. Rhodamine B and rhodamine 101 as reference substances for fluorescence quantum yield measurements. *J. Phys. Chem.* **84**, 1871–1872 (1980).

7 Grimm, J.B. & Lavis, L.D. Synthesis of rhodamines from fluoresceins using Pd-catalyzed C–N cross-coupling. *Org. Lett.* **13**, 6354–6357 (2011).

8 Cavallo, L., Moore, M.H., Corrie, J.E.T. & Fraternali, F. Quantum mechanics calculations on rhodamine dyes require inclusion of solvent water for accurate representation of the structure. *J. Phys. Chem. A* **108**, 7744–7751 (2004).

9 Pearson, W.H., Lian, B.W. & Bergmeier, S.C. in *Comprehensive Heterocyclic Chemistry II* Vol. 1A (eds A. R. Katritzky, C. W. Rees, & E. F. V. Scriven) 1–60 (Elsevier, 1996).

10 Smith, S.A., Hand, K.E., Love, M.L., Hill, G. & Magers, D.H. Conventional strain energies of azetidine and phosphetane: Can density functional theory yield reliable results? *J. Comp. Chem.* **34**, 558–565 (2013).

11 Beija, M., Afonso, C.A.M. & Martinho, J.M.G. Synthesis and applications of rhodamine derivatives as fluorescent probes. *Chem. Soc. Rev.* **38**, 2410–2433 (2009).

12 Los, G.V. *et al.* HaloTag: A novel protein labeling technology for cell imaging and protein analysis. *ACS Chem. Biol.* **3**, 373–382 (2008).

13 Encell, L.P. *et al.* Development of a dehalogenase-based protein fusion tag capable of rapid, selective and covalent attachment to customizable ligands. *Curr. Chem. Genomics* **6**, (Suppl 1-M7) 55–71 (2012).

14 Lavis, L.D. & Raines, R.T. Bright ideas for chemical biology. *ACS Chem. Biol.* **3**, 142–155 (2008).

15 Watkins, R.W., Lavis, L.D., Kung, V.M., Los, G.V. & Raines, R.T. Fluorogenic affinity label for the facile, rapid imaging of proteins in live cells. *Org. Biomol. Chem.* **7**, 3969–3975 (2009).

16 Neklesa, T.K. *et al.* Small-molecule hydrophobic tagging–induced degradation of HaloTag fusion proteins. *Nat. Chem. Biol.* **7**, 538–543 (2011).

17 Zhang, Z., Revyakin, A., Grimm, J.B., Lavis, L.D. & Tjian, R. Single-molecule tracking of the transcription cycle by sub-second RNA detection. *eLife* **3**, e01775 (2014).

18 Wu, B., Chao, J.A. & Singer, R.H. Fluorescence fluctuation spectroscopy enables quantitative imaging of single mRNAs in living cells. *Biophys. J.* **102**, 2936–2944 (2012).

19 Revyakin, A. *et al.* Transcription initiation by human RNA polymerase II visualized at single-molecule resolution. *Genes Dev.* **26**, 1691–1702 (2012).

20 Lukinavičius, G. *et al.* A near-infrared fluorophore for live-cell super-resolution microscopy of cellular proteins. *Nature Chem.* **5**, 132–139 (2013).

21 Egawa, T. *et al.* Development of a fluorescein analogue, TokyoMagenta, as a novel scaffold for fluorescence probes in red region. *Chem. Commun.* **47**, 4162–4164 (2011).

22 Kövér, J. & Antus, S. Facile deoxygenation of hydroxylated flavonoids by palladium-catalysed reduction of its triflate derivatives. *Z. Naturforsch., B: J. Chem. Sci.* **60**, 792–796 (2005).

23 Urgaonkar, S. & Verkade, J.G. Palladium/proazaphosphatrane-catalyzed amination of aryl halides possessing a phenol, alcohol, acetanilide, amide or an enolizable ketone functional group: efficacy of lithium bis(trimethylsilyl)amide as the base. *Adv. Synth. Catal.* **346**, 611–616 (2004).
24 Kollár, J., Hrdlovič, P., Chmela, Š., Sarakha, M. & Guyot, G. Synthesis and transient absorption spectra of derivatives of 1,8-naphthalic anhydrides and naphthalimides containing 2,2,6,6-tetramethylpiperidine; triplet route of deactivation. *J. Photochem. Photobiol., A* **170**, 151–159 (2005).
25 Whitaker, J.E. *et al.* Fluorescent rhodol derivatives: Versatile, photostable labels and tracers. *Anal. Biochem.* **207**, 267–279 (1992).
26 Sauers, R.R., Husain, S.N., Piechowski, A.P. & Bird, G.R. Shaping the absorption and fluorescence bands of a class of efficient, photoactive chromophores: synthesis and properties of some new 3H-xanthen-3-ones. *Dyes Pigments* **8**, 35–53 (1987).
27 Lee, L.G., Berry, G.M. & Chen, C.-H. Vita Blue: A new 633-nm excitable fluorescent dye for cell analysis. *Cytometry* **10**, 151–164 (1989).
28 Lavis, L.D., Rutkoski, T.J. & Raines, R.T. Tuning the pK_a of fluorescein to optimize binding assays. *Anal. Chem.* **79**, 6775–6782 (2007).

Origin	Bruker BioSpin GmbH
Solvent	CDCl3
Temperature	295.1
Pulse Sequence	zg30
Experiment	1D
Number of Scans	16
Acquisition Date	2013-07-05T16:00:00
Spectrometer Frequency	400.13
Spectral Width	8223.7
Lowest Frequency	-1645.8
Nucleus	1H
Acquired Size	32768
Spectral Size	65536

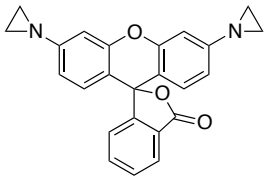

3

169.51
157.59
153.20
151.97
135.07
129.77
128.79
126.92
125.11
124.10
117.45
113.00
108.72
83.30
28.00

Origin	Bruker BioSpin GmbH
Solvent	CDCl3
Temperature	296.7
Pulse Sequence	zgpg30
Experiment	1D
Number of Scans	1024
Acquisition Date	2013-07-05T17:42:00
Spectrometer Frequency	100.62
Spectral Width	24038.5
Lowest Frequency	-1946.0
Nucleus	13C
Acquired Size	32768
Spectral Size	65536

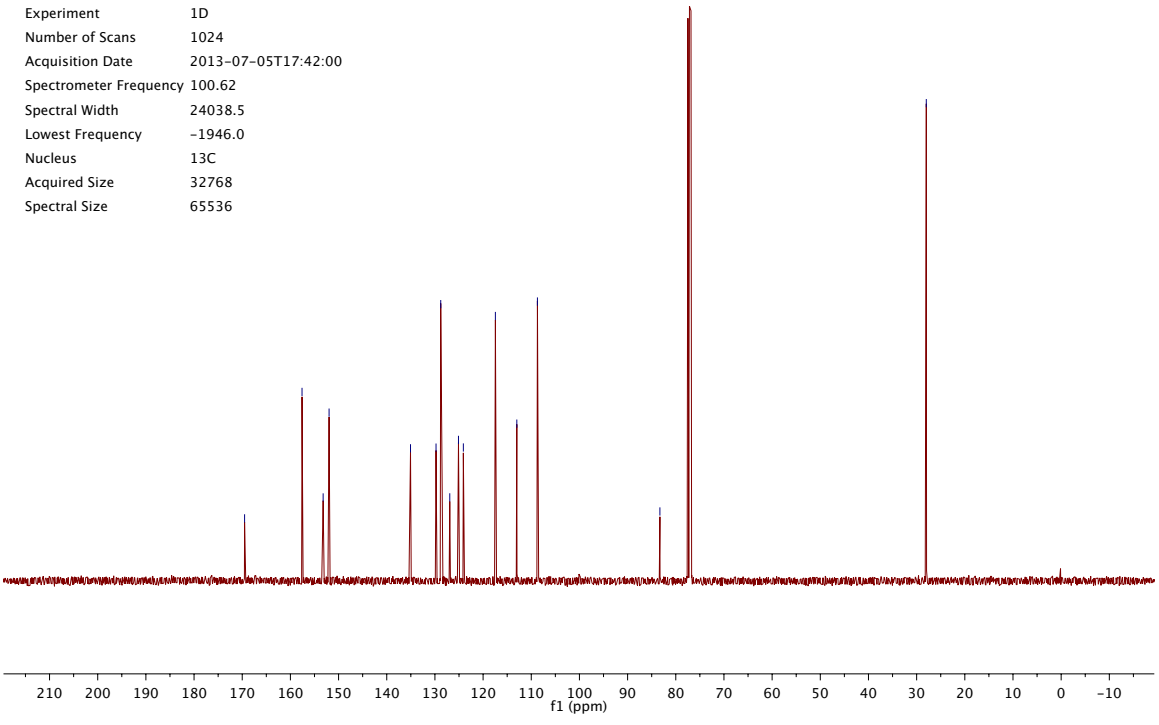

Origin	Bruker BioSpin GmbH
Solvent	CDCl3
Temperature	295.1
Pulse Sequence	zg30
Experiment	1D
Number of Scans	16
Acquisition Date	2013-07-05T21:05:00
Spectrometer Frequency	400.13
Spectral Width	8223.7
Lowest Frequency	-1646.1
Nucleus	1H
Acquired Size	32768
Spectral Size	65536

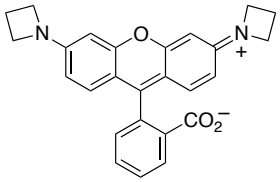

4

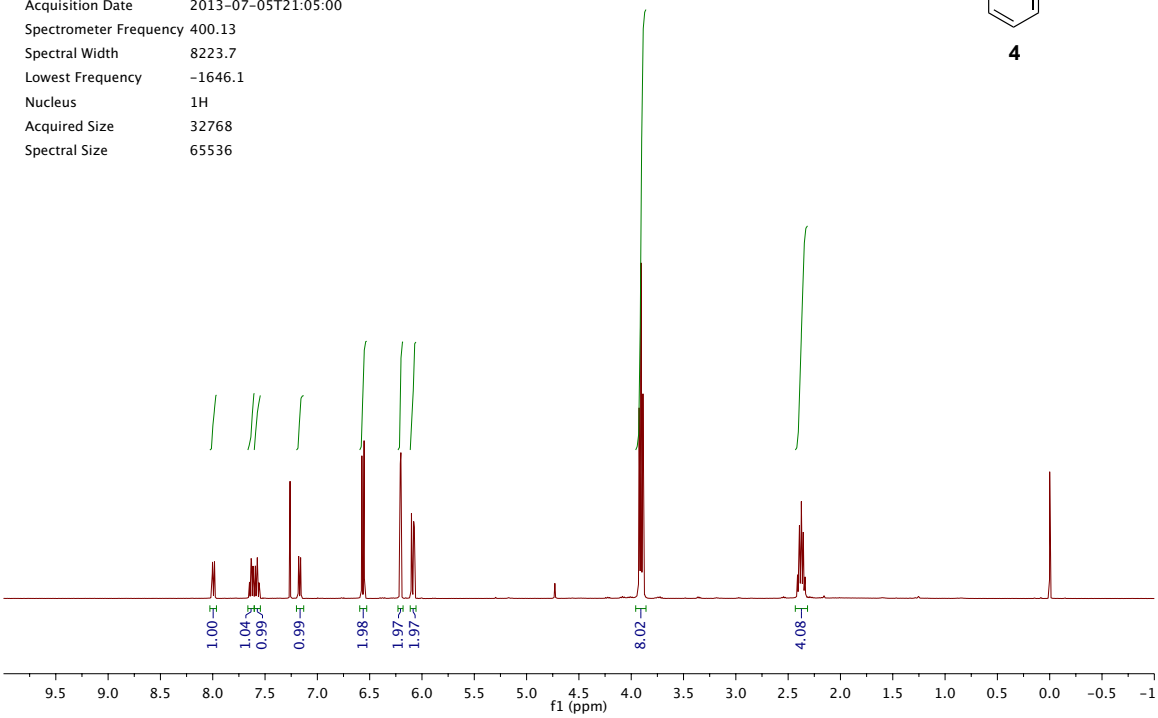

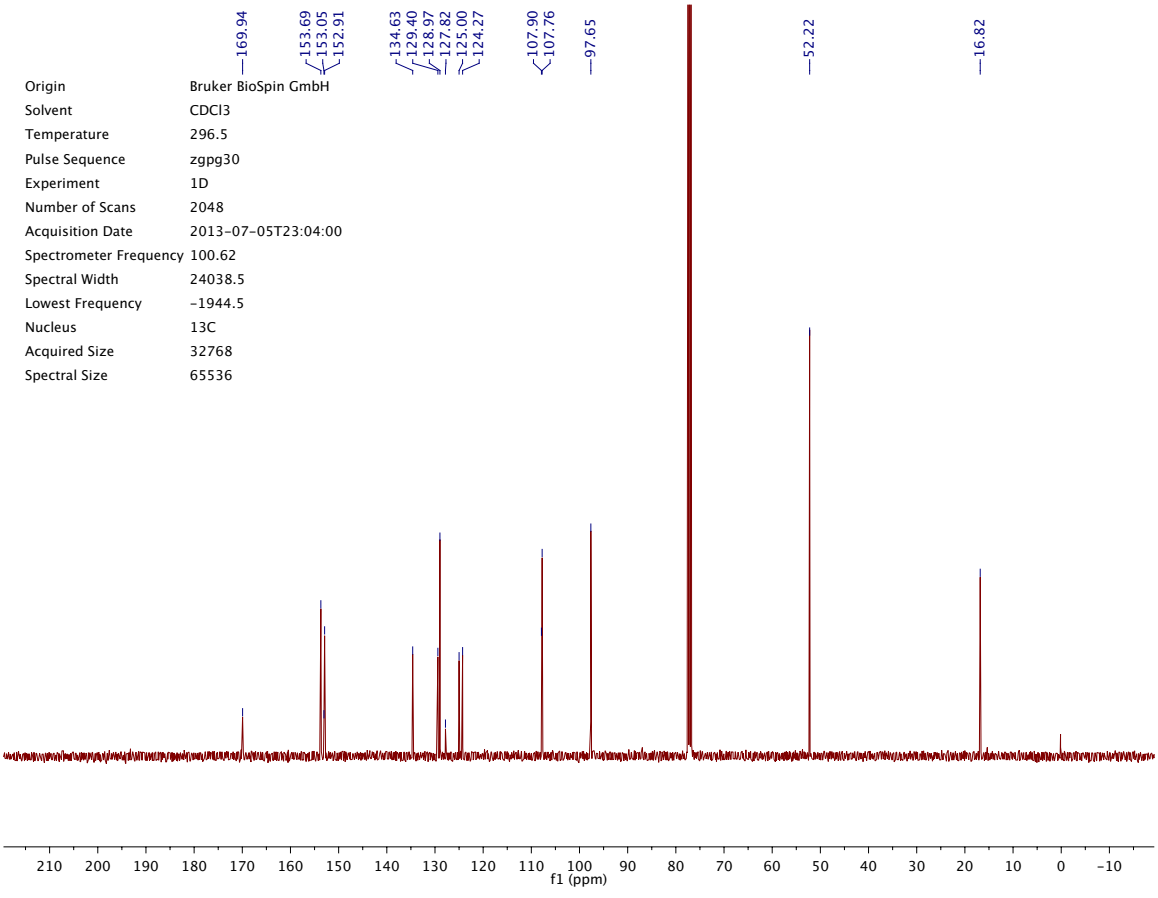

Origin	Bruker BioSpin GmbH
Solvent	CDCl3
Temperature	296.5
Pulse Sequence	zgpg30
Experiment	1D
Number of Scans	2048
Acquisition Date	2013-07-05T23:04:00
Spectrometer Frequency	100.62
Spectral Width	24038.5
Lowest Frequency	-1944.5
Nucleus	13C
Acquired Size	32768
Spectral Size	65536

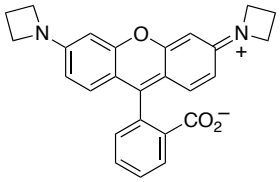
N
O
N
+
CO2−

4

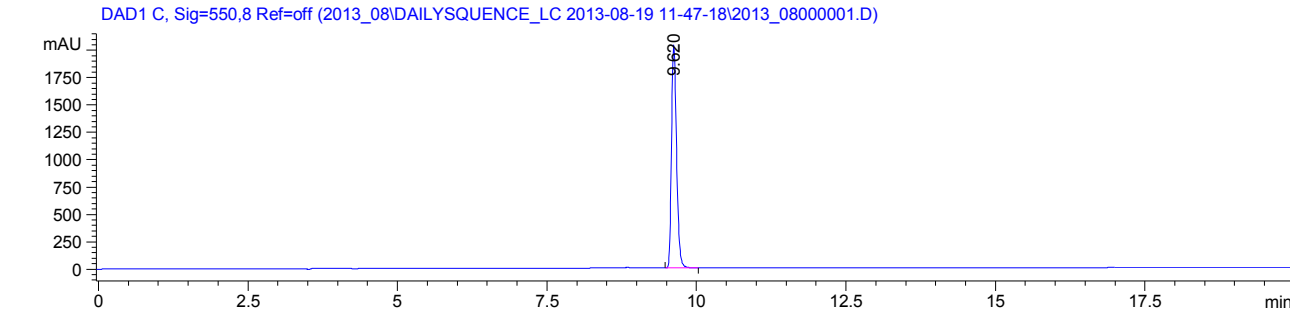
DAD1 C, Sig=550,8 Ref=off (2013_08\DAILYSQUENCE_LC 2013-08-19 11-47-18\2013_08000001.D)
mAU
1750
1500
1250
1000
750
500
250
0
9.620
0
2.5
5
7.5
10
12.5
15
17.5
min

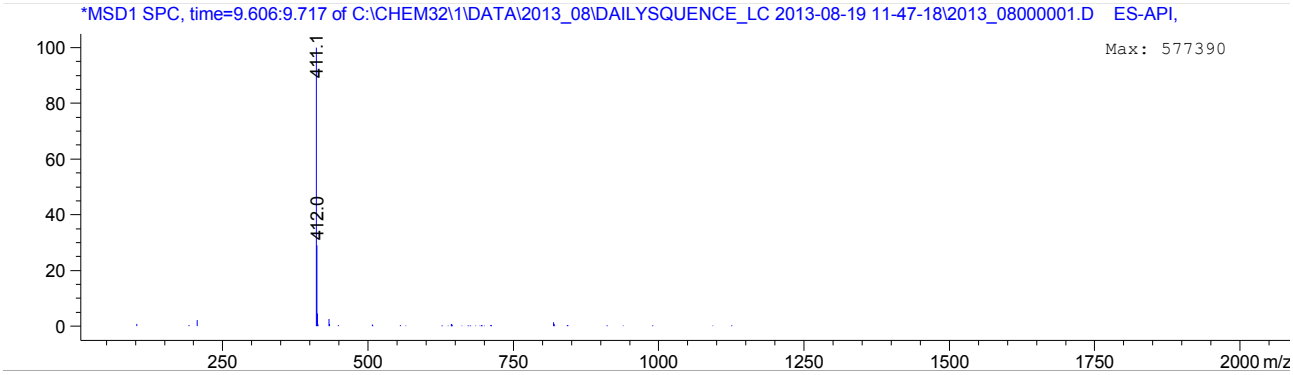
*MSD1 SPC, time=9.606:9.717 of C:\CHEM32\1\DATA\2013_08\DAILYSQUENCE_LC 2013-08-19 11-47-18\2013_08000001.D ES-API,
Max: 577390
100
80
60
40
20
0
411.1
412.0
250
500
750
1000
1250
1500
1750
2000 m/z

Origin	Bruker BioSpin GmbH
Solvent	MeOD
Temperature	300.0
Pulse Sequence	zg30
Experiment	1D
Number of Scans	16
Acquisition Date	2013-07-20T04:05:00
Spectrometer Frequency	400.13
Spectral Width	8223.7
Lowest Frequency	-1644.1
Nucleus	1H
Acquired Size	32768
Spectral Size	65536

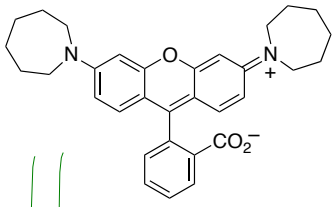

7

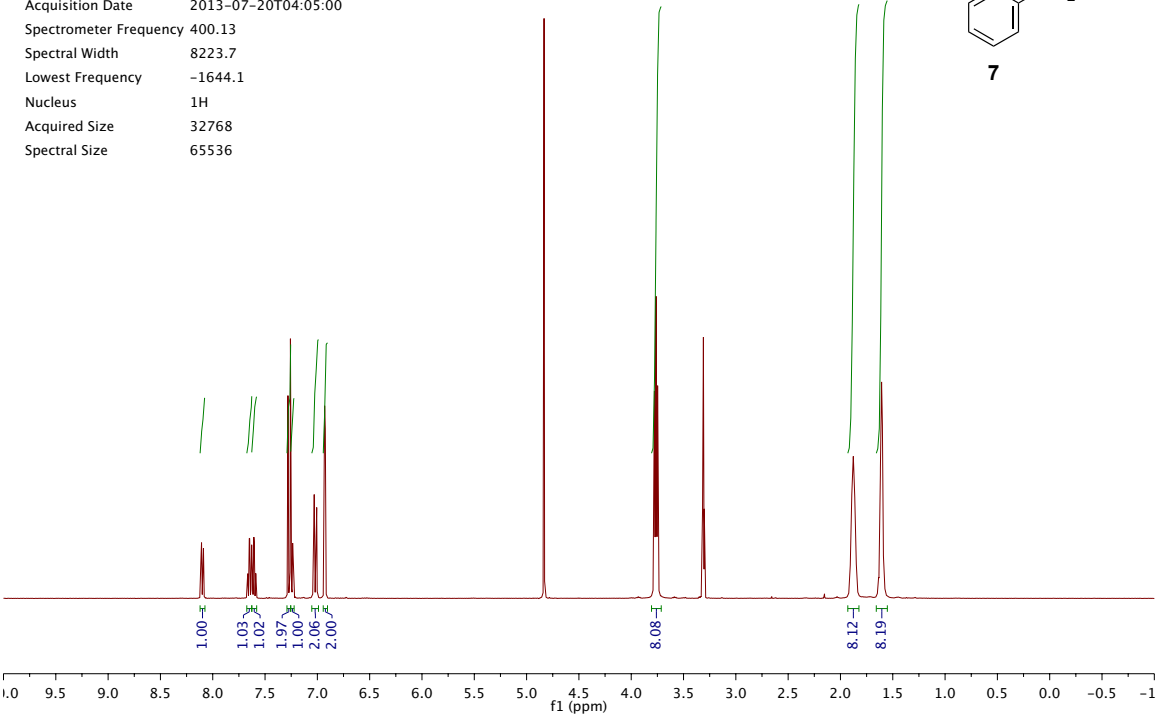

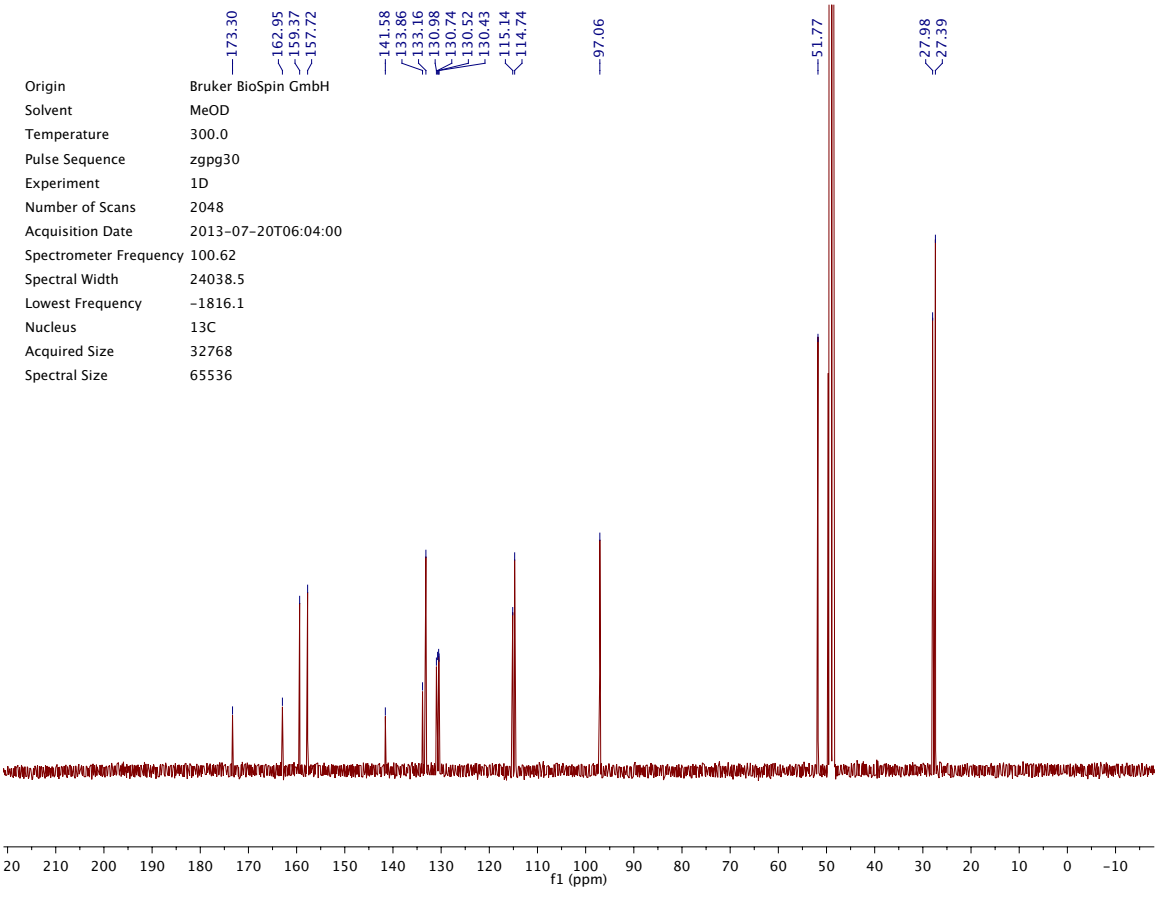

Origin	Bruker BioSpin GmbH
Solvent	MeOD
Temperature	300.0
Pulse Sequence	zgpg30
Experiment	1D
Number of Scans	2048
Acquisition Date	2013-07-20T06:04:00
Spectrometer Frequency	100.62
Spectral Width	24038.5
Lowest Frequency	-1816.1
Nucleus	13C
Acquired Size	32768
Spectral Size	65536

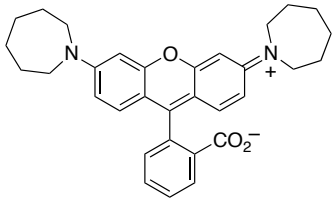
N
O
N
+
CO_2^-

7

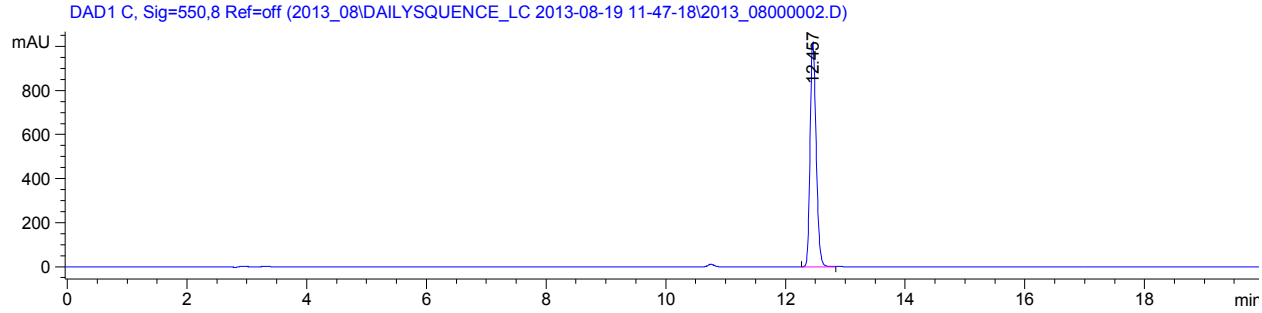
DAD1 C, Sig=550,8 Ref=off (2013_08\DAILYSQUENCE_LC 2013-08-19 11-47-18\2013_08000002.D)
mAU
800
600
400
200
0
12.457
0
2
4
6
8
10
12
14
16
18
mir

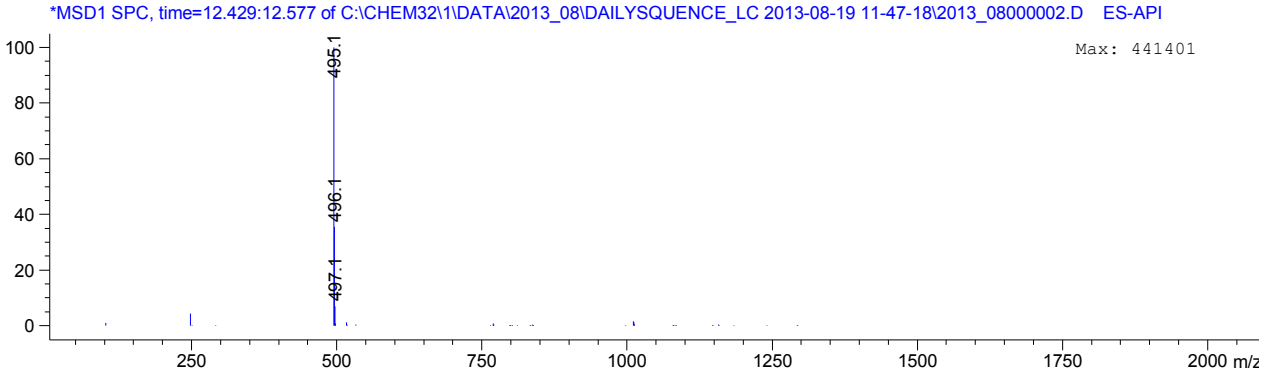
*MSD1 SPC, time=12.429:12.577 of C:\CHEM32\1\DATA\2013_08\DAILYSQUENCE_LC 2013-08-19 11-47-18\2013_08000002.D ES-API
Max: 441401
100
80
60
40
20
0
495.1
496.1
497.1
250
500
750
1000
1250
1500
1750
2000 m/z

Origin	Bruker BioSpin GmbH
Solvent	CDCl3
Temperature	300.0
Pulse Sequence	zg30
Experiment	1D
Number of Scans	16
Acquisition Date	2013-07-26T05:29:00
Spectrometer Frequency	400.13
Spectral Width	8223.7
Lowest Frequency	-1645.4
Nucleus	1H
Acquired Size	32768
Spectral Size	65536

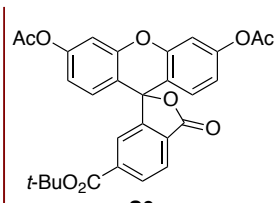

S3

Origin	Bruker BioSpin GmbH
Solvent	CDCl3
Temperature	300.0
Pulse Sequence	zgpg30
Experiment	1D
Number of Scans	2048
Acquisition Date	2013-07-26T07:28:00
Spectrometer Frequency	100.62
Spectral Width	24038.5
Lowest Frequency	-1943.5
Nucleus	13C
Acquired Size	32768
Spectral Size	65536

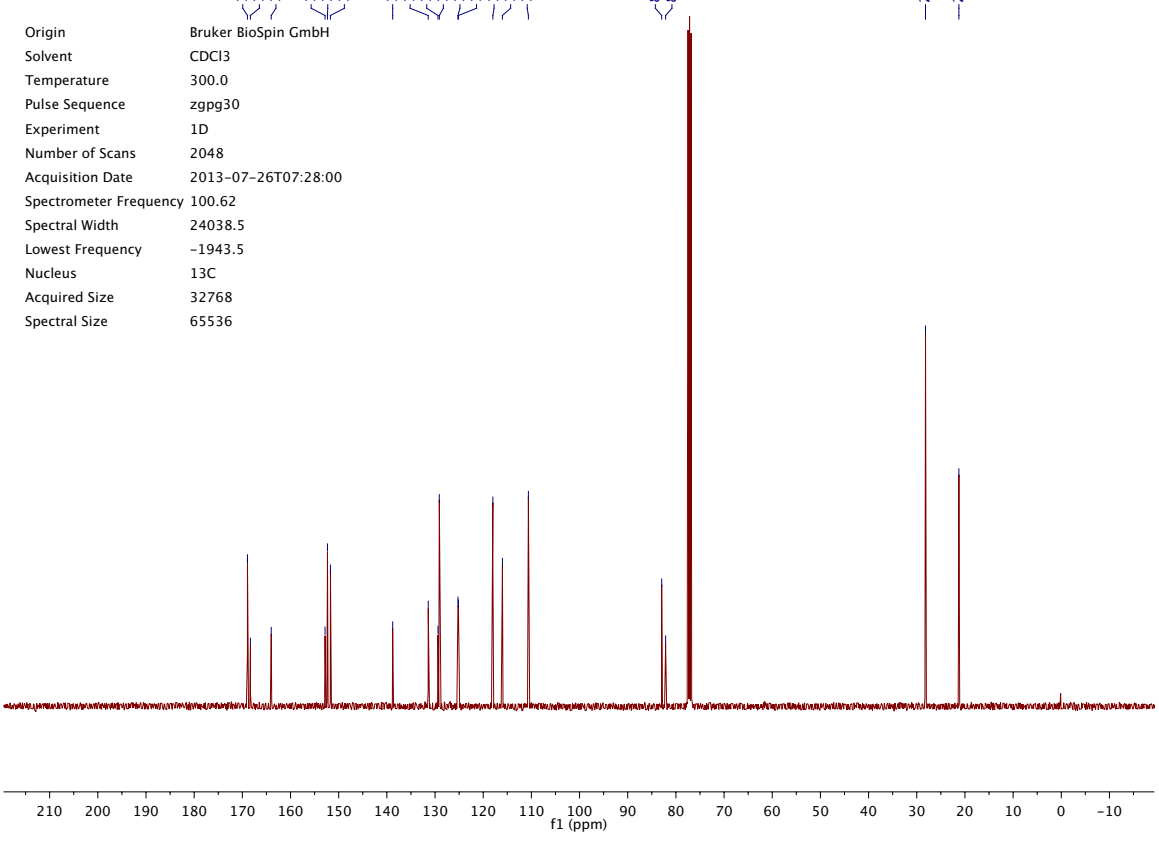

Origin	Bruker BioSpin GmbH
Solvent	CDCl3
Temperature	300.0
Pulse Sequence	zg30
Experiment	1D
Number of Scans	16
Acquisition Date	2013-07-26T21:38:00
Spectrometer Frequency	400.13
Spectral Width	8223.7
Lowest Frequency	-1645.8
Nucleus	1H
Acquired Size	32768
Spectral Size	65536

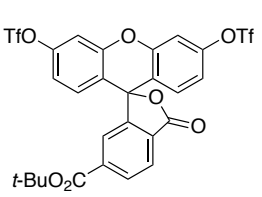

S4

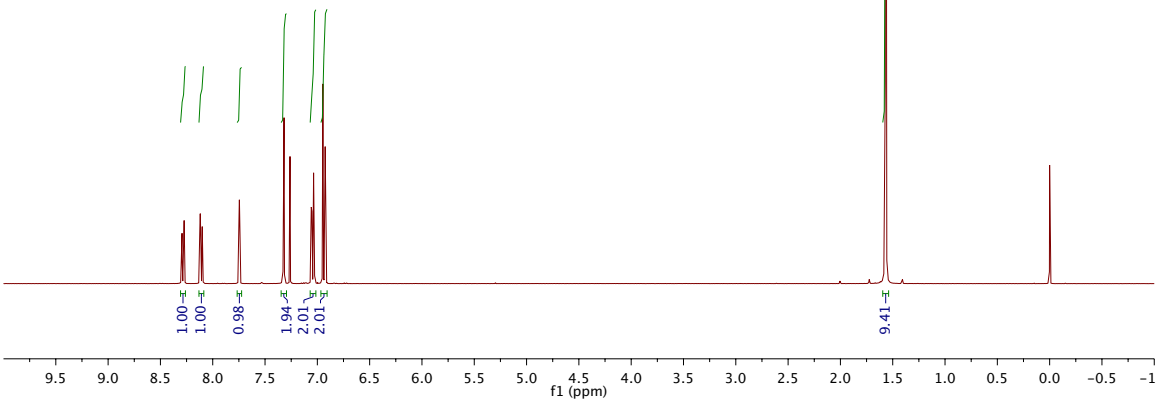

Origin	Bruker BioSpin GmbH
Solvent	CDCl3
Temperature	299.9
Pulse Sequence	zgpg30
Experiment	1D
Number of Scans	2048
Acquisition Date	2013-07-26T23:37:00
Spectrometer Frequency	100.62
Spectral Width	24038.5
Lowest Frequency	-1941.8
Nucleus	13C
Acquired Size	32768
Spectral Size	65536

Origin	Bruker BioSpin GmbH
Solvent	CDCl3
Temperature	300.0
Pulse Sequence	zg30
Experiment	1D
Number of Scans	16
Acquisition Date	2013-07-31T22:43:00
Spectrometer Frequency	400.13
Spectral Width	8223.7
Lowest Frequency	-1646.1
Nucleus	1H
Acquired Size	32768
Spectral Size	65536

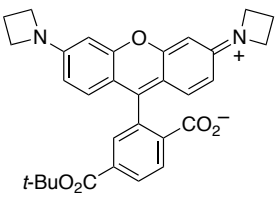

S5

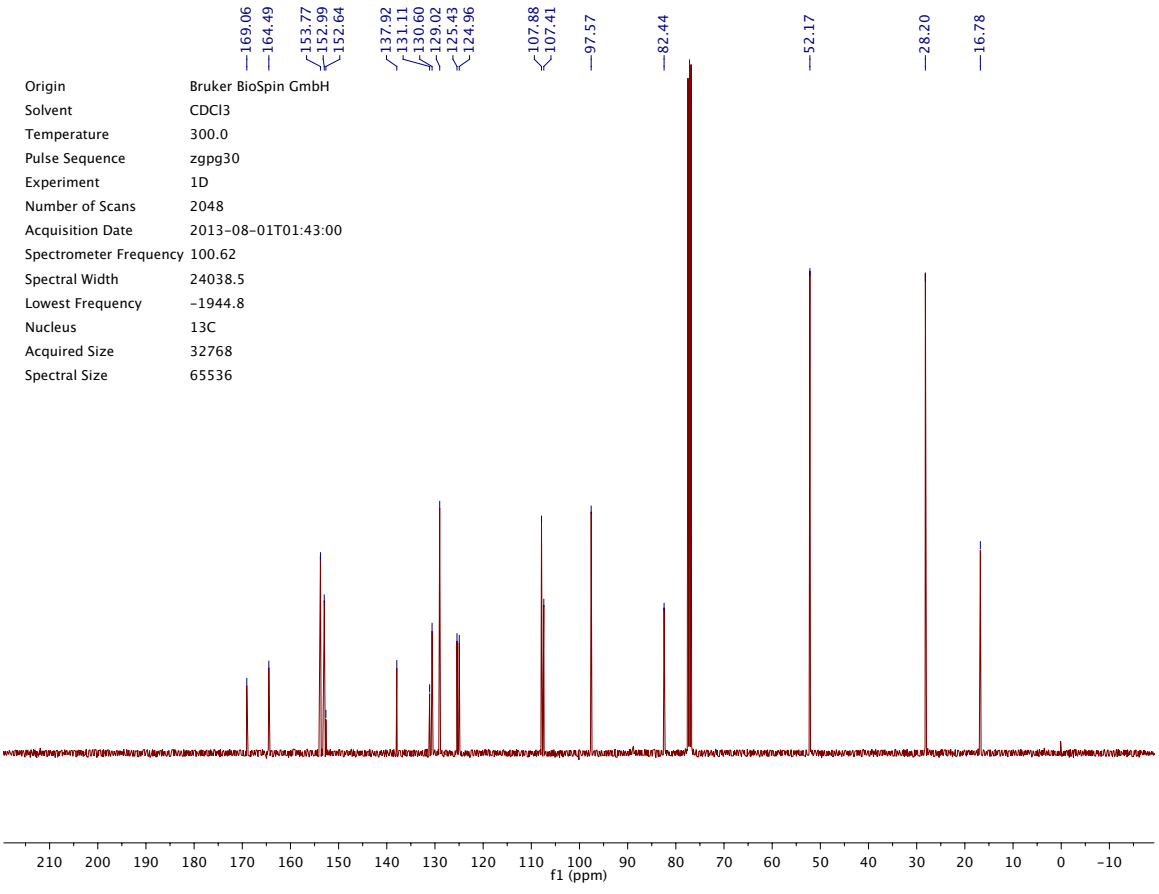

Origin	Bruker BioSpin GmbH
Solvent	CDCl3
Temperature	300.0
Pulse Sequence	zgpg30
Experiment	1D
Number of Scans	2048
Acquisition Date	2013-08-01T01:43:00
Spectrometer Frequency	100.62
Spectral Width	24038.5
Lowest Frequency	-1944.8
Nucleus	13C
Acquired Size	32768
Spectral Size	65536

Origin	Bruker BioSpin GmbH
Solvent	MeOD
Temperature	300.0
Pulse Sequence	zg30
Experiment	1D
Number of Scans	16
Acquisition Date	2013-08-12T09:48:00
Spectrometer Frequency	400.13
Spectral Width	8223.7
Lowest Frequency	-1644.0
Nucleus	1H
Acquired Size	32768
Spectral Size	65536

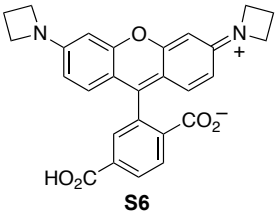

S6

Origin	Bruker BioSpin GmbH
Solvent	MeOD
Temperature	300.0
Pulse Sequence	zgpg30
Experiment	1D
Number of Scans	2048
Acquisition Date	2013-08-08T00:04:00
Spectrometer Frequency	100.62
Spectral Width	24038.5
Lowest Frequency	-1816.5
Nucleus	13C
Acquired Size	32768
Spectral Size	65536

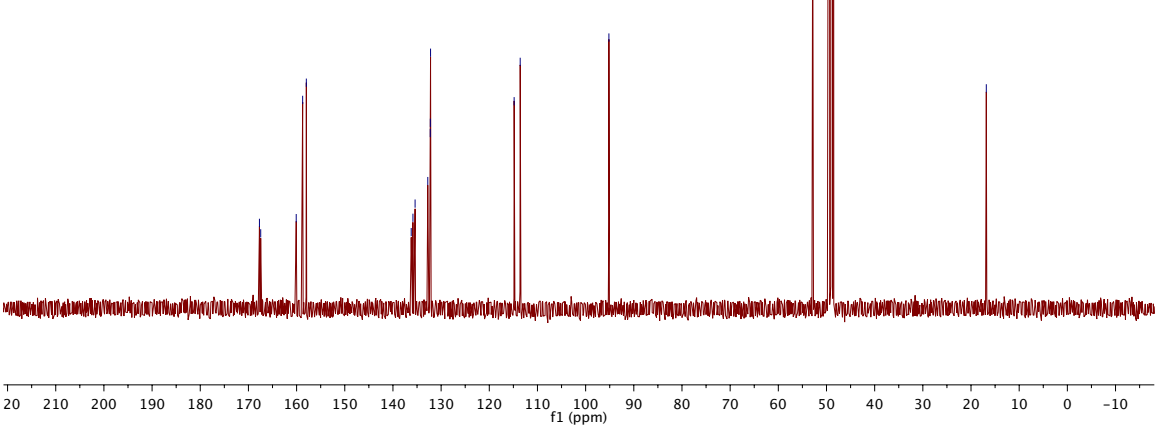

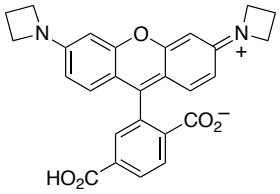
N
O
N
+
CO_2^-
HO_2C

S6

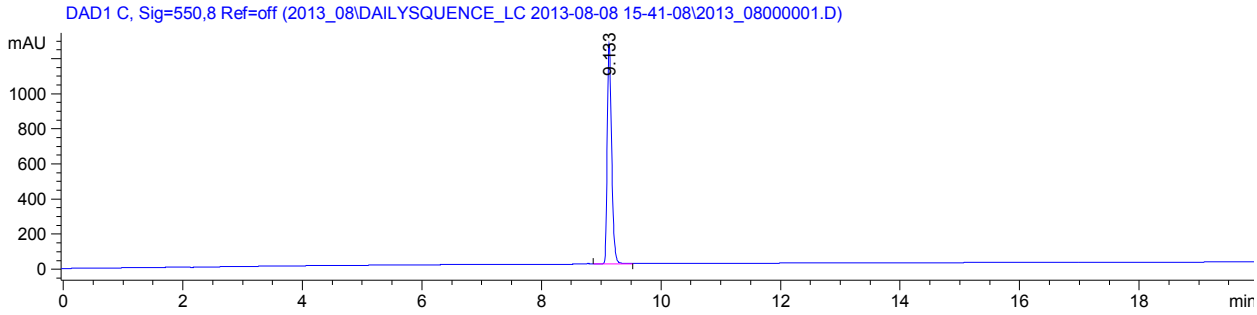
DAD1 C, Sig=550,8 Ref=off (2013_08\DAILYSQUENCE_LC 2013-08-08 15-41-08\2013_08000001.D)
mAU
1000
800
600
400
200
0
9.133
0
2
4
6
8
10
12
14
16
18
min

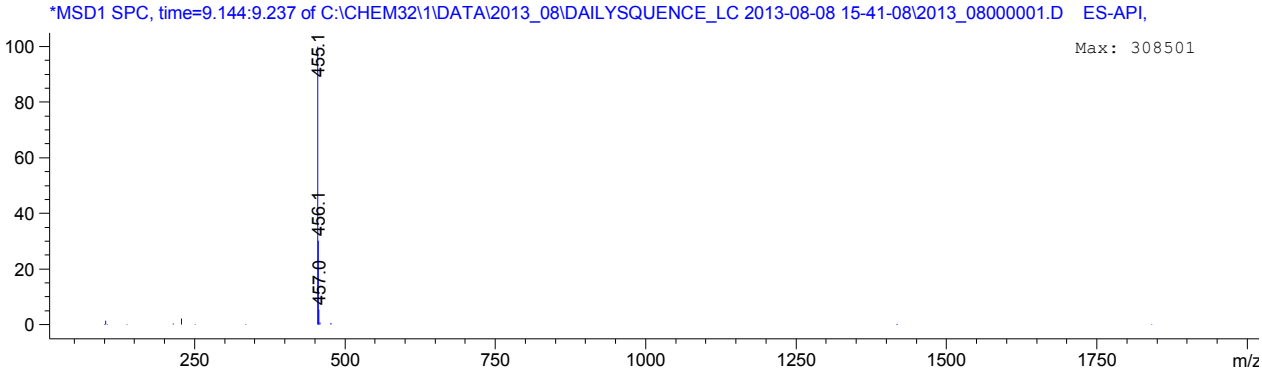
*MSD1 SPC, time=9.144:9.237 of C:\CHEM32\1\DATA\2013_08\DAILYSQUENCE_LC 2013-08-08 15-41-08\2013_08000001.D ES-API,
Max: 308501
100
80
60
40
20
0
455.1
456.1
457.0
250
500
750
1000
1250
1500
1750
m/z

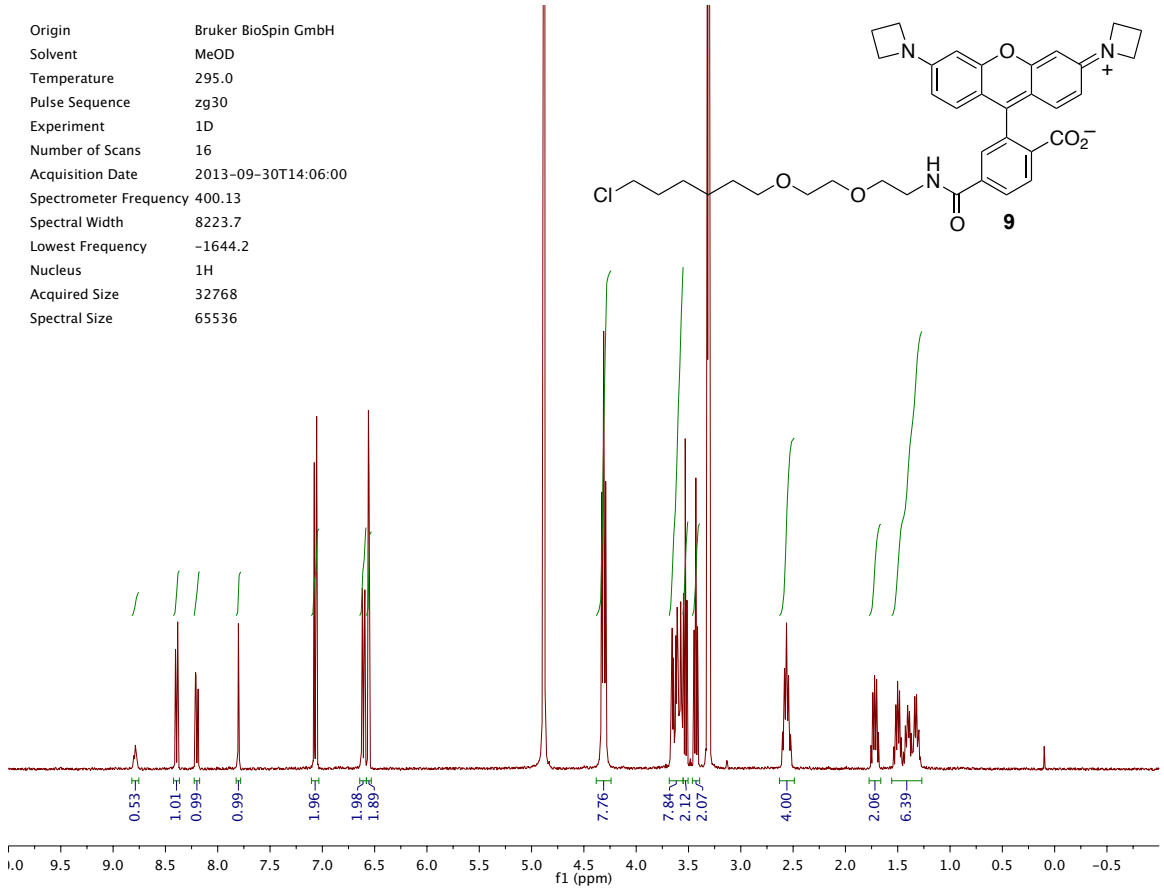
Origin Bruker BioSpin GmbH
Solvent MeOD
Temperature 295.0
Pulse Sequence zg30
Experiment 1D
Number of Scans 16
Acquisition Date 2013-09-30T14:06:00
Spectrometer Frequency 400.13
Spectral Width 8223.7
Lowest Frequency -1644.2
Nucleus 1H
Acquired Size 32768
Spectral Size 65536
Cl
O
O
H
N
O
CO_2^-
N
O
N
+
9
0.53
1.01
0.99
0.99
1.96
1.98
1.89
7.76
7.84
2.12
2.07
4.00
2.06
6.39
f1 (ppm)

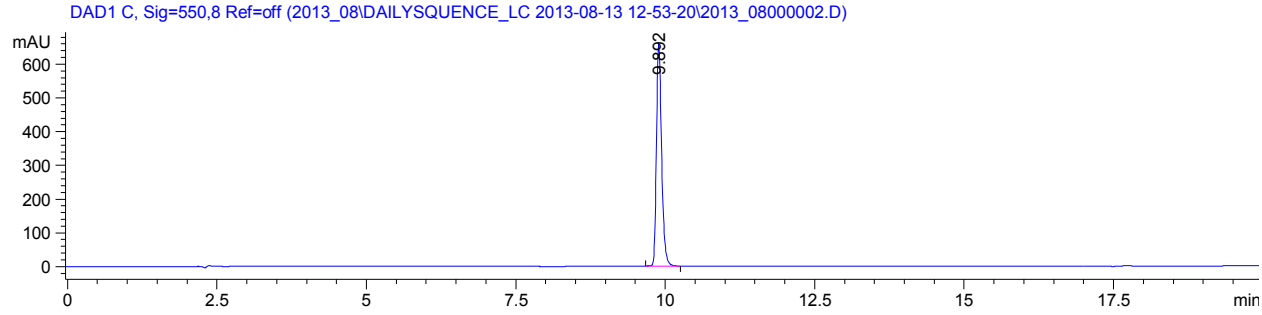
DAD1 C, Sig=550,8 Ref=off (2013_08\DAILYSQUENCE_LC 2013-08-13 12-53-20\2013_08000002.D)
mAU
9.892
min

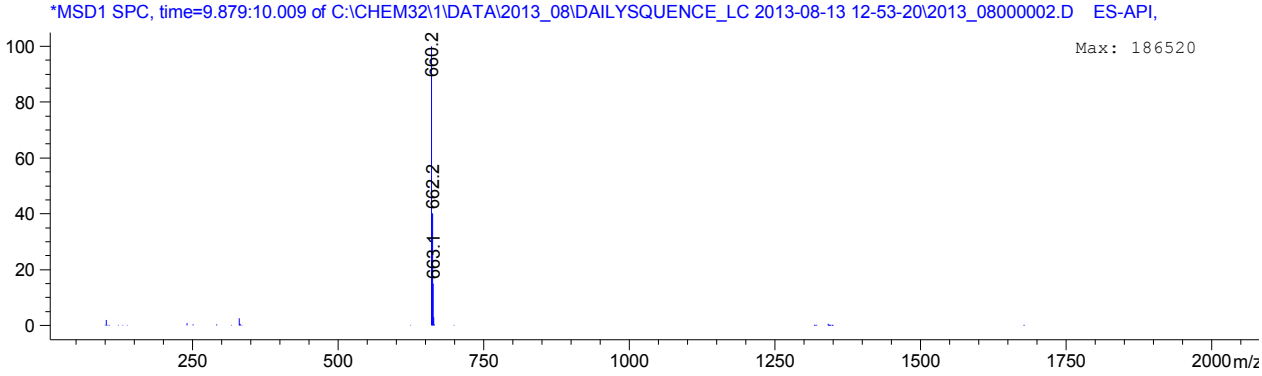
*MSD1 SPC, time=9.879:10.009 of C:\CHEM32\1\DATA\2013_08\DAILYSQUENCE_LC 2013-08-13 12-53-20\2013_08000002.D ES-API,
Max: 186520
660.2
662.2
663.1
m/z

Origin	Bruker BioSpin GmbH
Solvent	MeOD
Temperature	300.0
Pulse Sequence	zg30
Experiment	1D
Number of Scans	16
Acquisition Date	2013-10-28T09:49:00
Spectrometer Frequency	400.13
Spectral Width	8223.7
Lowest Frequency	-1644.0
Nucleus	1H
Acquired Size	32768
Spectral Size	65536

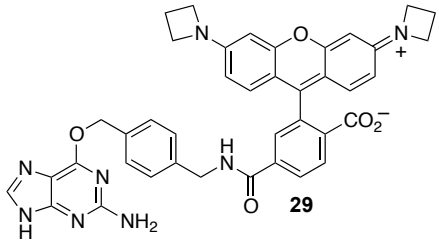

DAD1 C, Sig=550,8 Ref=off (2013_10\DAILYSQUENCE_LC 2013-10-24 14-06-01\2013_10000005.D)

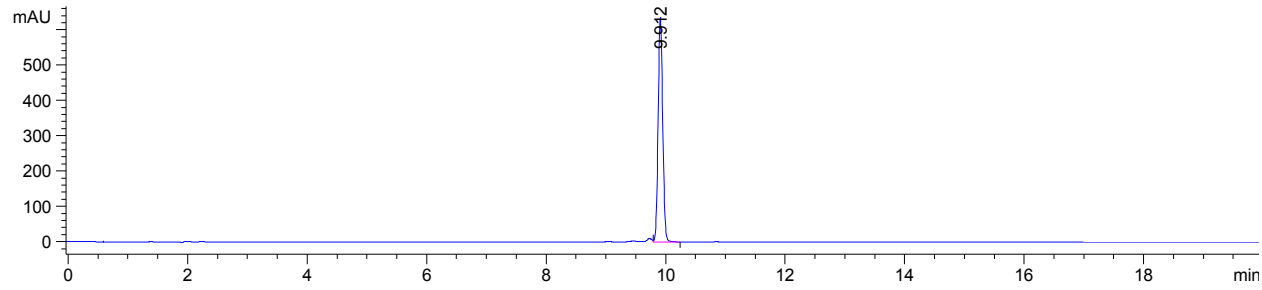

*MSD1 SPC, time=9.898:10.008 of C:\CHEM32\1\DATA\2013_10\DAILYSQUENCE_LC 2013-10-24 14-06-01\2013_10000005.D ES-API,

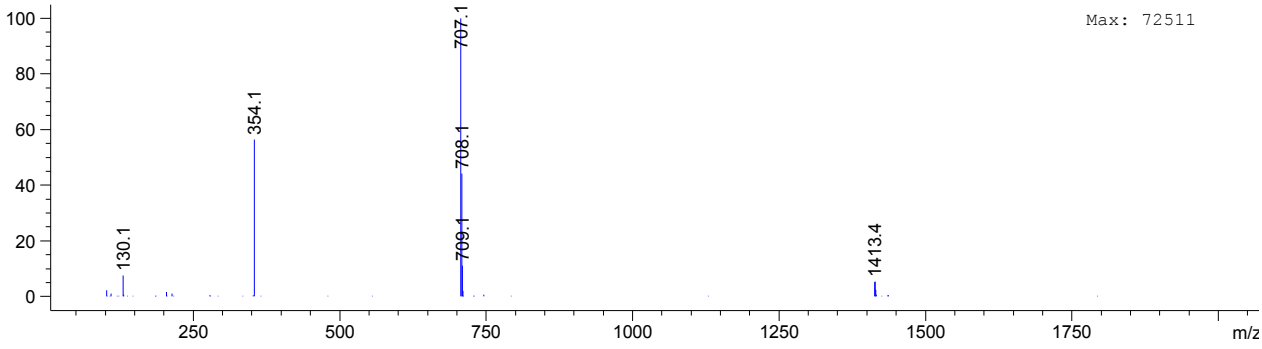

Origin	Bruker BioSpin GmbH
Solvent	CDCl3
Temperature	300.0
Pulse Sequence	zg30
Experiment	1D
Number of Scans	16
Acquisition Date	2011-07-12T09:17:00
Spectrometer Frequency	400.13
Spectral Width	8223.7
Lowest Frequency	-1649.8
Nucleus	1H
Acquired Size	32768
Spectral Size	32768

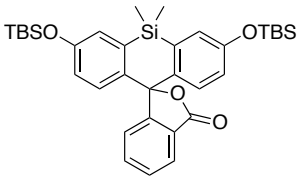

S12

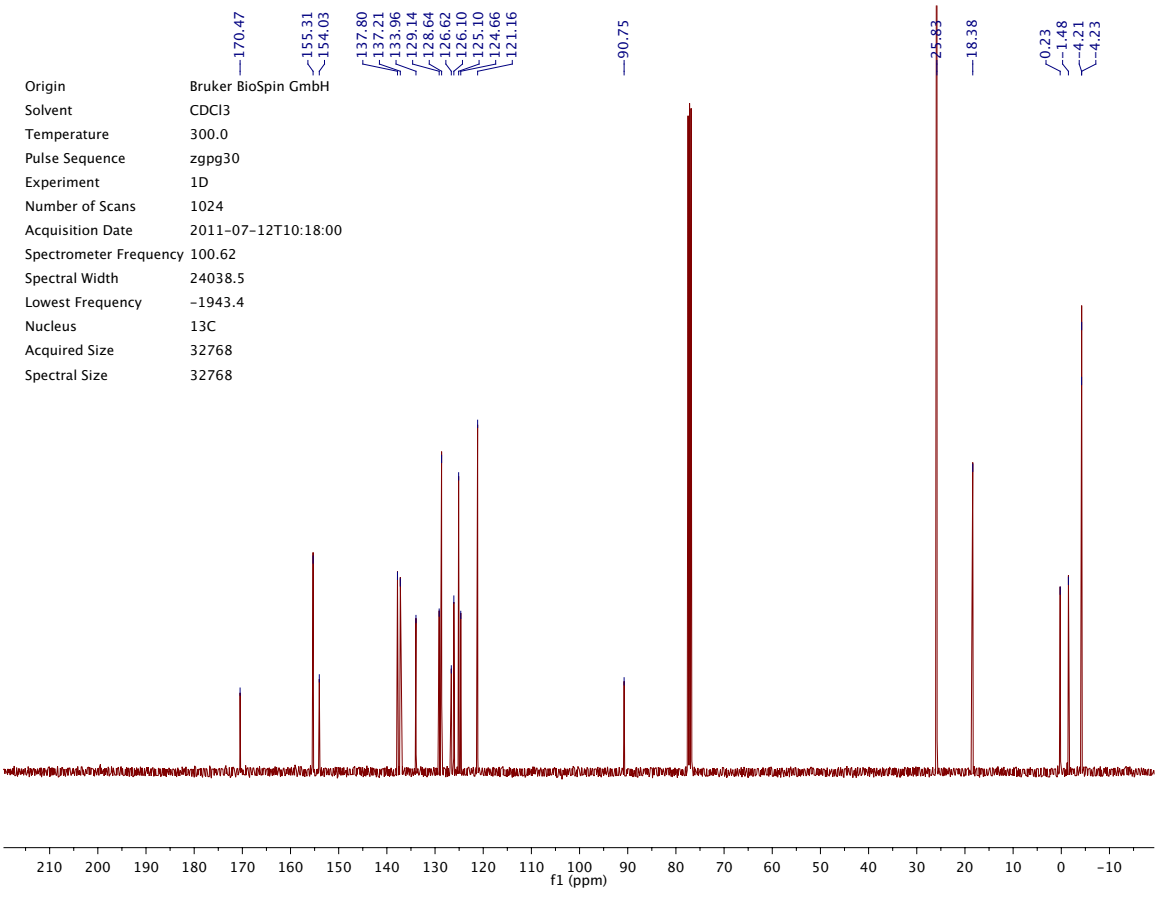

Origin	Bruker BioSpin GmbH
Solvent	CDCl3
Temperature	300.0
Pulse Sequence	zgpg30
Experiment	1D
Number of Scans	1024
Acquisition Date	2011-07-12T10:18:00
Spectrometer Frequency	100.62
Spectral Width	24038.5
Lowest Frequency	-1943.4
Nucleus	13C
Acquired Size	32768
Spectral Size	32768

Origin	Bruker BioSpin GmbH
Solvent	MeOD
Temperature	300.0
Pulse Sequence	zg30
Experiment	1D
Number of Scans	16
Acquisition Date	2011-07-14T09:06:00
Spectrometer Frequency	400.13
Spectral Width	8223.7
Lowest Frequency	-1644.2
Nucleus	1H
Acquired Size	32768
Spectral Size	32768

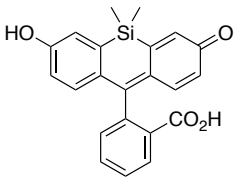

S13

Origin	Bruker BioSpin GmbH
Solvent	MeOD
Temperature	300.0
Pulse Sequence	zgpg30
Experiment	1D
Number of Scans	2048
Acquisition Date	2011-07-12T19:45:00
Spectrometer Frequency	100.62
Spectral Width	24038.5
Lowest Frequency	-1816.5
Nucleus	13C
Acquired Size	32768
Spectral Size	32768

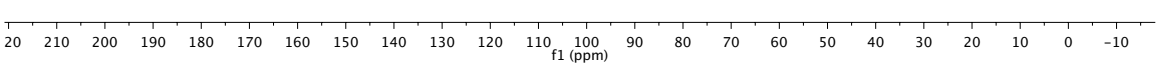

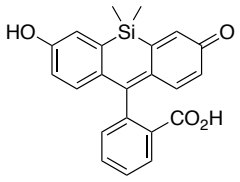
HO
Si
O
CO2H

S13

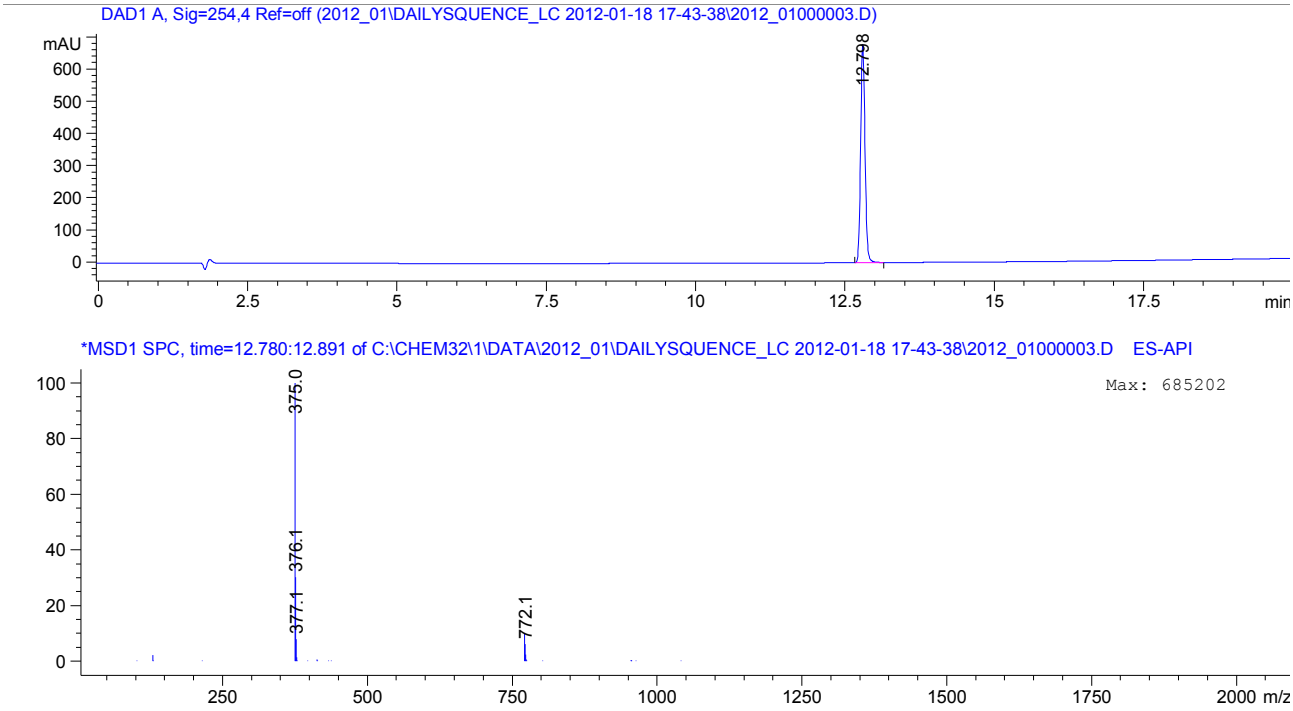
DAD1 A, Sig=254,4 Ref=off (2012_01\DAILYSQUENCE_LC 2012-01-18 17-43-38\2012_01000003.D)
mAU
600
500
400
300
200
100
0
12.798
0
2.5
5
7.5
10
12.5
15
17.5
min

*MSD1 SPC, time=12.780:12.891 of C:\CHEM32\1\DATA\2012_01\DAILYSQUENCE_LC 2012-01-18 17-43-38\2012_01000003.D ES-API
Max: 685202
100
80
60
40
20
0
375.0
376.1
377.1
772.1
250
500
750
1000
1250
1500
1750
2000 m/z

Origin	Bruker BioSpin GmbH
Solvent	CDCl3
Temperature	300.0
Pulse Sequence	zg30
Experiment	1D
Number of Scans	16
Acquisition Date	2011-07-14T12:12:00
Spectrometer Frequency	400.13
Spectral Width	8223.7
Lowest Frequency	-1646.6
Nucleus	1H
Acquired Size	32768
Spectral Size	32768

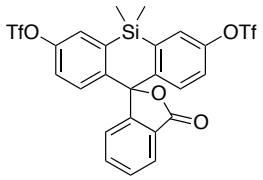

S14

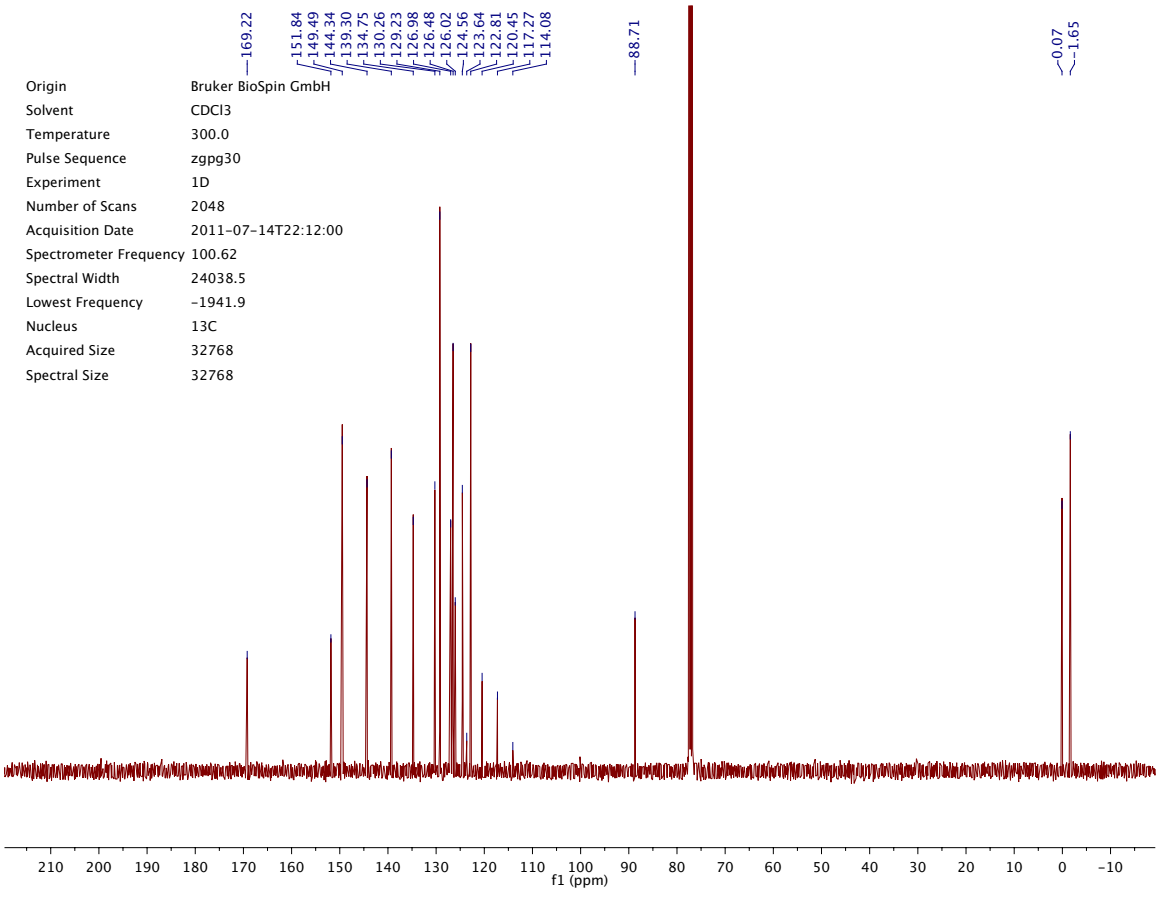

Origin	Bruker BioSpin GmbH
Solvent	CDCl3
Temperature	300.0
Pulse Sequence	zgpg30
Experiment	1D
Number of Scans	2048
Acquisition Date	2011-07-14T22:12:00
Spectrometer Frequency	100.62
Spectral Width	24038.5
Lowest Frequency	-1941.9
Nucleus	13C
Acquired Size	32768
Spectral Size	32768

Origin	Bruker BioSpin GmbH
Solvent	CDCl3
Temperature	300.0
Pulse Sequence	zg30
Experiment	1D
Number of Scans	16
Acquisition Date	2014-06-10T09:08:00
Spectrometer Frequency	400.13
Spectral Width	8223.7
Lowest Frequency	-1647.8
Nucleus	1H
Acquired Size	32768
Spectral Size	65536

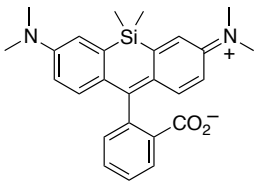

25

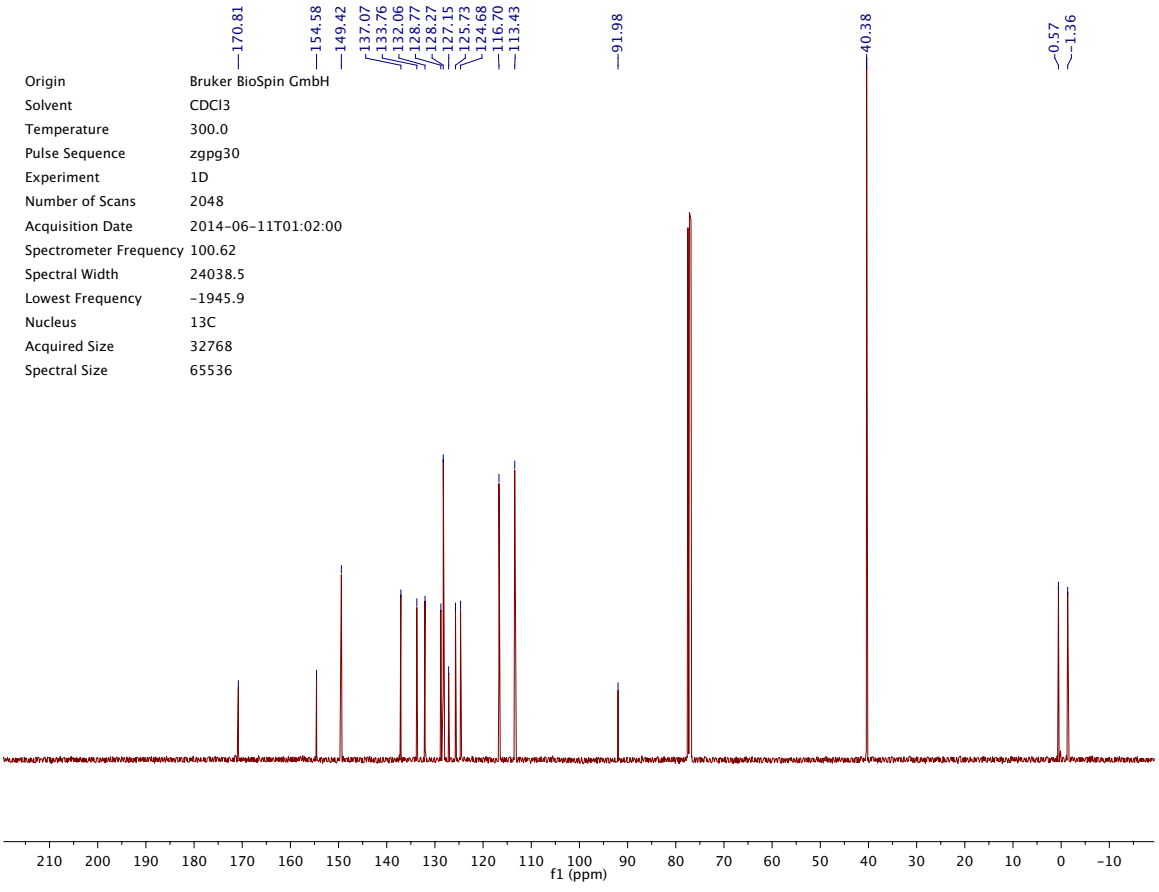

Origin	Bruker BioSpin GmbH
Solvent	CDCl3
Temperature	300.0
Pulse Sequence	zgpg30
Experiment	1D
Number of Scans	2048
Acquisition Date	2014-06-11T01:02:00
Spectrometer Frequency	100.62
Spectral Width	24038.5
Lowest Frequency	-1945.9
Nucleus	13C
Acquired Size	32768
Spectral Size	65536

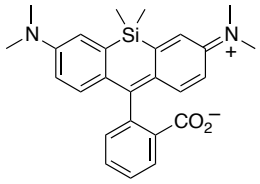
N
Si
N
+
CO_2^-

25

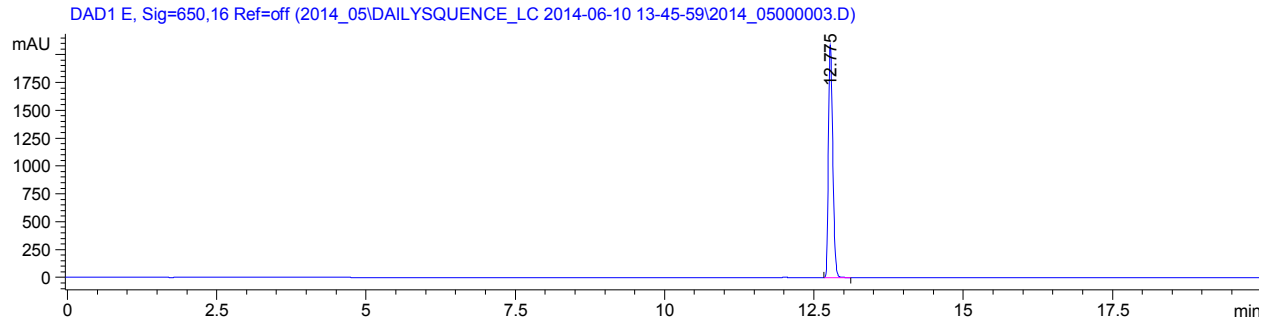
DAD1 E, Sig=650,16 Ref=off (2014_05\DAILYSQUENCE_LC 2014-06-10 13-45-59\2014_05000003.D)
mAU
1750
1500
1250
1000
750
500
250
0
12.775
0
2.5
5
7.5
10
12.5
15
17.5
min

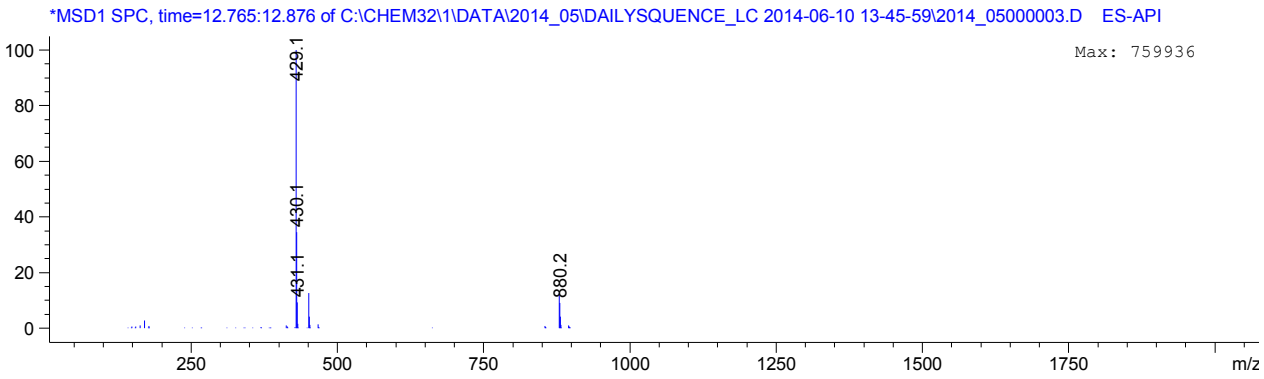
*MSD1 SPC, time=12.765:12.876 of C:\CHEM32\1\DATA\2014_05\DAILYSQUENCE_LC 2014-06-10 13-45-59\2014_05000003.D ES-API
Max: 759936
100
80
60
40
20
0
429.1
430.1
431.1
880.2
250
500
750
1000
1250
1500
1750
m/z

Origin	Bruker BioSpin GmbH
Solvent	CDCl3
Temperature	300.0
Pulse Sequence	zg30
Experiment	1D
Number of Scans	16
Acquisition Date	2013-07-31T11:57:00
Spectrometer Frequency	400.13
Spectral Width	8223.7
Lowest Frequency	-1647.1
Nucleus	1H
Acquired Size	32768
Spectral Size	65536

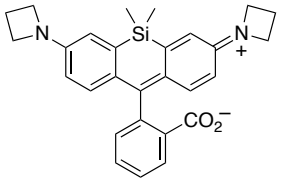

26

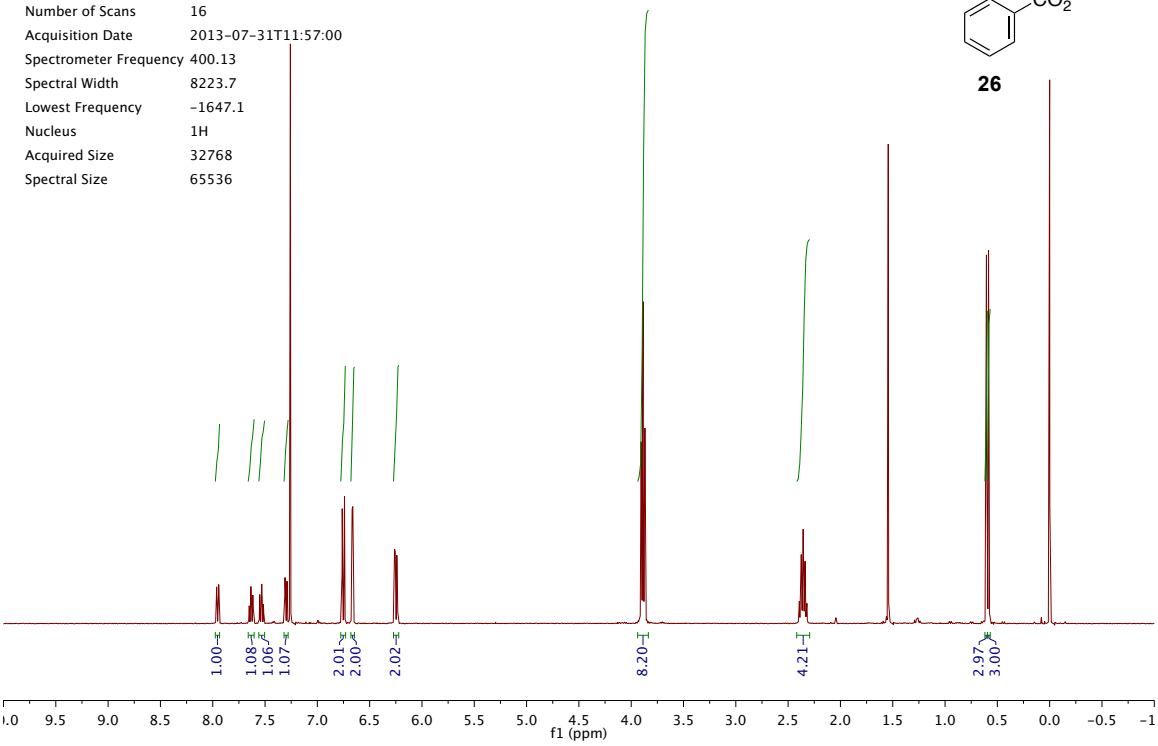

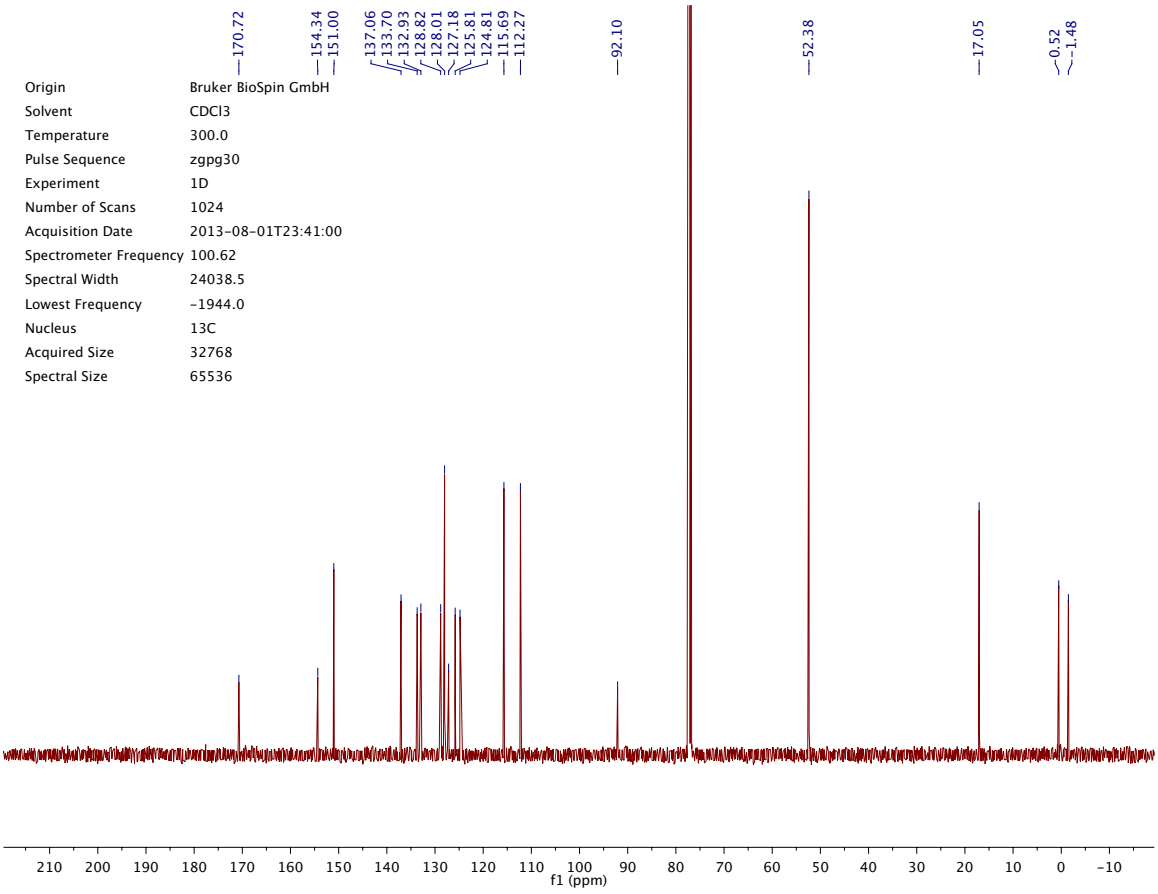

Origin	Bruker BioSpin GmbH
Solvent	CDCl3
Temperature	300.0
Pulse Sequence	zgpg30
Experiment	1D
Number of Scans	1024
Acquisition Date	2013-08-01T23:41:00
Spectrometer Frequency	100.62
Spectral Width	24038.5
Lowest Frequency	-1944.0
Nucleus	13C
Acquired Size	32768
Spectral Size	65536

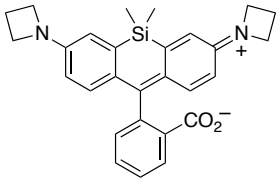
N
Si
N
+
CO2−

26

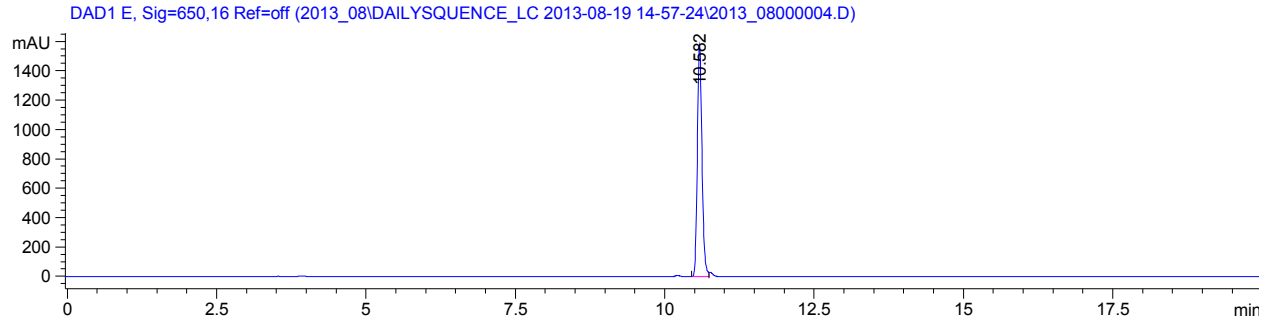
DAD1 E, Sig=650,16 Ref=off (2013_08\DAILYSQUENCE_LC 2013-08-19 14-57-24\2013_08000004.D)
mAU
1400
1200
1000
800
600
400
200
0
10.582
0
2.5
5
7.5
10
12.5
15
17.5
min

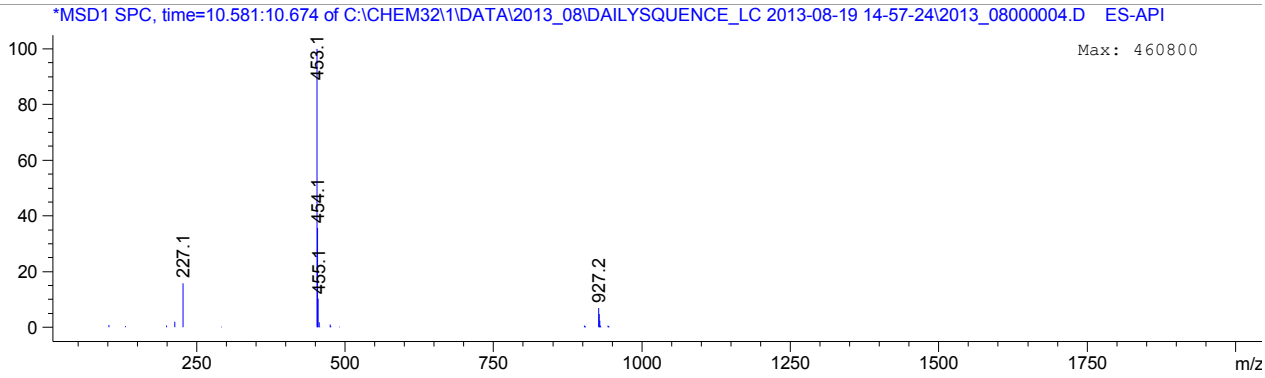
*MSD1 SPC, time=10.581:10.674 of C:\CHEM32\1\DATA\2013_08\DAILYSQUENCE_LC 2013-08-19 14-57-24\2013_08000004.D ES-API
Max: 460800
100
80
60
40
20
0
453.1
454.1
455.1
227.1
927.2
250
500
750
1000
1250
1500
1750
m/z

Origin	Bruker BioSpin GmbH
Solvent	CDCl3
Temperature	297.6
Pulse Sequence	zg30
Experiment	1D
Number of Scans	16
Acquisition Date	2012-04-05T15:50:00
Spectrometer Frequency	400.13
Spectral Width	8223.7
Lowest Frequency	-1645.8
Nucleus	1H
Acquired Size	32768
Spectral Size	65536

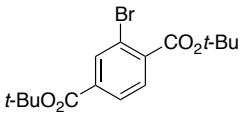

S16

Origin	Bruker BioSpin GmbH
Solvent	CDCl3
Temperature	299.9
Pulse Sequence	zgpg30
Experiment	1D
Number of Scans	1024
Acquisition Date	2013-08-20T23:45:00
Spectrometer Frequency	100.62
Spectral Width	24038.5
Lowest Frequency	-1942.5
Nucleus	13C
Acquired Size	32768
Spectral Size	65536

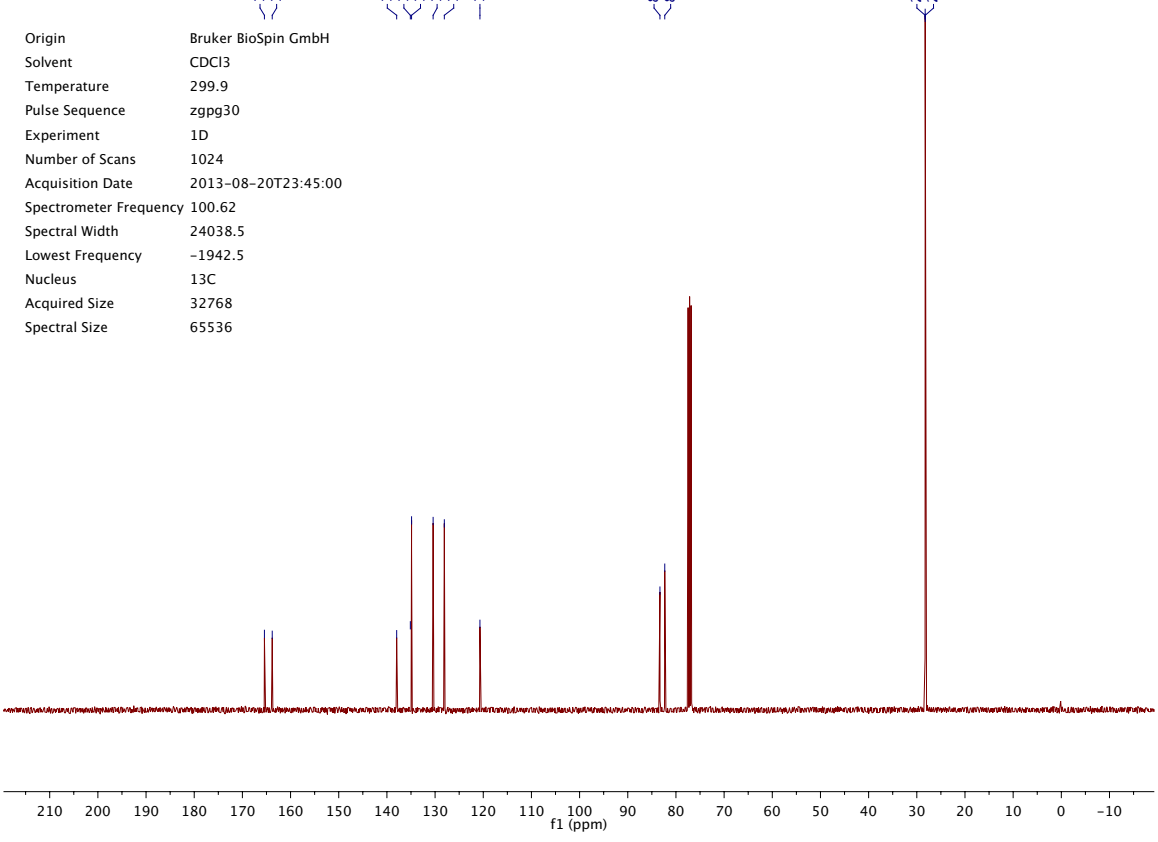

Origin	Bruker BioSpin GmbH
Solvent	CDCl3
Temperature	300.0
Pulse Sequence	zg30
Experiment	1D
Number of Scans	16
Acquisition Date	2013-07-25T21:05:00
Spectrometer Frequency	400.13
Spectral Width	8223.7
Lowest Frequency	-1647.5
Nucleus	1H
Acquired Size	32768
Spectral Size	65536

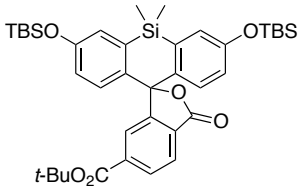

S17

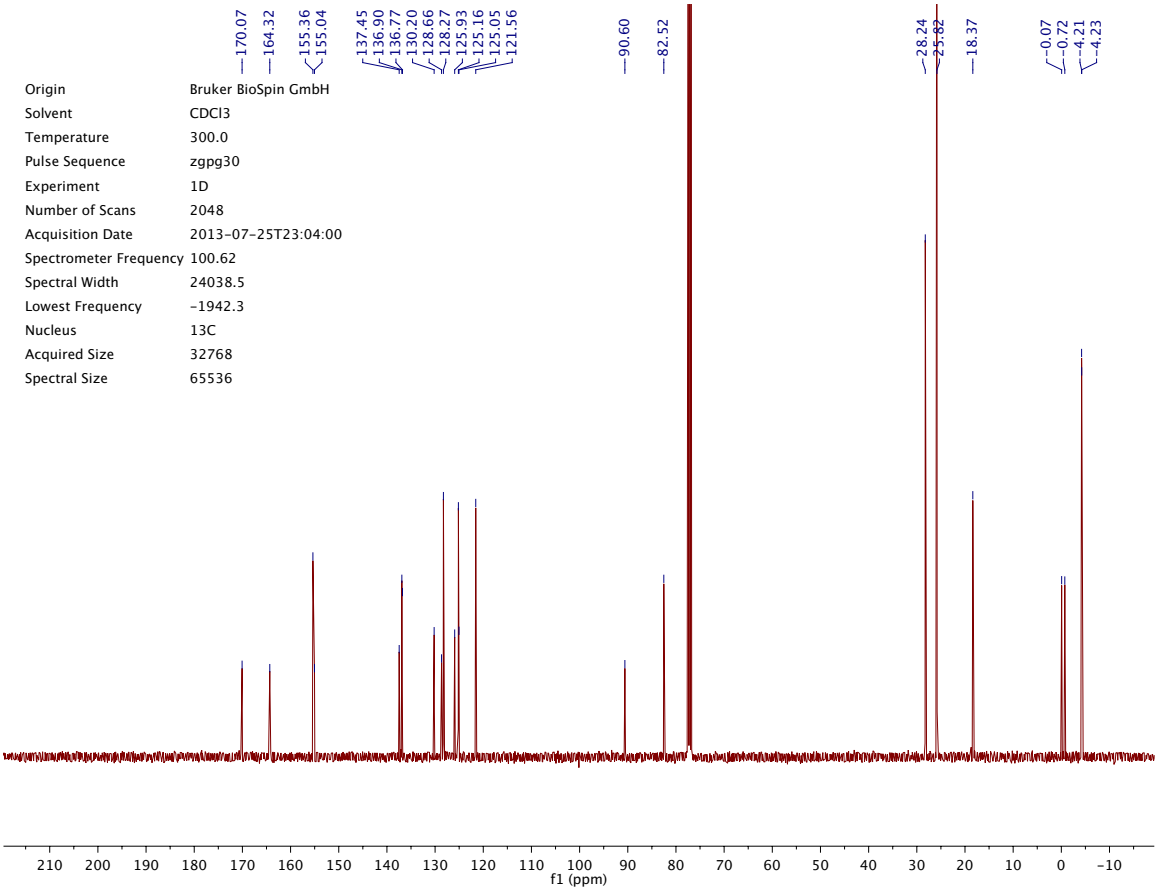

Origin	Bruker BioSpin GmbH
Solvent	CDCl3
Temperature	300.0
Pulse Sequence	zgpg30
Experiment	1D
Number of Scans	2048
Acquisition Date	2013-07-25T23:04:00
Spectrometer Frequency	100.62
Spectral Width	24038.5
Lowest Frequency	-1942.3
Nucleus	13C
Acquired Size	32768
Spectral Size	65536

Origin	Bruker BioSpin GmbH
Solvent	CDCl3
Temperature	300.0
Pulse Sequence	zg30
Experiment	1D
Number of Scans	16
Acquisition Date	2013-08-06T00:40:00
Spectrometer Frequency	400.13
Spectral Width	8223.7
Lowest Frequency	-1646.2
Nucleus	1H
Acquired Size	32768
Spectral Size	65536

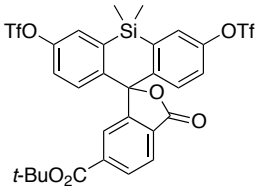

S18

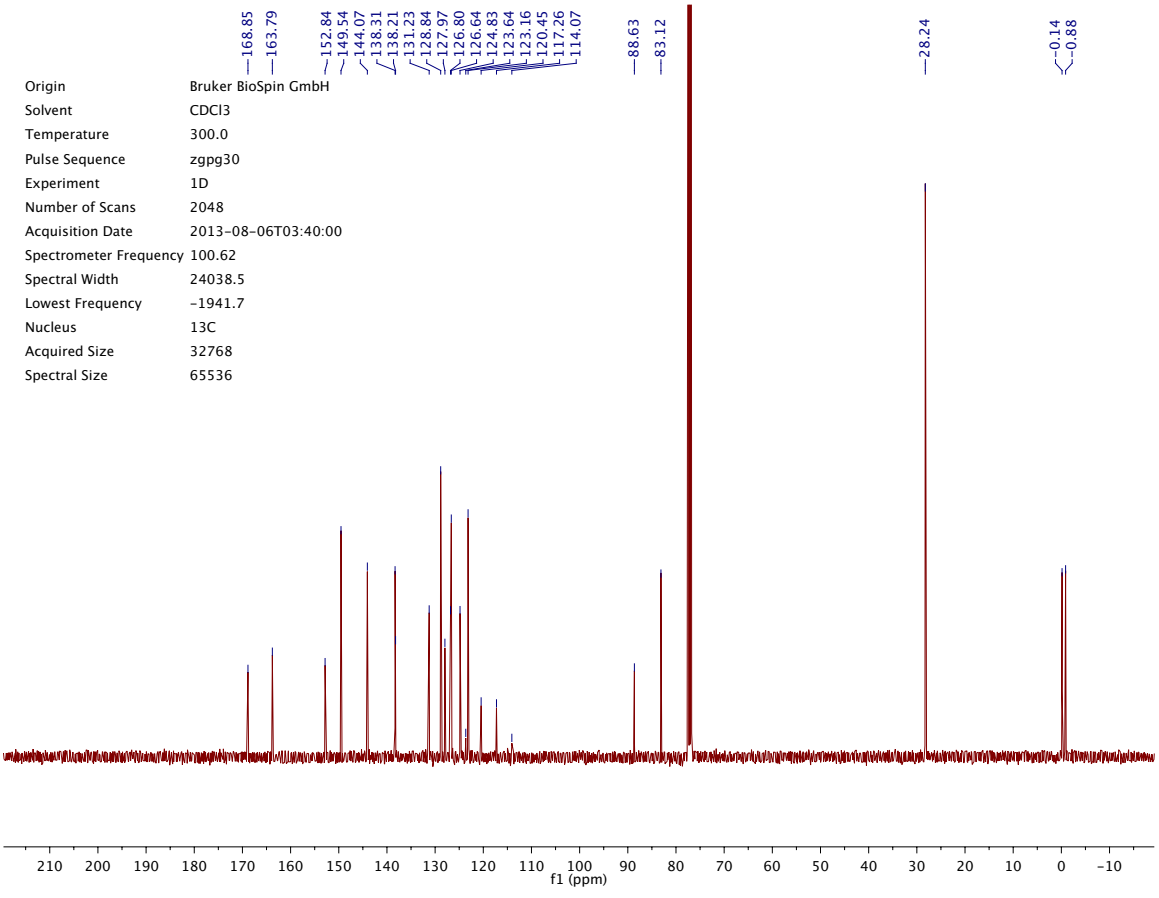

Origin	Bruker BioSpin GmbH
Solvent	CDCl3
Temperature	300.0
Pulse Sequence	zgpg30
Experiment	1D
Number of Scans	2048
Acquisition Date	2013-08-06T03:40:00
Spectrometer Frequency	100.62
Spectral Width	24038.5
Lowest Frequency	-1941.7
Nucleus	13C
Acquired Size	32768
Spectral Size	65536

Origin	Bruker BioSpin GmbH
Solvent	CDCl3
Temperature	300.0
Pulse Sequence	zg30
Experiment	1D
Number of Scans	16
Acquisition Date	2013-08-01T10:19:00
Spectrometer Frequency	400.13
Spectral Width	8223.7
Lowest Frequency	-1647.1
Nucleus	1H
Acquired Size	32768
Spectral Size	65536

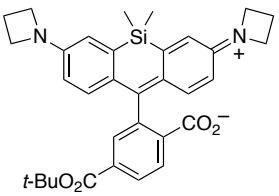

S19

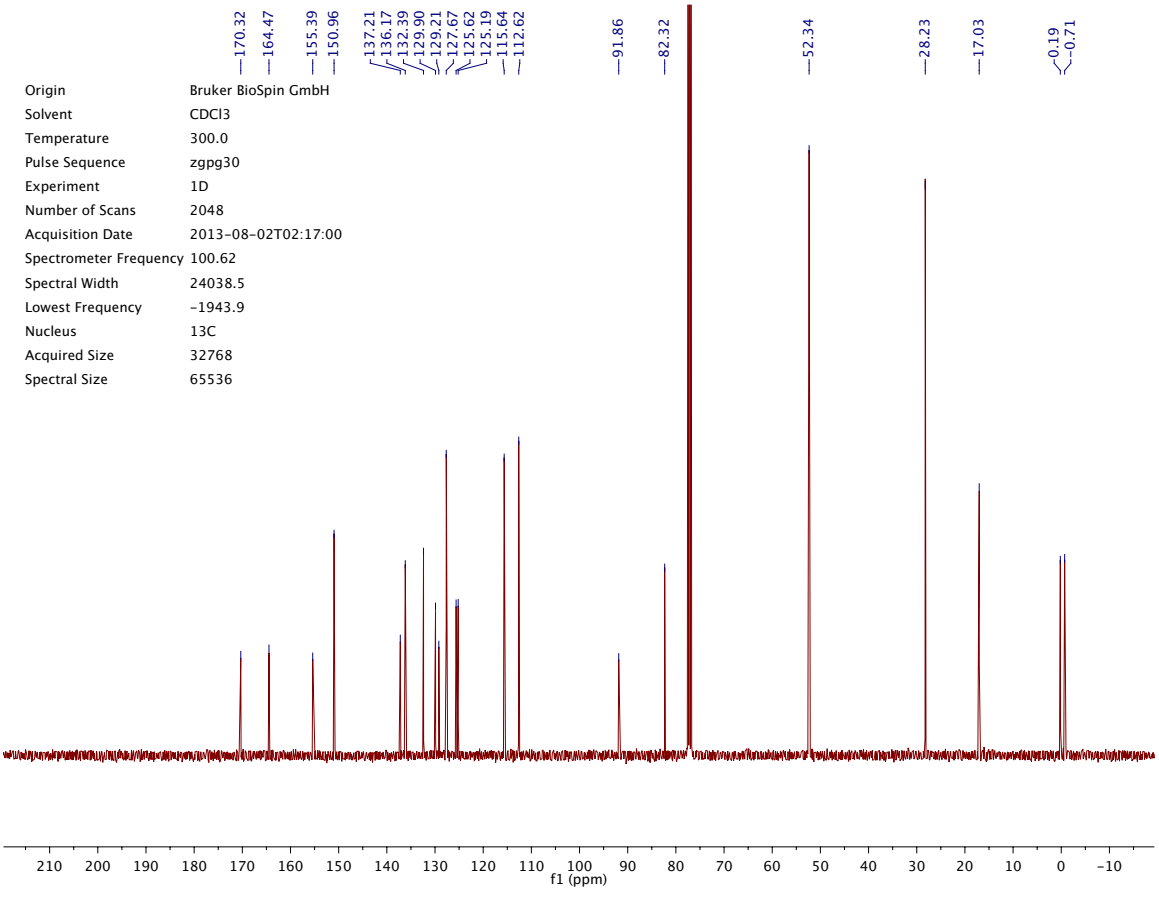

Origin	Bruker BioSpin GmbH
Solvent	CDCl3
Temperature	300.0
Pulse Sequence	zgpg30
Experiment	1D
Number of Scans	2048
Acquisition Date	2013-08-02T02:17:00
Spectrometer Frequency	100.62
Spectral Width	24038.5
Lowest Frequency	-1943.9
Nucleus	13C
Acquired Size	32768
Spectral Size	65536

Origin	Bruker BioSpin GmbH
Solvent	CDCl3
Temperature	300.0
Pulse Sequence	zg30
Experiment	1D
Number of Scans	16
Acquisition Date	2014-06-11T09:28:00
Spectrometer Frequency	400.13
Spectral Width	8223.7
Lowest Frequency	-1647.3
Nucleus	1H
Acquired Size	32768
Spectral Size	65536

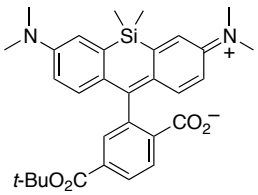

S20

Origin	Bruker BioSpin GmbH
Solvent	CDCl3
Temperature	300.0
Pulse Sequence	zgpg30
Experiment	1D
Number of Scans	2048
Acquisition Date	2014-06-12T01:33:00
Spectrometer Frequency	100.62
Spectral Width	24038.5
Lowest Frequency	-1944.3
Nucleus	13C
Acquired Size	32768
Spectral Size	65536

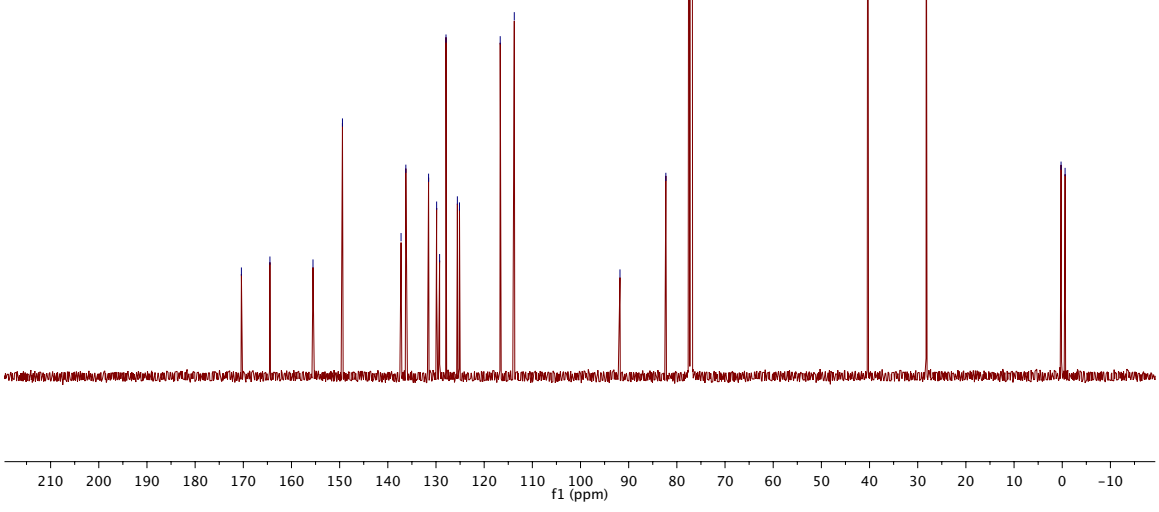

Origin	Bruker BioSpin GmbH
Solvent	MeOD
Temperature	300.0
Pulse Sequence	zg30
Experiment	1D
Number of Scans	16
Acquisition Date	2013-08-14T14:05:00
Spectrometer Frequency	400.13
Spectral Width	8223.7
Lowest Frequency	-1644.2
Nucleus	1H
Acquired Size	32768
Spectral Size	65536

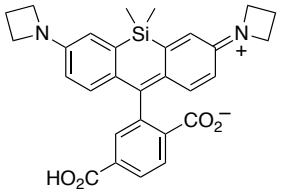

S21

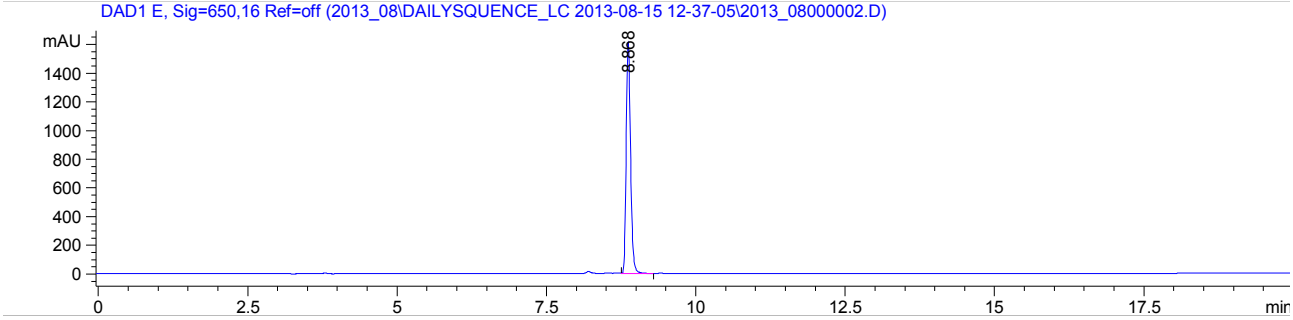

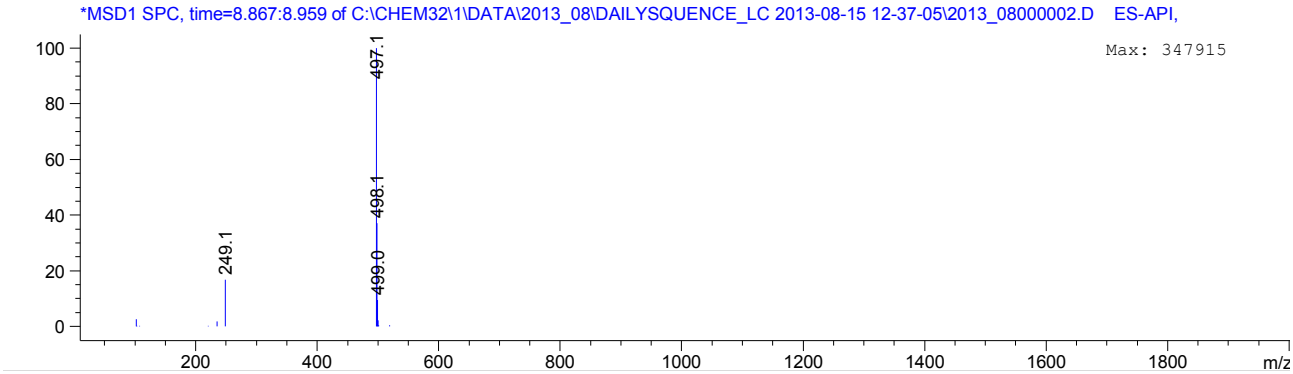

Origin	Bruker BioSpin GmbH
Solvent	CDCl3
Temperature	300.0
Pulse Sequence	zg30
Experiment	1D
Number of Scans	16
Acquisition Date	2014-01-28T09:26:00
Spectrometer Frequency	400.13
Spectral Width	8223.7
Lowest Frequency	-1646.6
Nucleus	1H
Acquired Size	32768
Spectral Size	65536

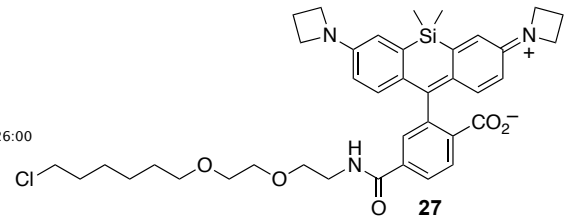

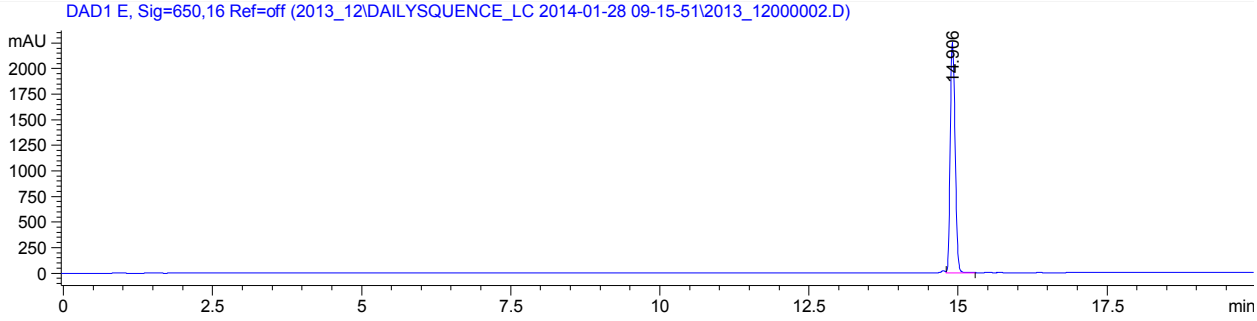

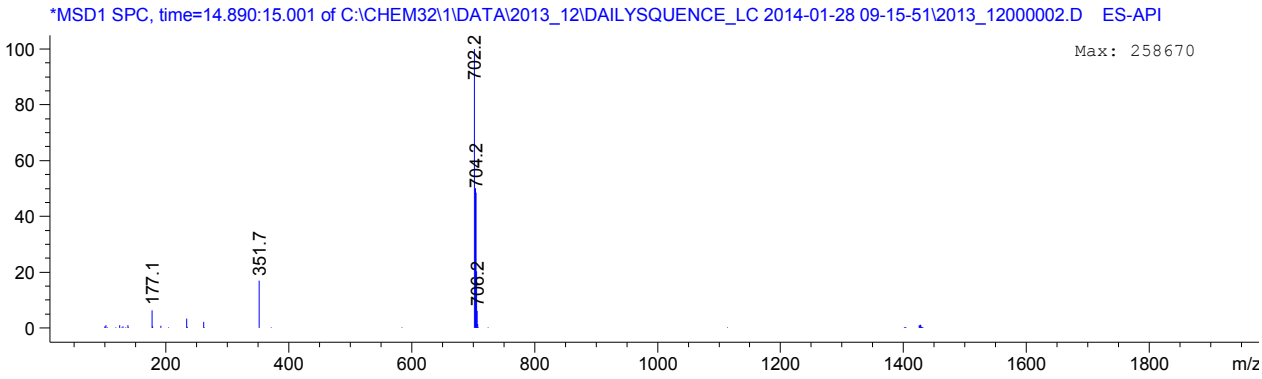

Origin	Bruker BioSpin GmbH
Solvent	DMSO
Temperature	300.0
Pulse Sequence	zg30
Experiment	1D
Number of Scans	16
Acquisition Date	2014-07-22T15:44:00
Spectrometer Frequency	400.13
Spectral Width	8223.7
Lowest Frequency	-1638.3
Nucleus	1H
Acquired Size	32768
Spectral Size	65536

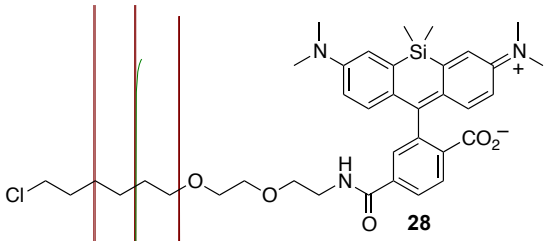

28

DAD1 E, Sig=650,16 Ref=off (2014_06\DAILYSQUENCE_LC 2014-06-17 15-33-18\2014_06000008.D)

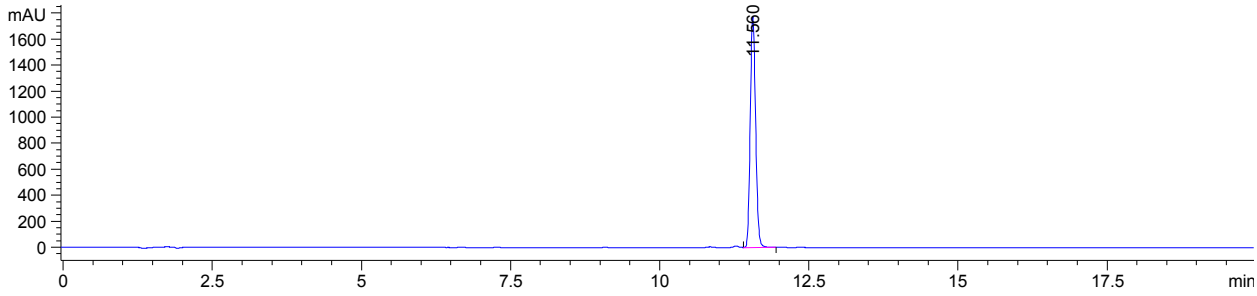

*MSD1 SPC, time=11.528:11.657 of C:\CHEM32\1\DATA\2014_06\DAILYSQUENCE_LC 2014-06-17 15-33-18\2014_06000008.D ES-API

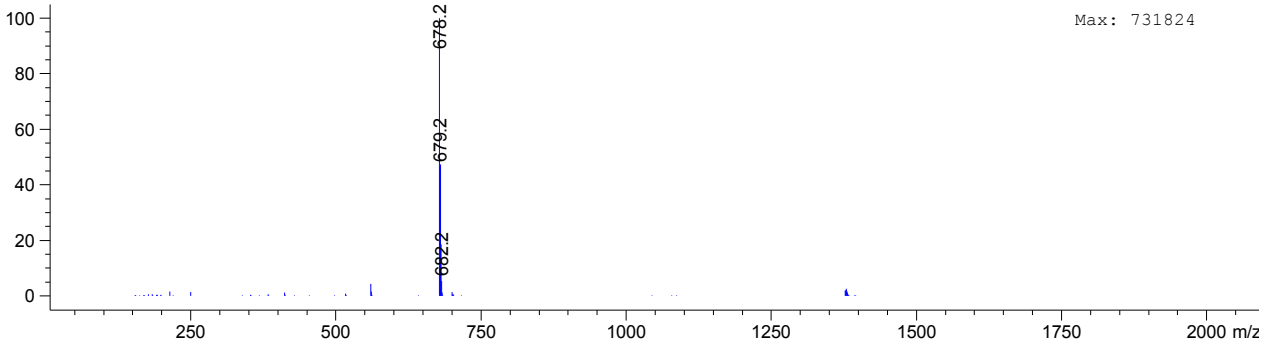

Origin	Bruker BioSpin GmbH
Solvent	CDCl3
Temperature	300.0
Pulse Sequence	zg30
Experiment	1D
Number of Scans	16
Acquisition Date	2014-07-09T15:25:00
Spectrometer Frequency	400.13
Spectral Width	8223.7
Lowest Frequency	-1646.0
Nucleus	1H
Acquired Size	32768
Spectral Size	65536

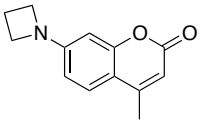

12

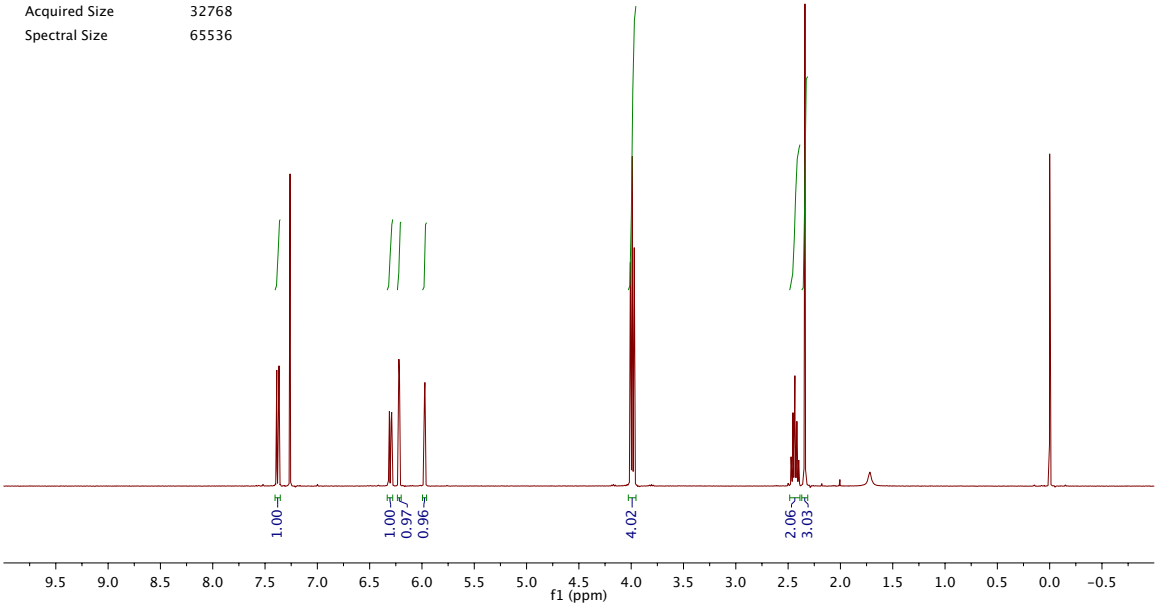

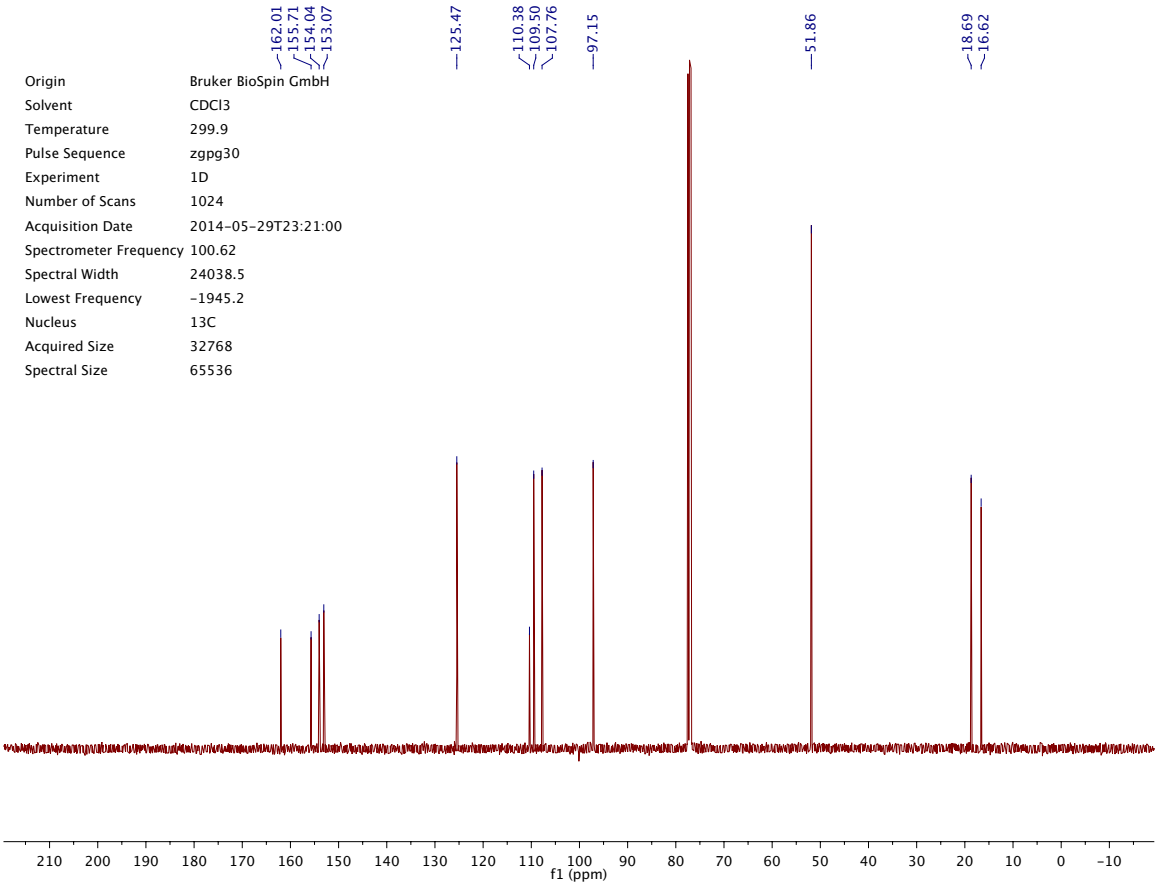

Origin	Bruker BioSpin GmbH
Solvent	CDCl3
Temperature	299.9
Pulse Sequence	zgpg30
Experiment	1D
Number of Scans	1024
Acquisition Date	2014-05-29T23:21:00
Spectrometer Frequency	100.62
Spectral Width	24038.5
Lowest Frequency	-1945.2
Nucleus	13C
Acquired Size	32768
Spectral Size	65536

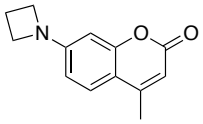

12

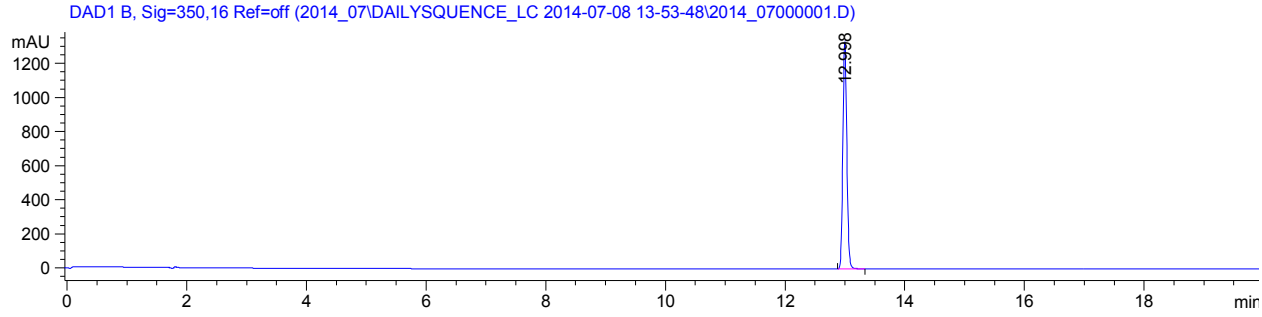
DAD1 B, Sig=350,16 Ref=off (2014_07\DAILYSQUENCE_LC 2014-07-08 13-53-48\2014_07000001.D)
mAU
1200
1000
800
600
400
200
0
12.998
0
2
4
6
8
10
12
14
16
18
min

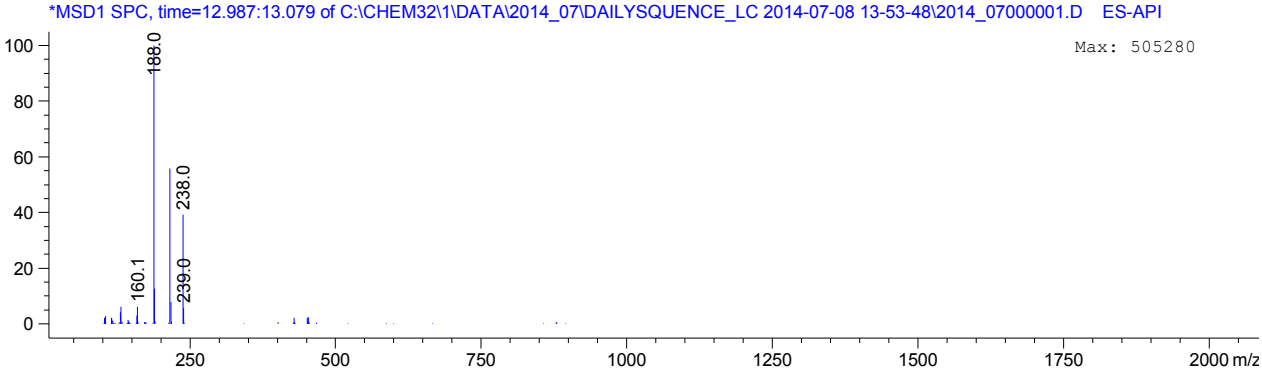
*MSD1 SPC, time=12.987:13.079 of C:\CHEM32\1\DATA\2014_07\DAILYSQUENCE_LC 2014-07-08 13-53-48\2014_07000001.D ES-API
Max: 505280
100
80
60
40
20
0
188.0
238.0
160.1
239.0
250
500
750
1000
1250
1500
1750
2000 m/z

Origin	Bruker BioSpin GmbH
Solvent	CDCl3
Temperature	300.0
Pulse Sequence	zg30
Experiment	1D
Number of Scans	16
Acquisition Date	2014-05-16T14:31:00
Spectrometer Frequency	400.13
Spectral Width	8223.7
Lowest Frequency	-1647.3
Nucleus	1H
Acquired Size	32768
Spectral Size	65536

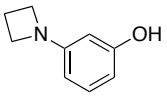

S25

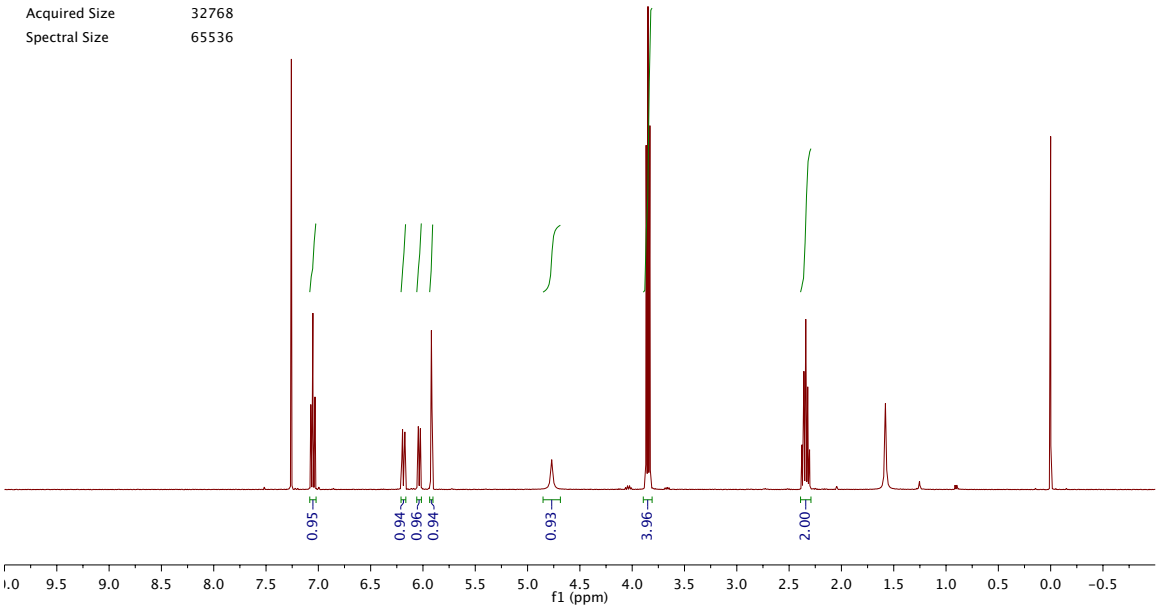

Origin	Bruker BioSpin GmbH
Solvent	CDCl3
Temperature	300.0
Pulse Sequence	zgpg30
Experiment	1D
Number of Scans	2048
Acquisition Date	2014-08-08T23:04:00
Spectrometer Frequency	100.62
Spectral Width	24038.5
Lowest Frequency	-1944.3
Nucleus	13C
Acquired Size	32768
Spectral Size	65536

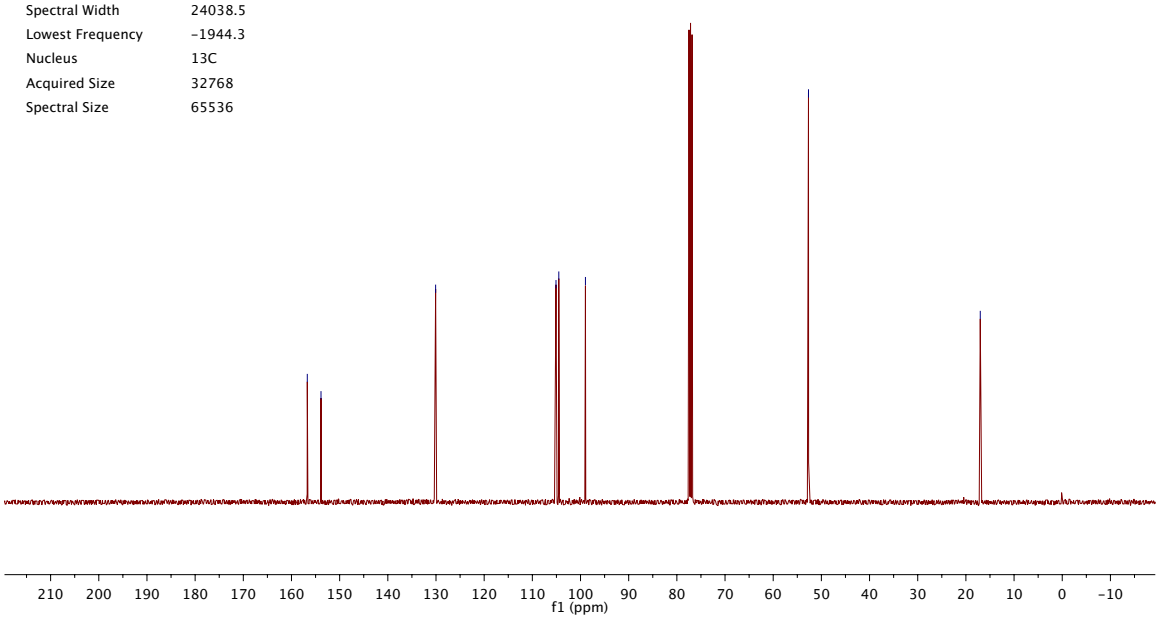

Origin	Bruker BioSpin GmbH
Solvent	CDCl3
Temperature	300.0
Pulse Sequence	zg30
Experiment	1D
Number of Scans	16
Acquisition Date	2014-08-06T15:50:00
Spectrometer Frequency	400.13
Spectral Width	8223.7
Lowest Frequency	-1646.3
Nucleus	1H
Acquired Size	32768
Spectral Size	65536

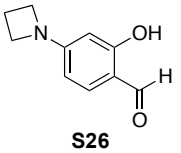

S26

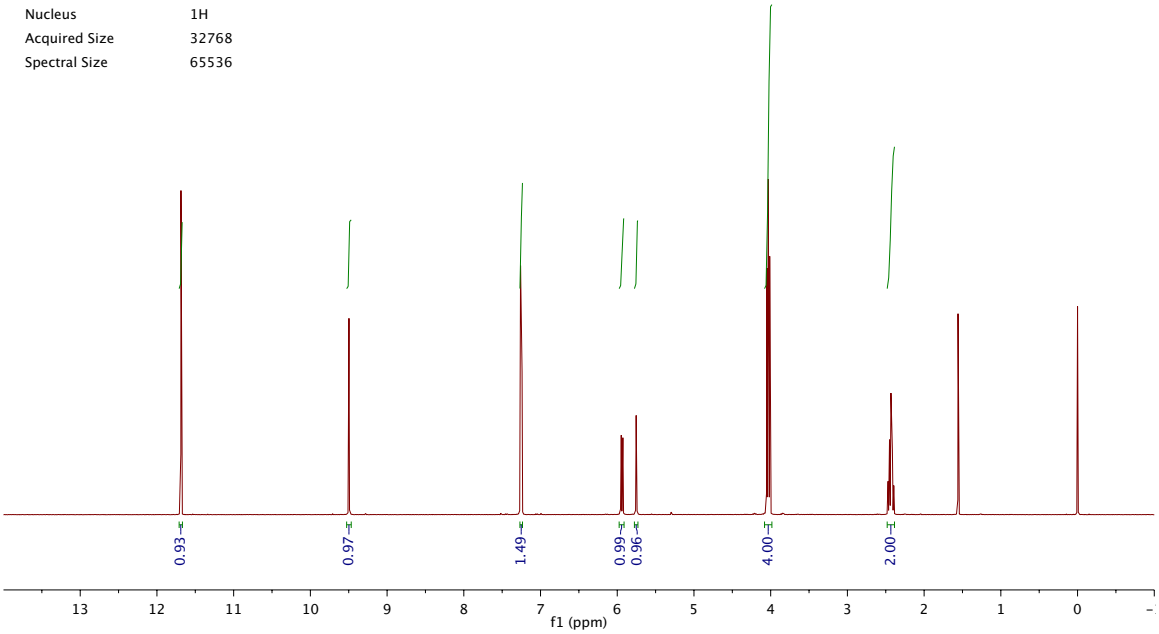

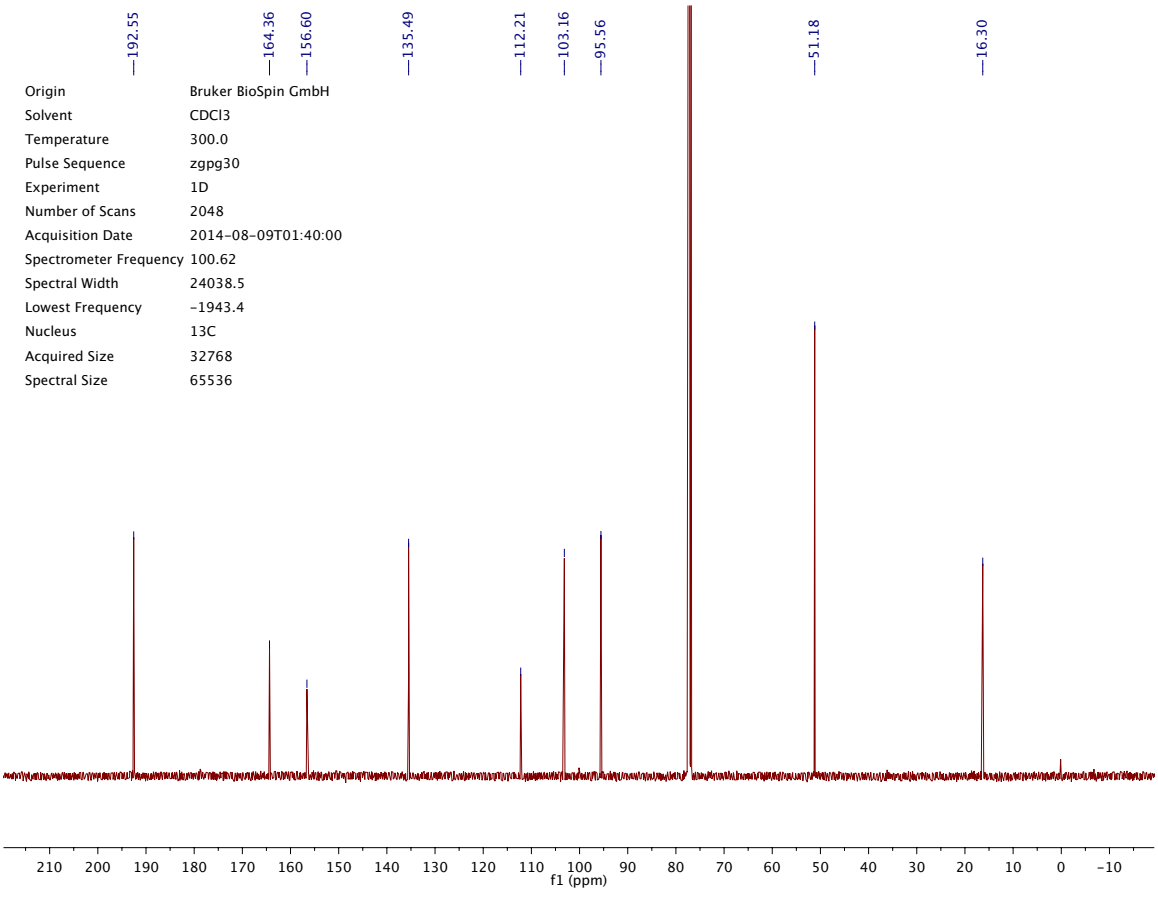

Origin	Bruker BioSpin GmbH
Solvent	CDCl3
Temperature	300.0
Pulse Sequence	zgpg30
Experiment	1D
Number of Scans	2048
Acquisition Date	2014-08-09T01:40:00
Spectrometer Frequency	100.62
Spectral Width	24038.5
Lowest Frequency	-1943.4
Nucleus	13C
Acquired Size	32768
Spectral Size	65536

Origin	Bruker BioSpin GmbH
Solvent	CDCl3
Temperature	300.0
Pulse Sequence	zg30
Experiment	1D
Number of Scans	16
Acquisition Date	2014-08-09T02:16:00
Spectrometer Frequency	400.13
Spectral Width	8223.7
Lowest Frequency	-1637.6
Nucleus	1H
Acquired Size	32768
Spectral Size	65536

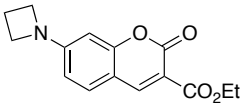

S27

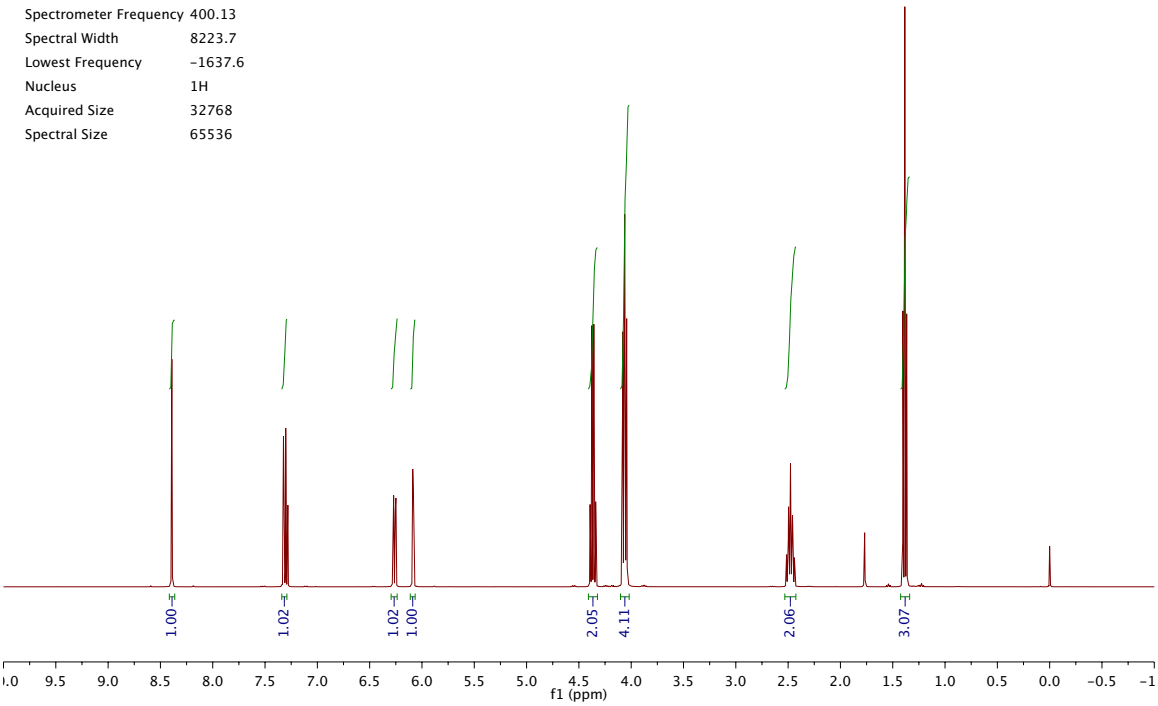

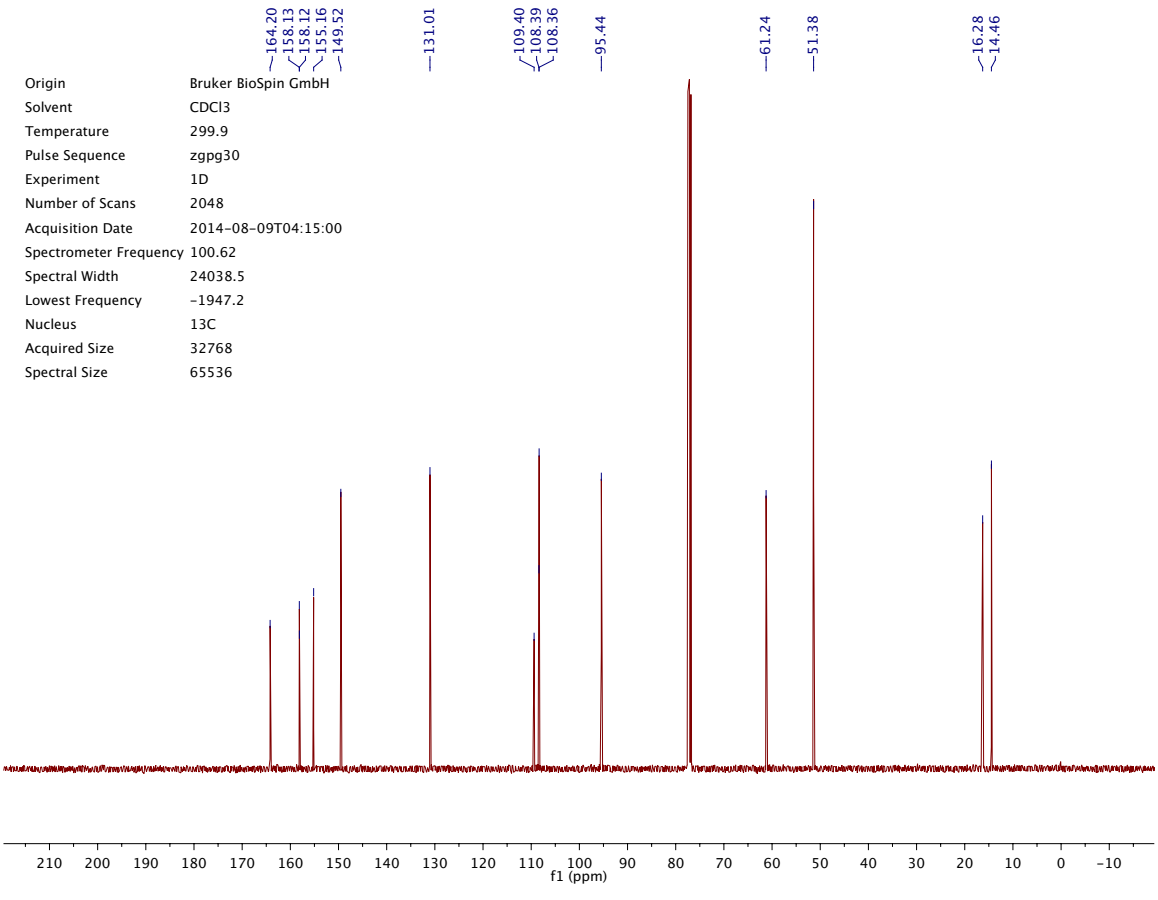

Origin	Bruker BioSpin GmbH
Solvent	CDCl3
Temperature	299.9
Pulse Sequence	zgpg30
Experiment	1D
Number of Scans	2048
Acquisition Date	2014-08-09T04:15:00
Spectrometer Frequency	100.62
Spectral Width	24038.5
Lowest Frequency	-1947.2
Nucleus	13C
Acquired Size	32768
Spectral Size	65536

Origin	Bruker BioSpin GmbH
Solvent	DMSO
Temperature	300.0
Pulse Sequence	zg30
Experiment	1D
Number of Scans	16
Acquisition Date	2014-07-02T11:28:00
Spectrometer Frequency	400.13
Spectral Width	8223.7
Lowest Frequency	-1638.7
Nucleus	1H
Acquired Size	32768
Spectral Size	65536

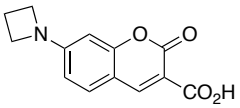

14

Origin	Bruker BioSpin GmbH
Solvent	DMSO
Temperature	300.0
Pulse Sequence	zgpg30
Experiment	1D
Number of Scans	1024
Acquisition Date	2014-07-18T13:07:00
Spectrometer Frequency	100.62
Spectral Width	24038.5
Lowest Frequency	-2005.6
Nucleus	13C
Acquired Size	32768
Spectral Size	65536

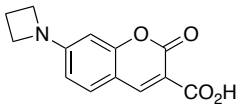
N
O
O
CO2H

14

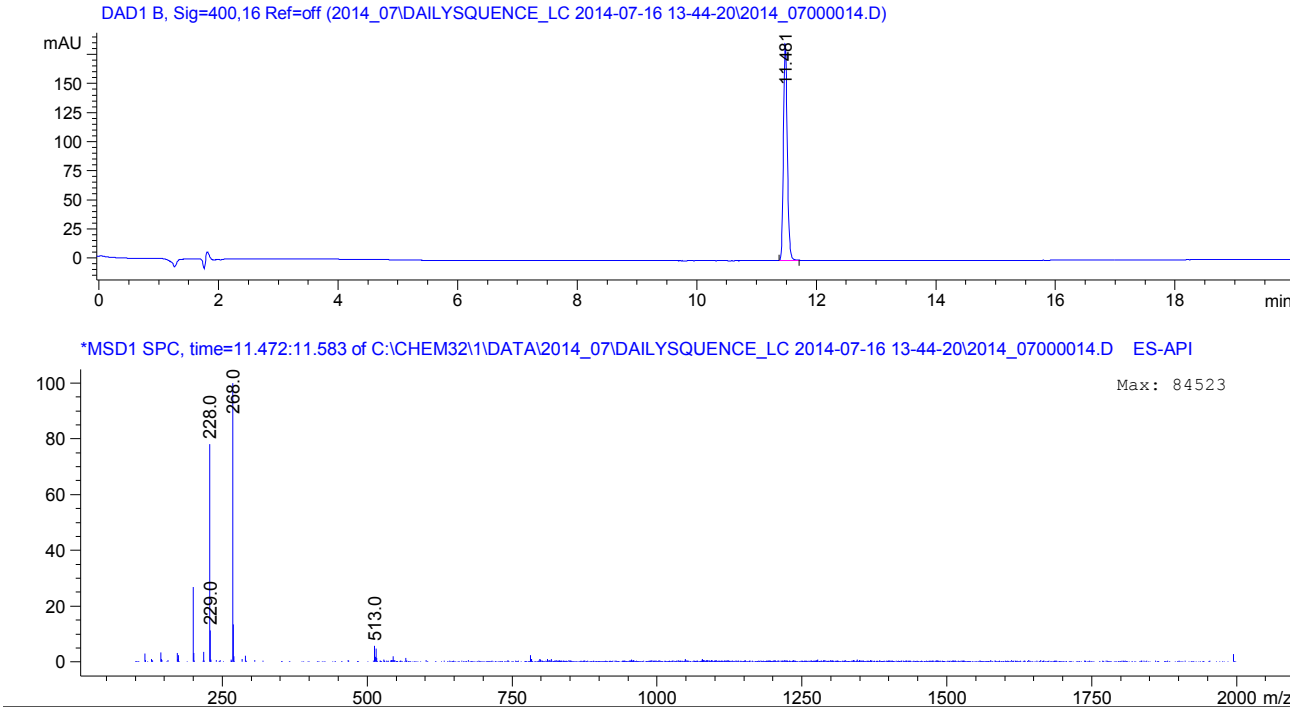
DAD1 B, Sig=400,16 Ref=off (2014_07\DAILYSQUENCE_LC 2014-07-16 13-44-20\2014_07000014.D)
mAU
150
125
100
75
50
25
0
11.481
0
2
4
6
8
10
12
14
16
18
min
*MSD1 SPC, time=11.472:11.583 of C:\CHEM32\1\DATA\2014_07\DAILYSQUENCE_LC 2014-07-16 13-44-20\2014_07000014.D ES-API
Max: 84523
100
80
60
40
20
0
228.0
268.0
229.0
513.0
250
500
750
1000
1250
1500
1750
2000 m/z

Origin	Bruker BioSpin GmbH
Solvent	MeOD
Temperature	300.0
Pulse Sequence	zg30
Experiment	1D
Number of Scans	16
Acquisition Date	2014-07-25T11:08:00
Spectrometer Frequency	400.13
Spectral Width	8223.7
Lowest Frequency	-1644.1
Nucleus	1H
Acquired Size	32768
Spectral Size	65536

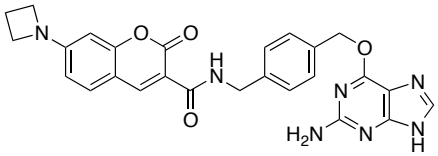

31

DAD1 B, Sig=400,16 Ref=off (2014_06\DAILYSQUENCE_LC 2014-07-01 16-57-28\2014_06000001.D)

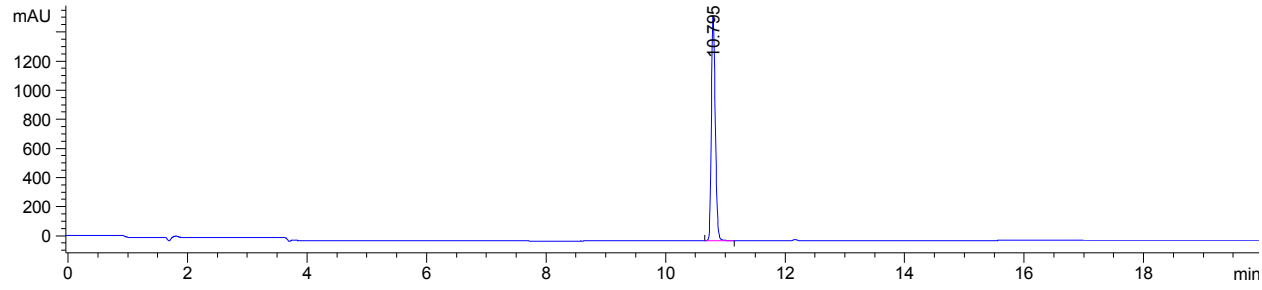

*MSD1 SPC, time=10.770:10.899 of C:\CHEM32\1\DATA\2014_06\DAILYSQUENCE_LC 2014-07-01 16-57-28\2014_06000001.D ES-API

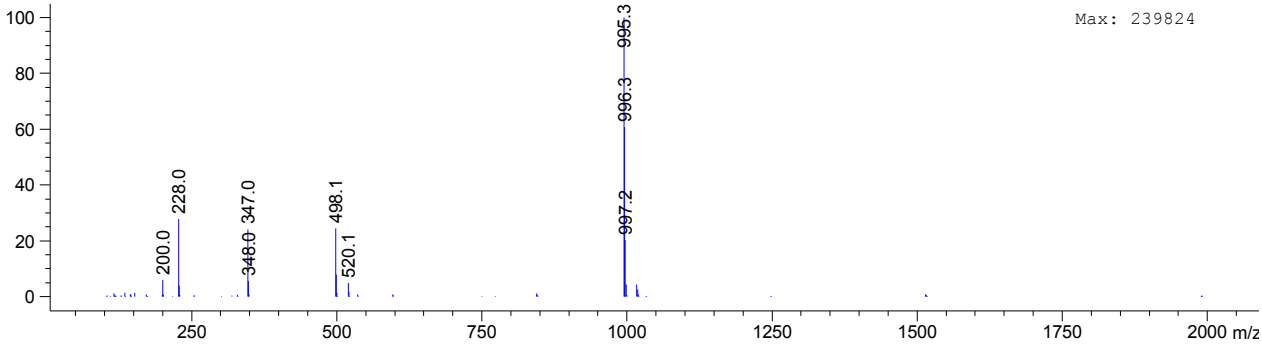

Origin	Bruker BioSpin GmbH
Solvent	CDCl3
Temperature	300.0
Pulse Sequence	zg30
Experiment	1D
Number of Scans	16
Acquisition Date	2014-05-16T17:24:00
Spectrometer Frequency	400.13
Spectral Width	8223.7
Lowest Frequency	-1646.2
Nucleus	1H
Acquired Size	32768
Spectral Size	65536

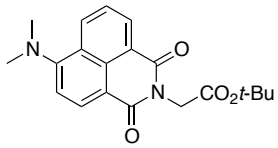

S29

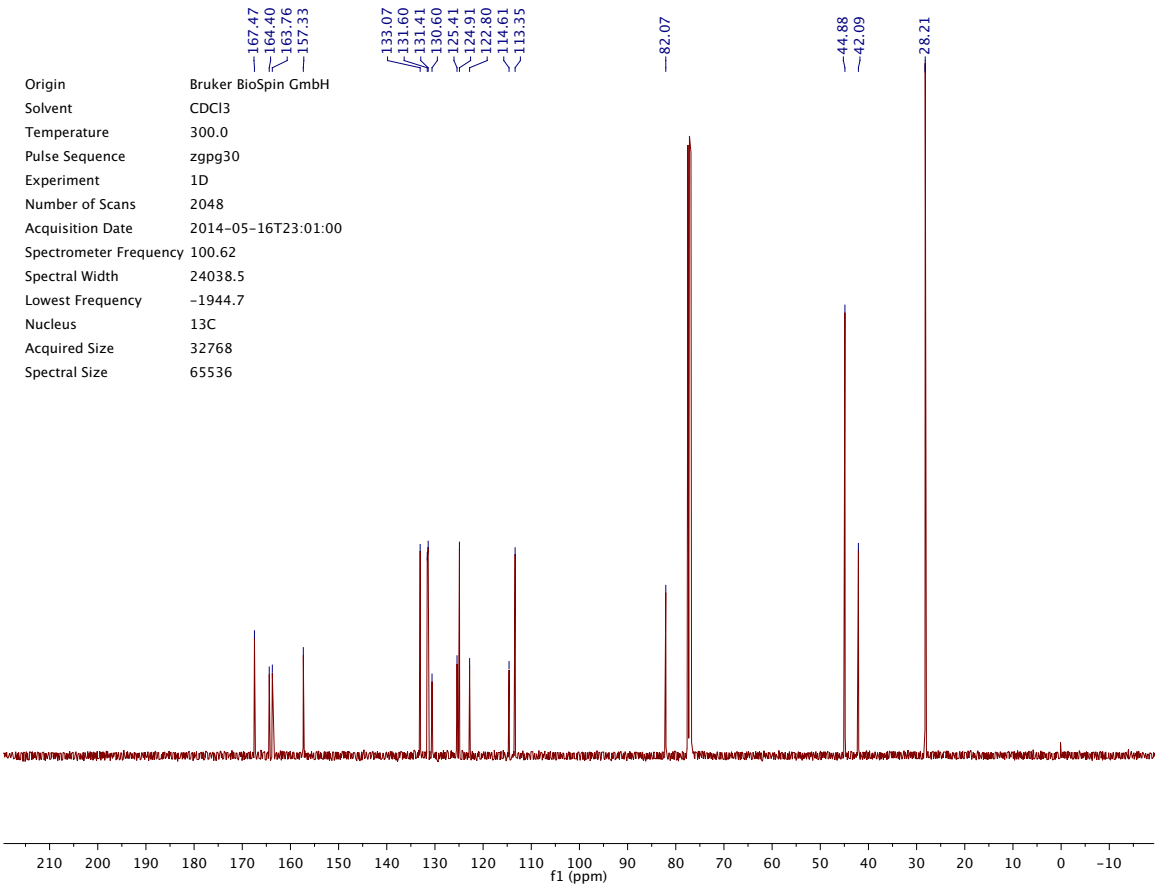

Origin	Bruker BioSpin GmbH
Solvent	CDCl3
Temperature	300.0
Pulse Sequence	zgpg30
Experiment	1D
Number of Scans	2048
Acquisition Date	2014-05-16T23:01:00
Spectrometer Frequency	100.62
Spectral Width	24038.5
Lowest Frequency	-1944.7
Nucleus	13C
Acquired Size	32768
Spectral Size	65536

Origin	Bruker BioSpin GmbH
Solvent	DMSO
Temperature	300.0
Pulse Sequence	zg30
Experiment	1D
Number of Scans	16
Acquisition Date	2014-05-21T16:39:00
Spectrometer Frequency	400.13
Spectral Width	8223.7
Lowest Frequency	-1638.5
Nucleus	1H
Acquired Size	32768
Spectral Size	65536

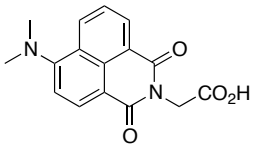

15

Origin	Bruker BioSpin GmbH
Solvent	DMSO
Temperature	300.0
Pulse Sequence	zgpg30
Experiment	1D
Number of Scans	1024
Acquisition Date	2014-06-09T22:01:00
Spectrometer Frequency	100.62
Spectral Width	24038.5
Lowest Frequency	-2006.0
Nucleus	13C
Acquired Size	32768
Spectral Size	65536

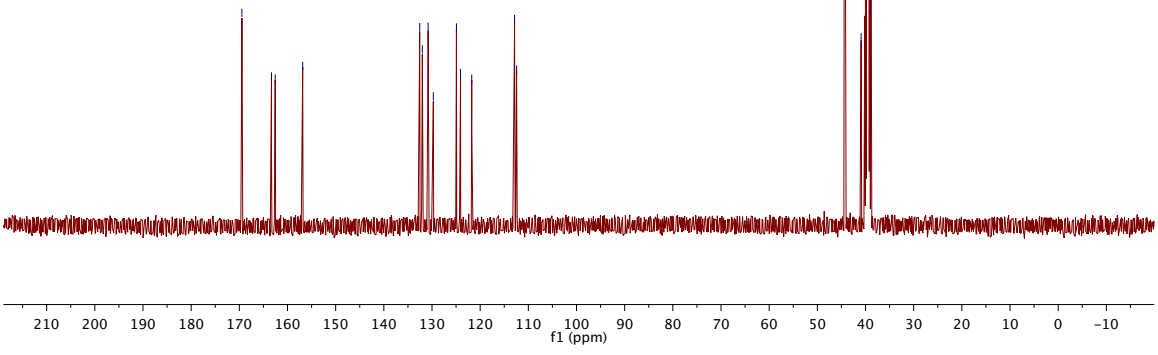

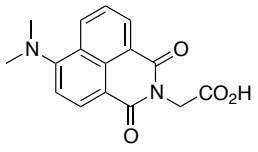
N
O
N
CO2H
O

15

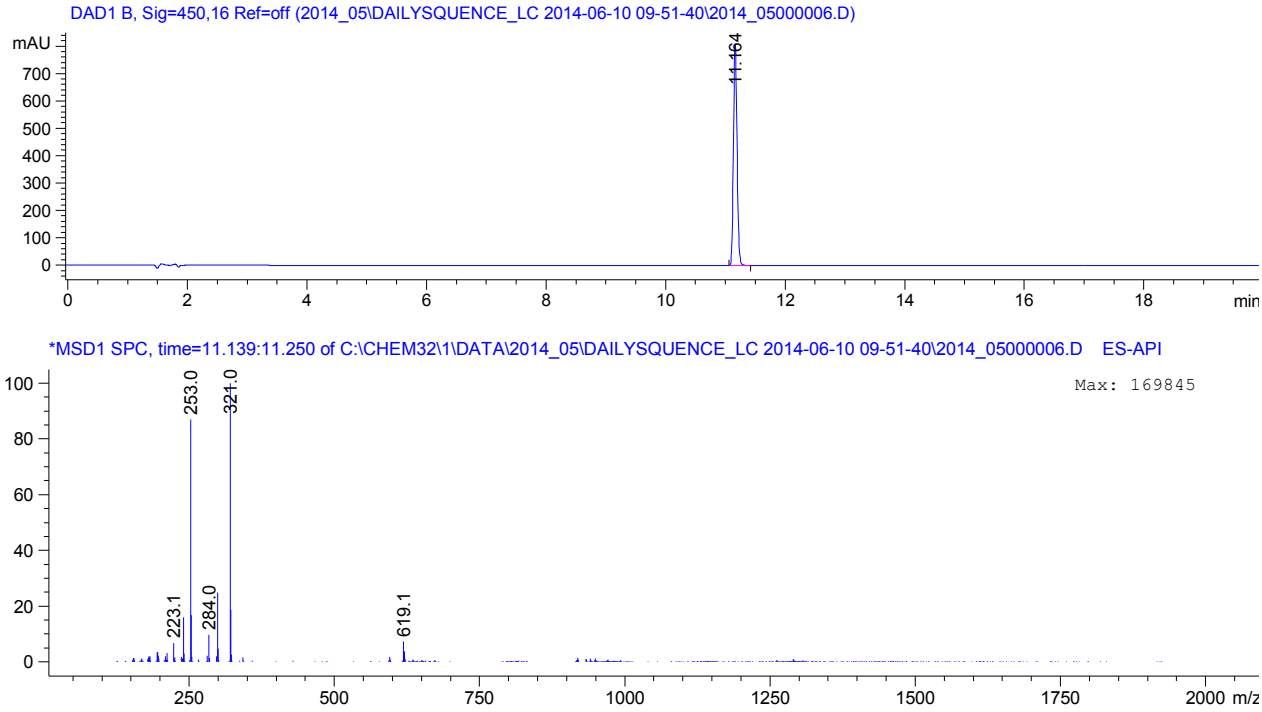
DAD1 B, Sig=450,16 Ref=off (2014_05\DAILYSQUENCE_LC 2014-06-10 09-51-40\2014_05000006.D)
mAU
700
600
500
400
300
200
100
0
11.164
0
2
4
6
8
10
12
14
16
18
min

*MSD1 SPC, time=11.139:11.250 of C:\CHEM32\1\DATA\2014_05\DAILYSQUENCE_LC 2014-06-10 09-51-40\2014_05000006.D ES-API
Max: 169845
100
80
60
40
20
0
253.0
321.0
223.1
284.0
619.1
250
500
750
1000
1250
1500
1750
2000 m/z

Origin	Bruker BioSpin GmbH
Solvent	CDCl3
Temperature	300.0
Pulse Sequence	zg30
Experiment	1D
Number of Scans	16
Acquisition Date	2014-05-13T14:27:00
Spectrometer Frequency	400.13
Spectral Width	8223.7
Lowest Frequency	-1646.3
Nucleus	1H
Acquired Size	32768
Spectral Size	65536

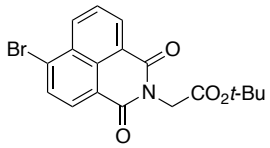

S31

Origin	Bruker BioSpin GmbH
Solvent	CDCl3
Temperature	300.0
Pulse Sequence	zgpg30
Experiment	1D
Number of Scans	2048
Acquisition Date	2014-05-13T23:01:00
Spectrometer Frequency	100.62
Spectral Width	24038.5
Lowest Frequency	-1943.7
Nucleus	13C
Acquired Size	32768
Spectral Size	65536

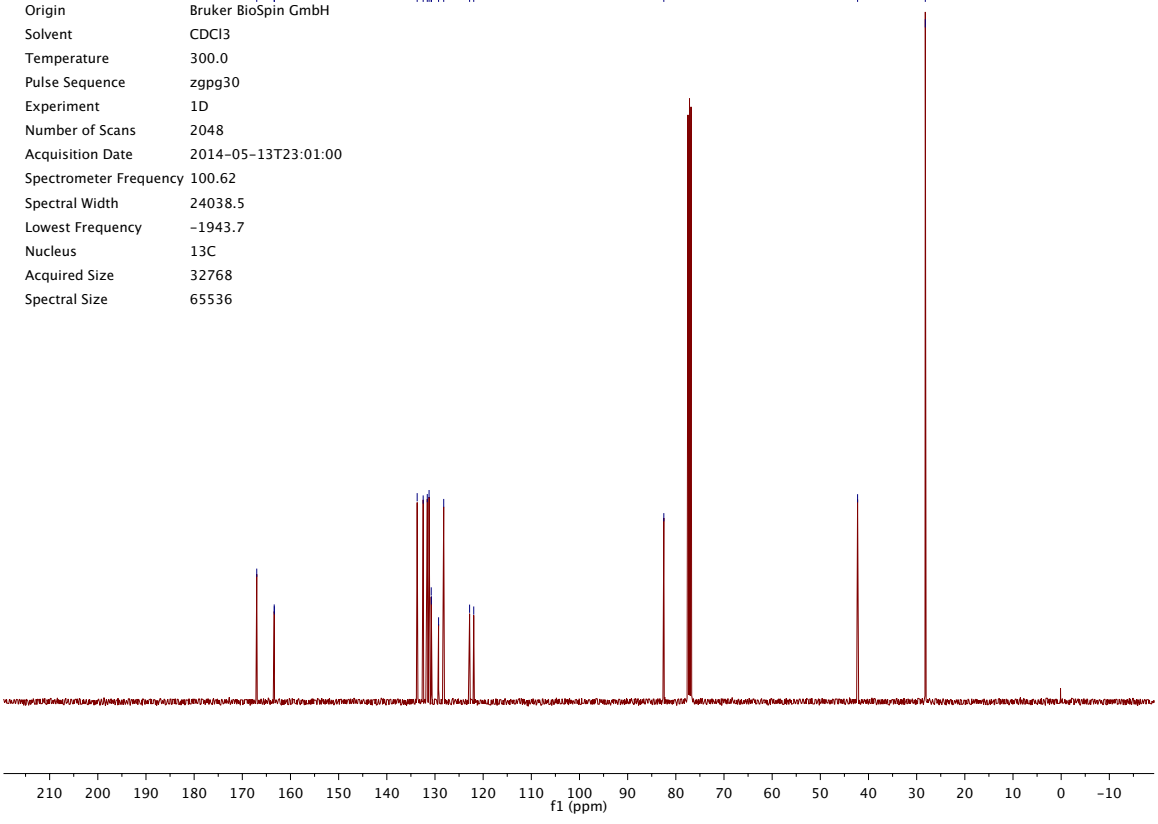

Origin	Bruker BioSpin GmbH
Solvent	CDCl3
Temperature	300.0
Pulse Sequence	zg30
Experiment	1D
Number of Scans	16
Acquisition Date	2014-05-15T17:08:00
Spectrometer Frequency	400.13
Spectral Width	8223.7
Lowest Frequency	-1646.2
Nucleus	1H
Acquired Size	32768
Spectral Size	65536

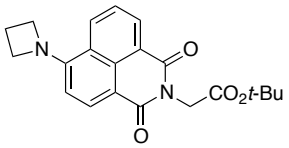

S32

Origin	Bruker BioSpin GmbH
Solvent	CDCl3
Temperature	300.0
Pulse Sequence	zgpg30
Experiment	1D
Number of Scans	2048
Acquisition Date	2014-05-17T01:36:00
Spectrometer Frequency	100.62
Spectral Width	24038.5
Lowest Frequency	-1944.8
Nucleus	13C
Acquired Size	32768
Spectral Size	65536

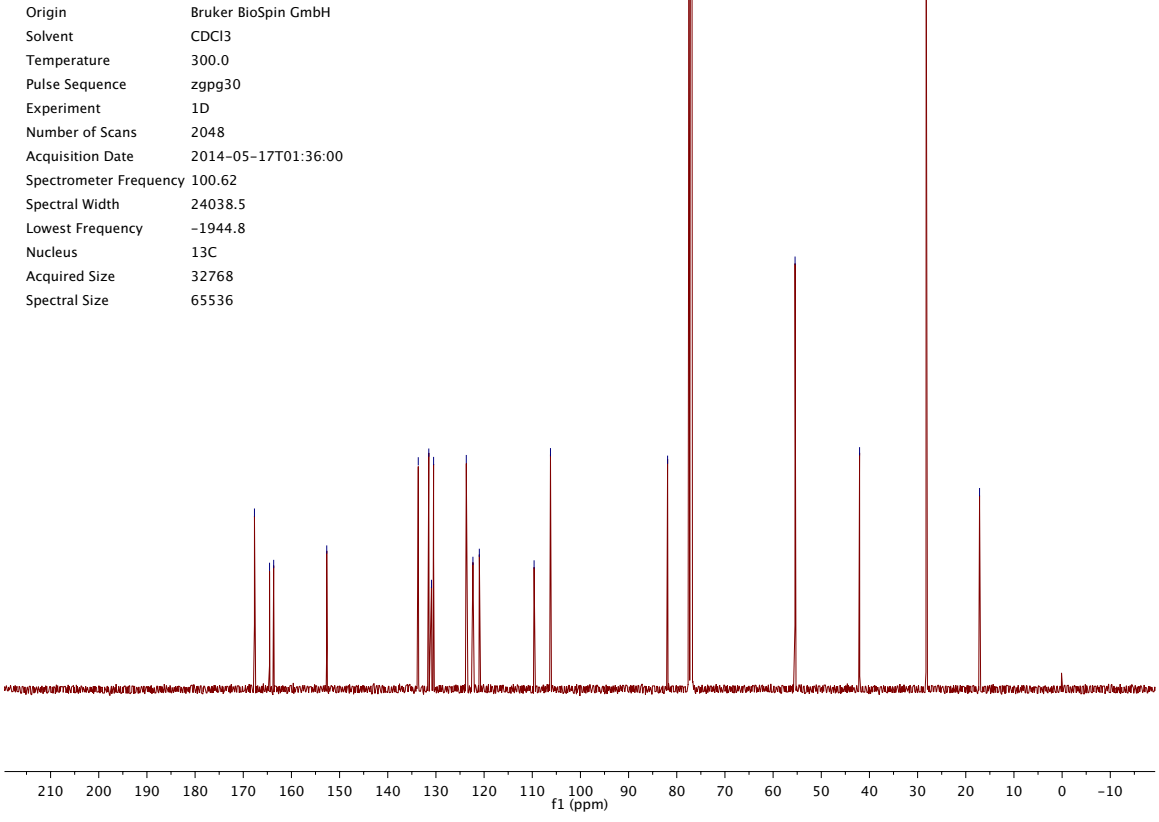

Origin	Bruker BioSpin GmbH
Solvent	DMSO
Temperature	300.0
Pulse Sequence	zg30
Experiment	1D
Number of Scans	16
Acquisition Date	2014-05-23T09:29:00
Spectrometer Frequency	400.13
Spectral Width	8223.7
Lowest Frequency	-1638.3
Nucleus	1H
Acquired Size	32768
Spectral Size	65536

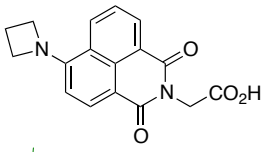

16

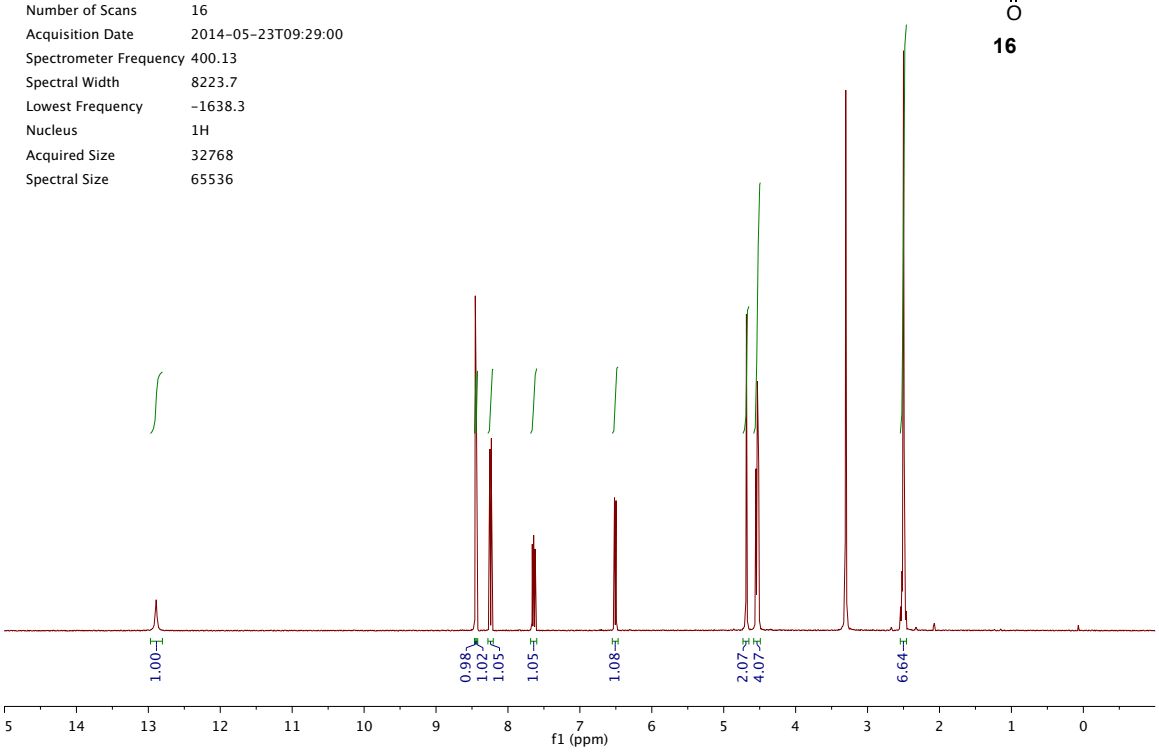

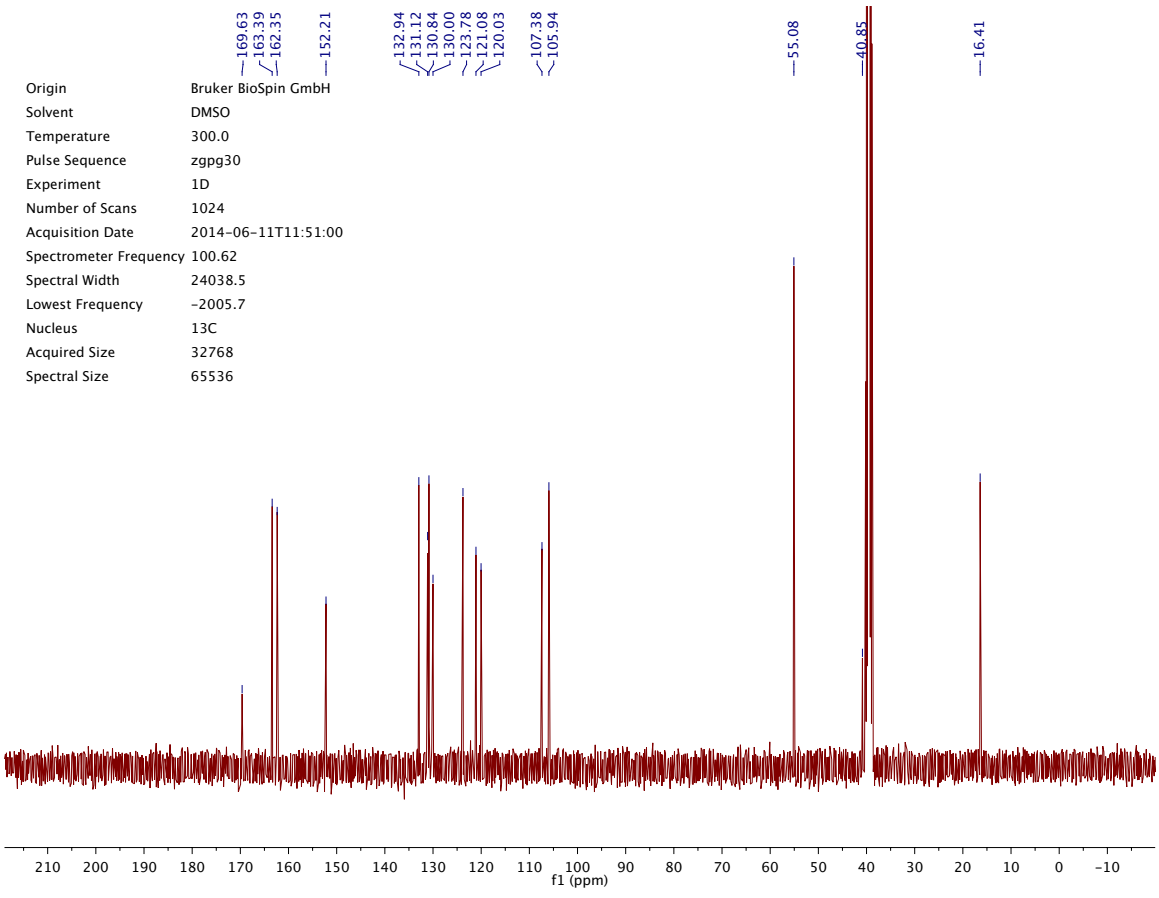

Origin	Bruker BioSpin GmbH
Solvent	DMSO
Temperature	300.0
Pulse Sequence	zgpg30
Experiment	1D
Number of Scans	1024
Acquisition Date	2014-06-11T11:51:00
Spectrometer Frequency	100.62
Spectral Width	24038.5
Lowest Frequency	-2005.7
Nucleus	13C
Acquired Size	32768
Spectral Size	65536

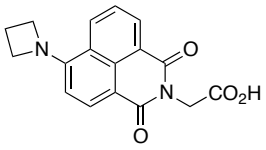
N
O
N
CO2H
O

16

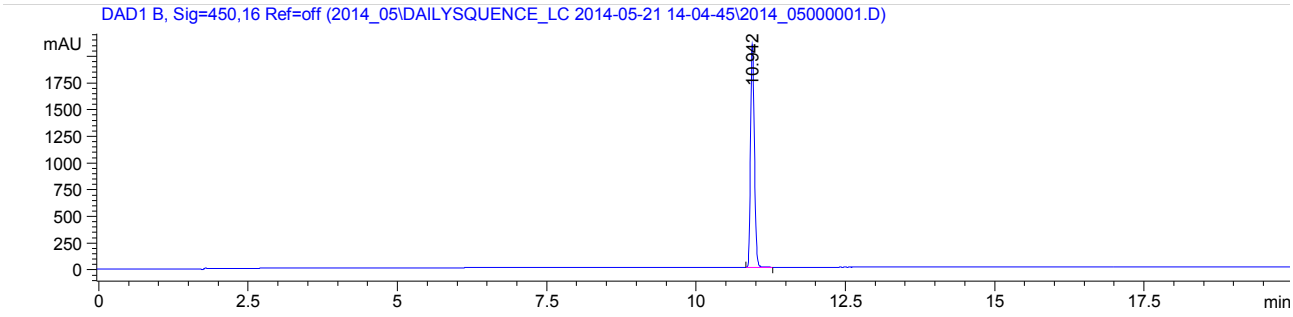
DAD1 B, Sig=450,16 Ref=off (2014_05\DAILYSQUENCE_LC 2014-05-21 14-04-45\2014_05000001.D)
mAU
1750
1500
1250
1000
750
500
250
0
10.942
0
2.5
5
7.5
10
12.5
15
17.5
min

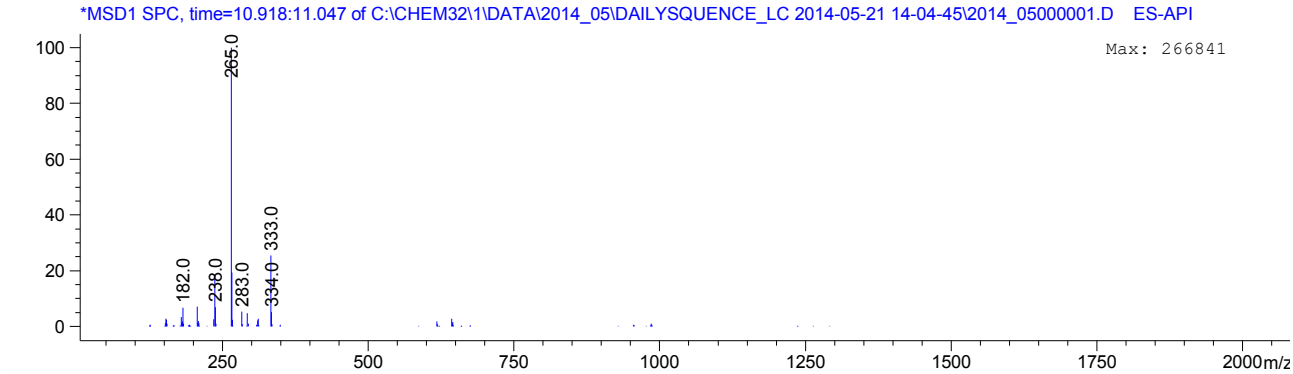
*MSD1 SPC, time=10.918:11.047 of C:\CHEM32\1\DATA\2014_05\DAILYSQUENCE_LC 2014-05-21 14-04-45\2014_05000001.D ES-API
Max: 266841
100
80
60
40
20
0
265.0
182.0
238.0
283.0
334.0
333.0
250
500
750
1000
1250
1500
1750
2000
m/z

Origin	Bruker BioSpin GmbH
Solvent	CDCl3
Temperature	300.0
Pulse Sequence	zg30
Experiment	1D
Number of Scans	16
Acquisition Date	2014-05-15T17:13:00
Spectrometer Frequency	400.13
Spectral Width	8223.7
Lowest Frequency	-1646.6
Nucleus	1H
Acquired Size	32768
Spectral Size	65536

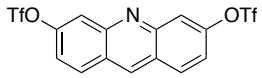

S35

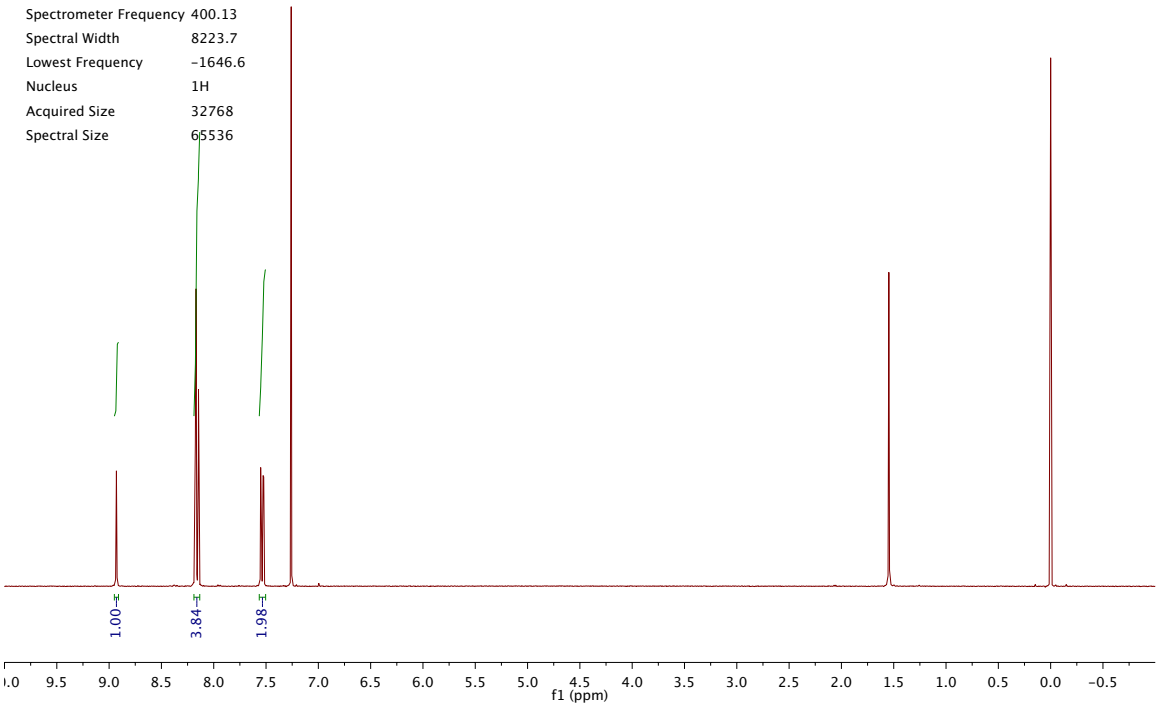

151.05
149.47
137.02
131.23
125.70
123.73
121.44
120.78
120.54
117.35
114.16

Origin	Bruker BioSpin GmbH
Solvent	CDCl3
Temperature	300.0
Pulse Sequence	zgpg30
Experiment	1D
Number of Scans	2048
Acquisition Date	2014-05-15T23:04:00
Spectrometer Frequency	100.62
Spectral Width	24038.5
Lowest Frequency	-1941.6
Nucleus	13C
Acquired Size	32768
Spectral Size	65536

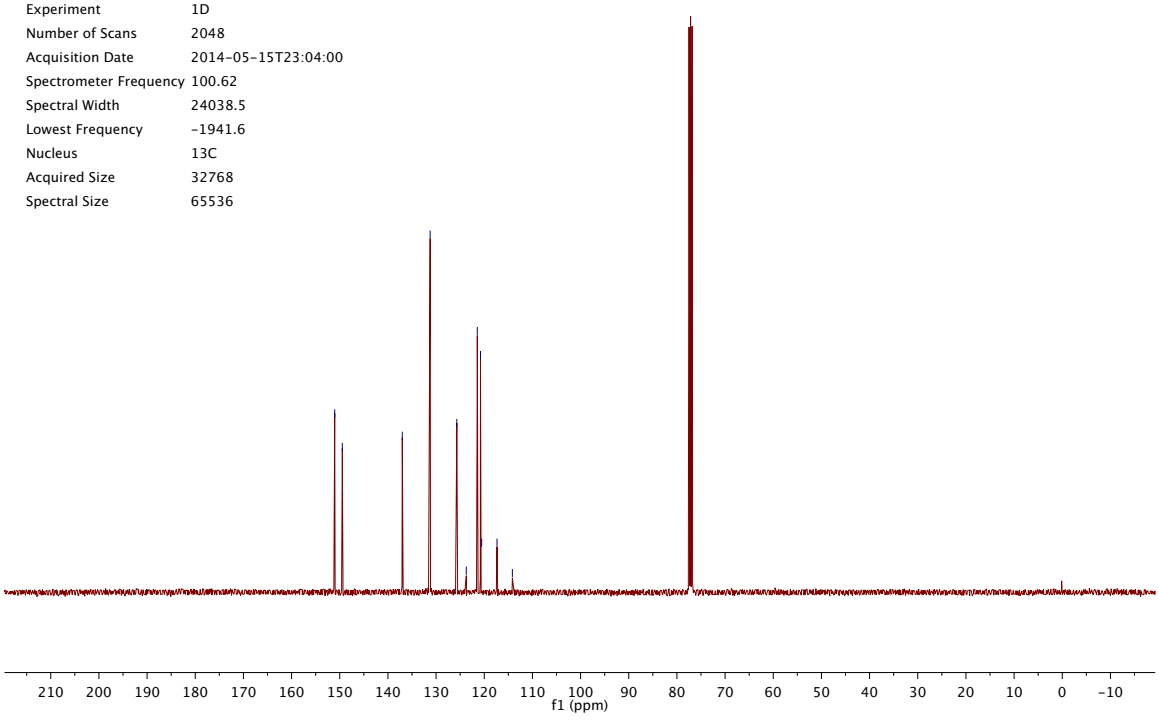

Origin	Bruker BioSpin GmbH
Solvent	MeOD
Temperature	300.0
Pulse Sequence	zg30
Experiment	1D
Number of Scans	16
Acquisition Date	2014-03-07T14:40:00
Spectrometer Frequency	400.13
Spectral Width	8223.7
Lowest Frequency	-1644.1
Nucleus	1H
Acquired Size	32768
Spectral Size	65536

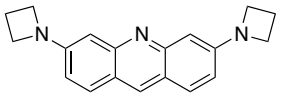

18

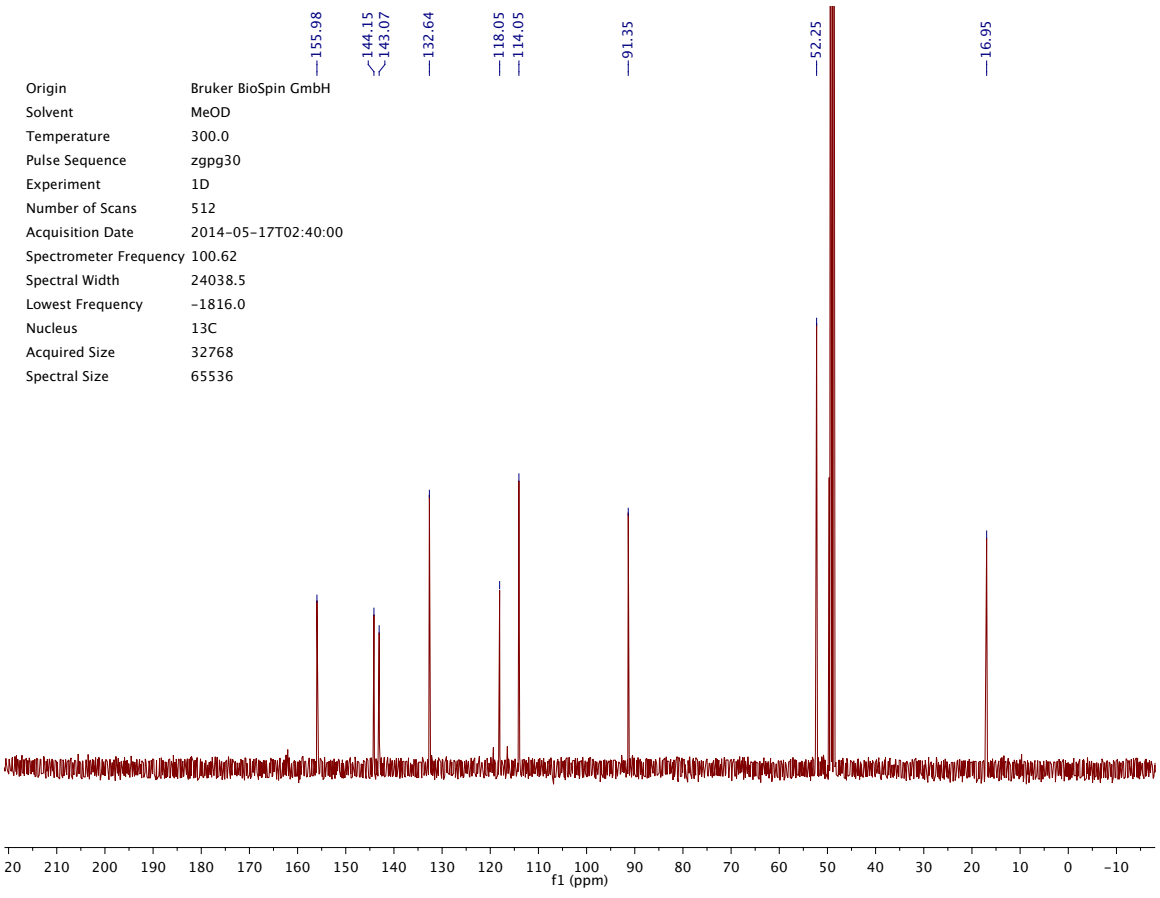

Origin	Bruker BioSpin GmbH
Solvent	MeOD
Temperature	300.0
Pulse Sequence	zgpg30
Experiment	1D
Number of Scans	512
Acquisition Date	2014-05-17T02:40:00
Spectrometer Frequency	100.62
Spectral Width	24038.5
Lowest Frequency	-1816.0
Nucleus	13C
Acquired Size	32768
Spectral Size	65536

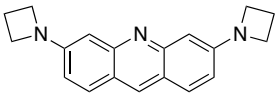

18

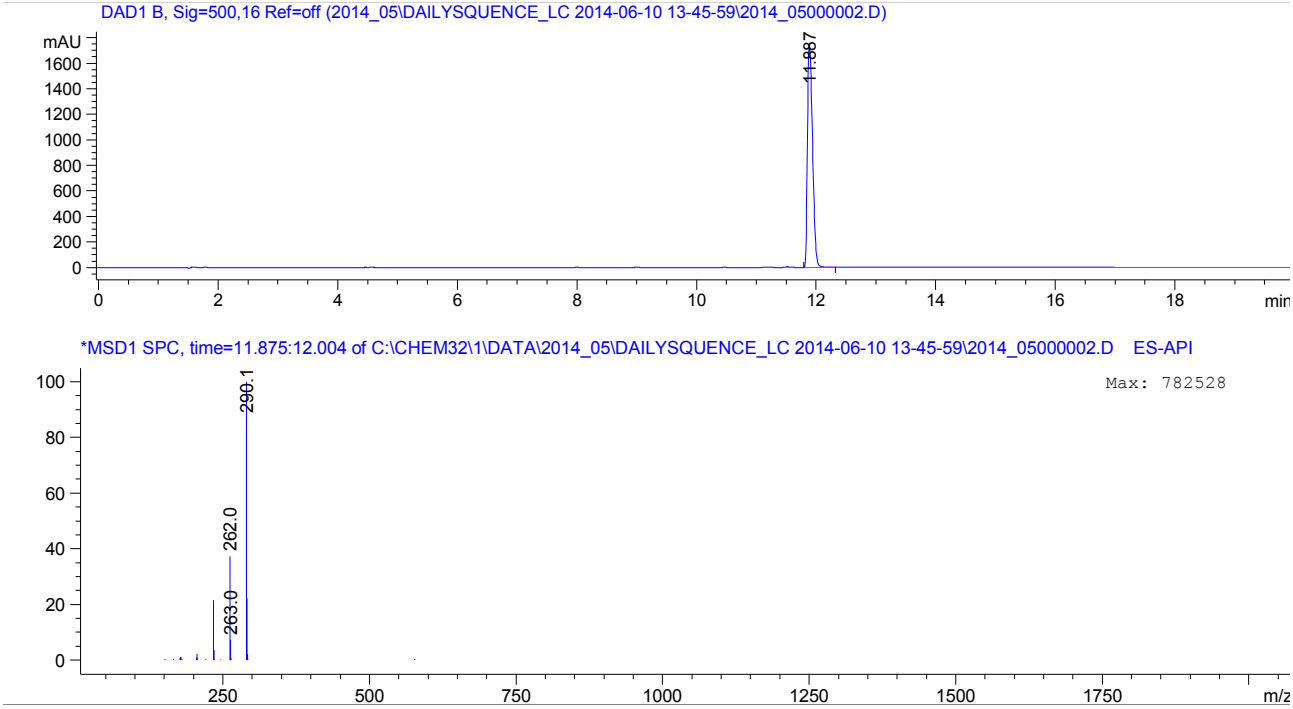
DAD1 B, Sig=500,16 Ref=off (2014_05\DAILYSQUENCE_LC 2014-06-10 13-45-59\2014_05000002.D)
mAU
1600
1400
1200
1000
800
600
400
200
0
11.987
0
2
4
6
8
10
12
14
16
18
min
*MSD1 SPC, time=11.875:12.004 of C:\CHEM32\1\DATA\2014_05\DAILYSQUENCE_LC 2014-06-10 13-45-59\2014_05000002.D ES-API
Max: 782528
100
80
60
40
20
0
290.1
262.0
263.0
250
500
750
1000
1250
1500
1750
m/z

Origin	Bruker BioSpin GmbH
Solvent	MeOD
Temperature	300.0
Pulse Sequence	zg30
Experiment	1D
Number of Scans	16
Acquisition Date	2014-06-20T14:44:00
Spectrometer Frequency	400.13
Spectral Width	8223.7
Lowest Frequency	-1644.1
Nucleus	1H
Acquired Size	32768
Spectral Size	65536

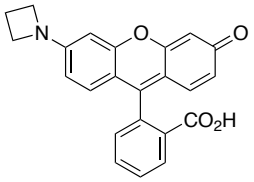

20

Origin	Bruker BioSpin GmbH
Solvent	MeOD
Temperature	300.0
Pulse Sequence	zgpg30
Experiment	1D
Number of Scans	8192
Acquisition Date	2014-07-09T04:54:00
Spectrometer Frequency	100.62
Spectral Width	24038.5
Lowest Frequency	-1816.2
Nucleus	13C
Acquired Size	32768
Spectral Size	65536

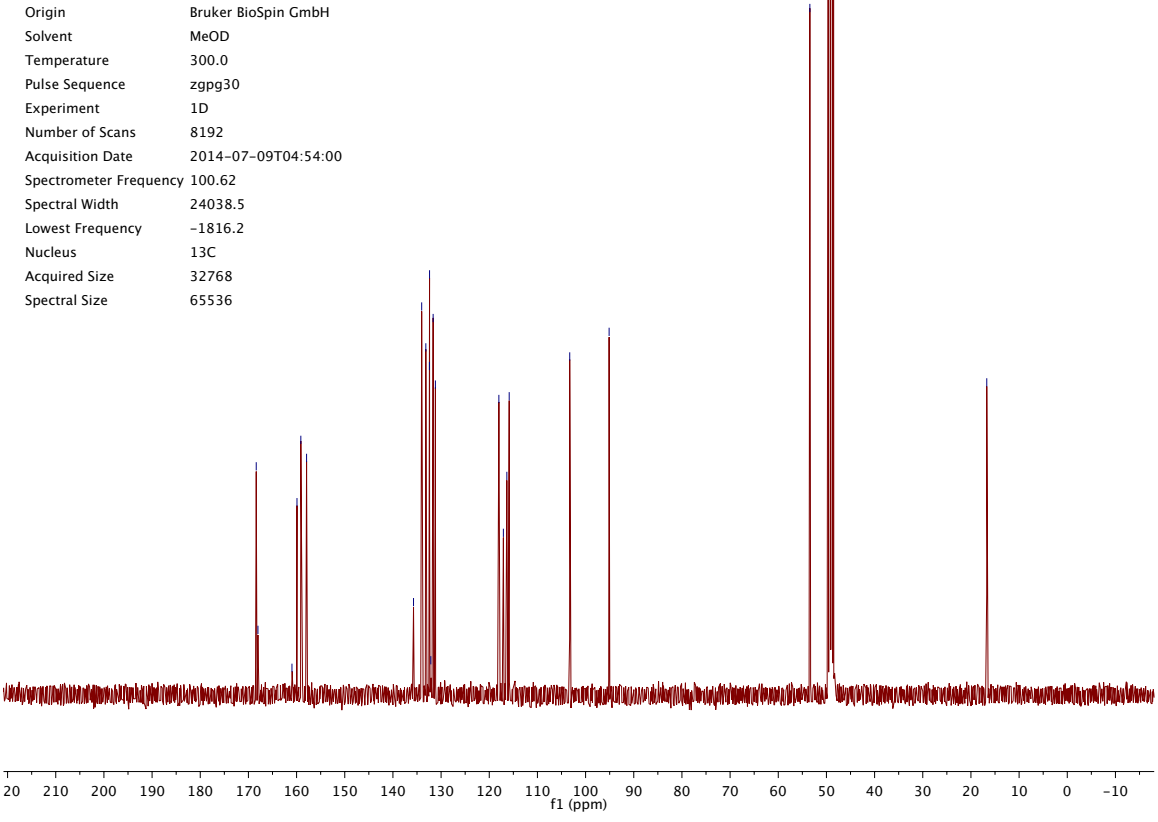

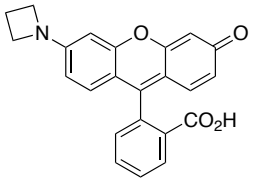
N
O
O
CO_2H

20

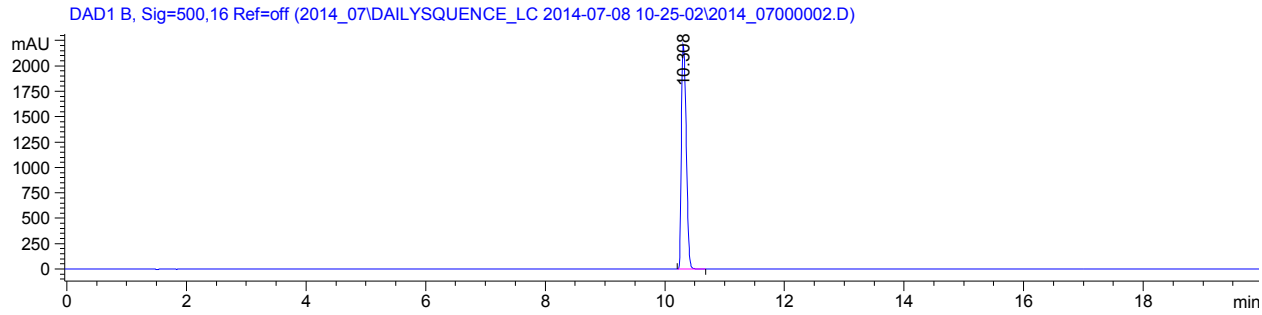
DAD1 B, Sig=500,16 Ref=off (2014_07\DAILYSQUENCE_LC 2014-07-08 10-25-02\2014_07000002.D)
mAU
2000
1750
1500
1250
1000
750
500
250
0
10.398
0
2
4
6
8
10
12
14
16
18
min

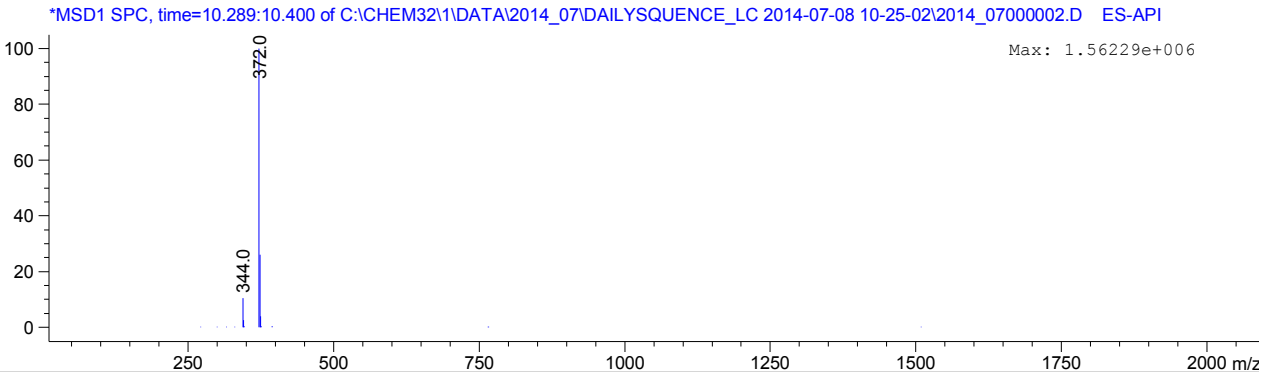
*MSD1 SPC, time=10.289:10.400 of C:\CHEM32\1\DATA\2014_07\DAILYSQUENCE_LC 2014-07-08 10-25-02\2014_07000002.D ES-API
Max: 1.56229e+006
100
80
60
40
20
0
372.0
344.0
250
500
750
1000
1250
1500
1750
2000 m/z

Origin	Bruker BioSpin GmbH
Solvent	CDCl3
Temperature	300.0
Pulse Sequence	zg30
Experiment	1D
Number of Scans	16
Acquisition Date	2014-06-11T09:23:00
Spectrometer Frequency	400.13
Spectral Width	8223.7
Lowest Frequency	-1647.6
Nucleus	1H
Acquired Size	32768
Spectral Size	65536

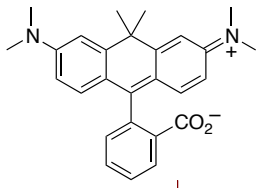

21

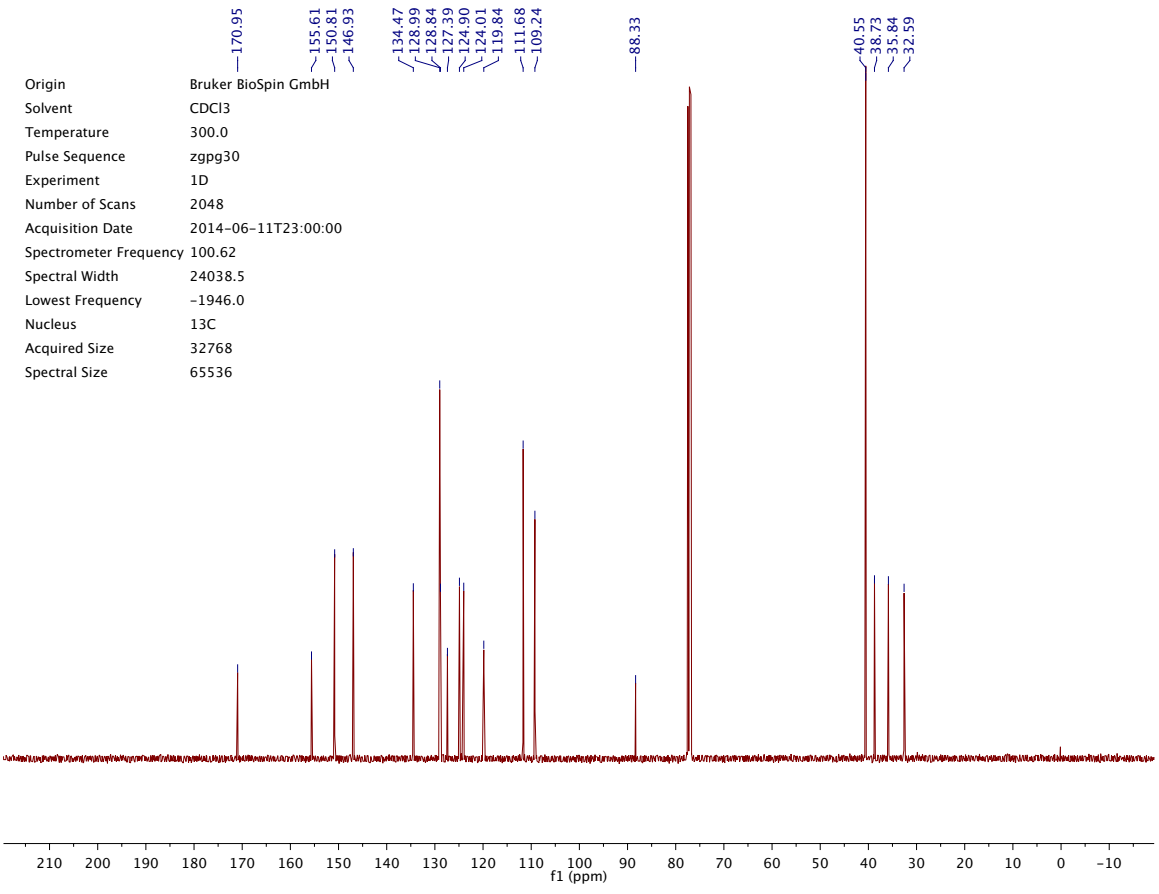

Origin	Bruker BioSpin GmbH
Solvent	CDCl3
Temperature	300.0
Pulse Sequence	zgpg30
Experiment	1D
Number of Scans	2048
Acquisition Date	2014-06-11T23:00:00
Spectrometer Frequency	100.62
Spectral Width	24038.5
Lowest Frequency	-1946.0
Nucleus	13C
Acquired Size	32768
Spectral Size	65536

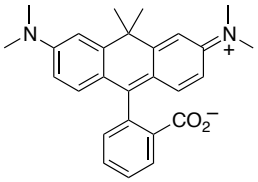

21

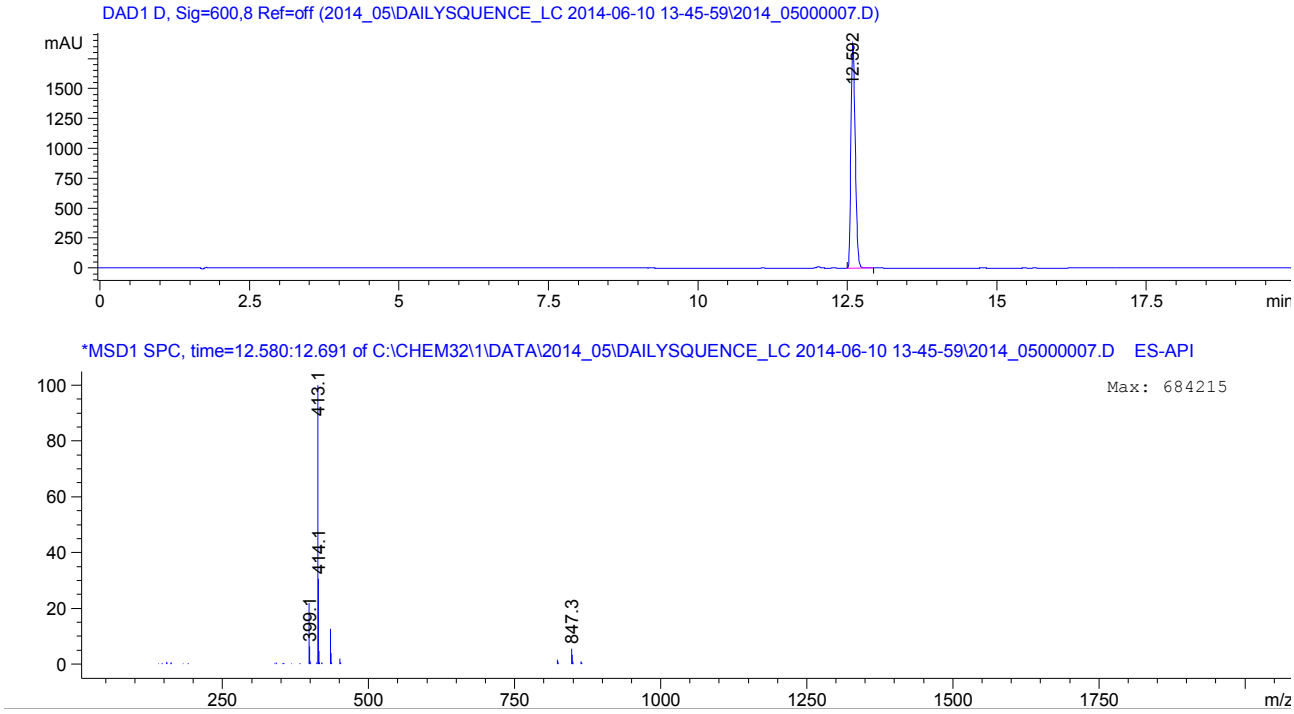
DAD1 D, Sig=600,8 Ref=off (2014_05\DAILYSQUENCE_LC 2014-06-10 13-45-59\2014_05000007.D)
mAU
1500
1250
1000
750
500
250
0
12.592
0
2.5
5
7.5
10
12.5
15
17.5
min
*MSD1 SPC, time=12.580:12.691 of C:\CHEM32\1\DATA\2014_05\DAILYSQUENCE_LC 2014-06-10 13-45-59\2014_05000007.D ES-API
Max: 684215
100
80
60
40
20
0
413.1
414.1
399.1
847.3
250
500
750
1000
1250
1500
1750
m/z

Origin	Bruker BioSpin GmbH
Solvent	CDCl3
Temperature	300.0
Pulse Sequence	zg30
Experiment	1D
Number of Scans	16
Acquisition Date	2013-07-31T11:42:00
Spectrometer Frequency	400.13
Spectral Width	8223.7
Lowest Frequency	-1647.0
Nucleus	1H
Acquired Size	32768
Spectral Size	65536

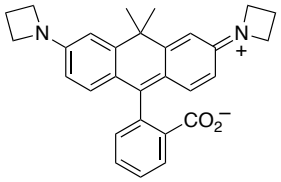

22

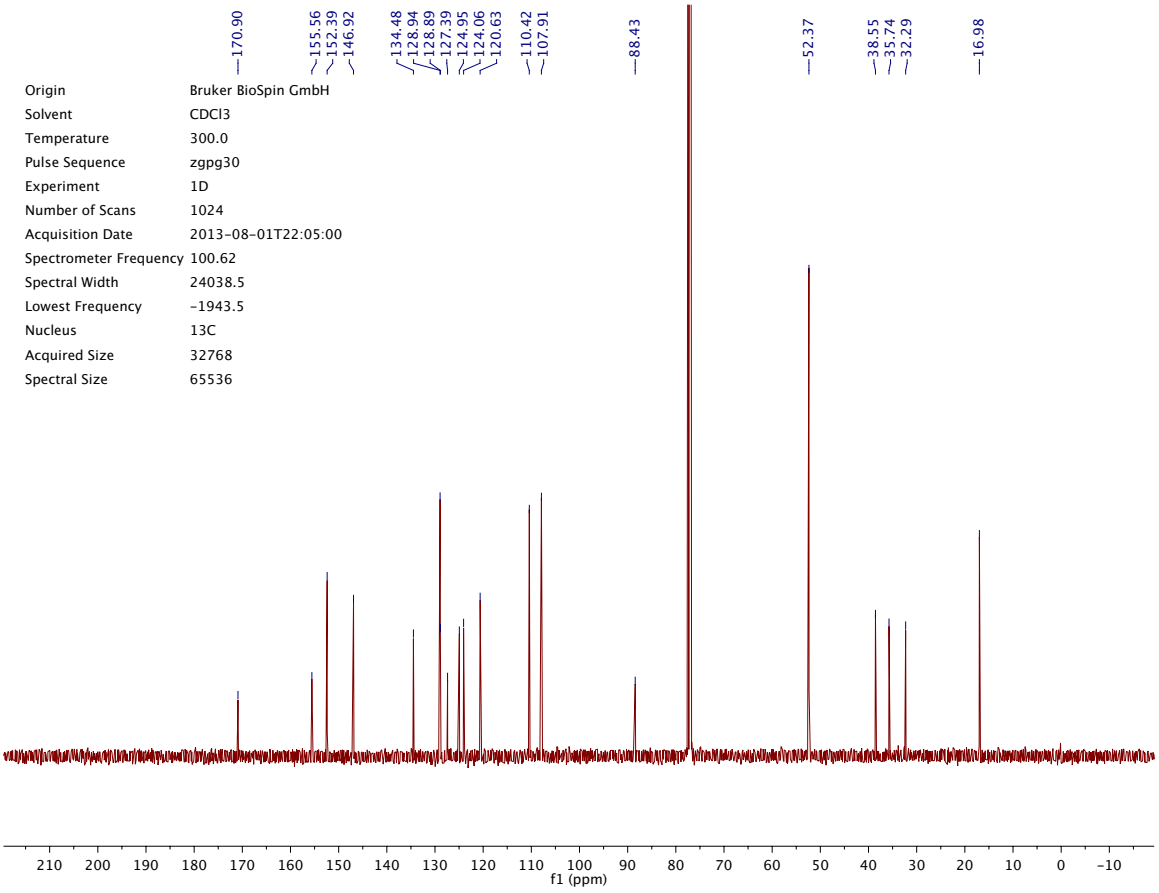

Origin	Bruker BioSpin GmbH
Solvent	CDCl3
Temperature	300.0
Pulse Sequence	zgpg30
Experiment	1D
Number of Scans	1024
Acquisition Date	2013-08-01T22:05:00
Spectrometer Frequency	100.62
Spectral Width	24038.5
Lowest Frequency	-1943.5
Nucleus	13C
Acquired Size	32768
Spectral Size	65536

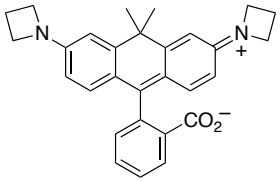

22

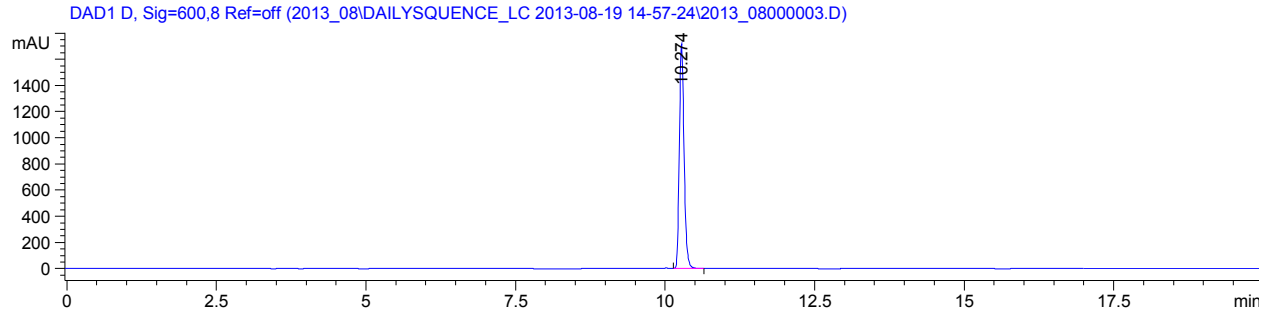
DAD1 D, Sig=600,8 Ref=off (2013_08\DAILYSQUENCE_LC 2013-08-19 14-57-24\2013_08000003.D)
mAU
1400
1200
1000
800
600
400
200
0
10.274
0
2.5
5
7.5
10
12.5
15
17.5
min

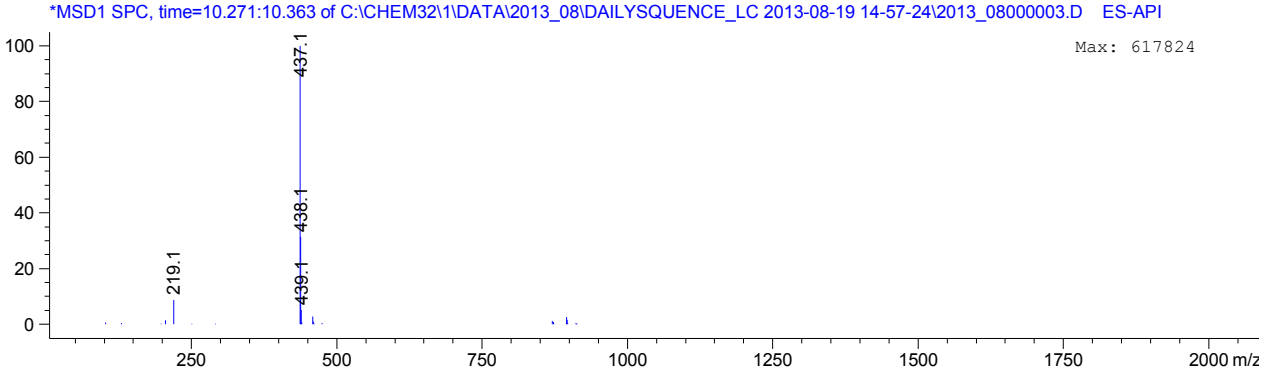
*MSD1 SPC, time=10.271:10.363 of C:\CHEM32\1\DATA\2013_08\DAILYSQUENCE_LC 2013-08-19 14-57-24\2013_08000003.D ES-API
Max: 617824
100
80
60
40
20
0
437.1
438.1
439.1
219.1
250
500
750
1000
1250
1500
1750
2000 m/z

Origin	Bruker BioSpin GmbH
Solvent	CDCl3
Temperature	300.0
Pulse Sequence	zg30
Experiment	1D
Number of Scans	16
Acquisition Date	2014-07-08T10:49:00
Spectrometer Frequency	400.13
Spectral Width	8223.7
Lowest Frequency	-1646.9
Nucleus	1H
Acquired Size	32768
Spectral Size	65536

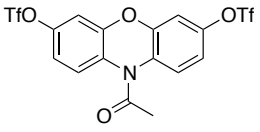

S39

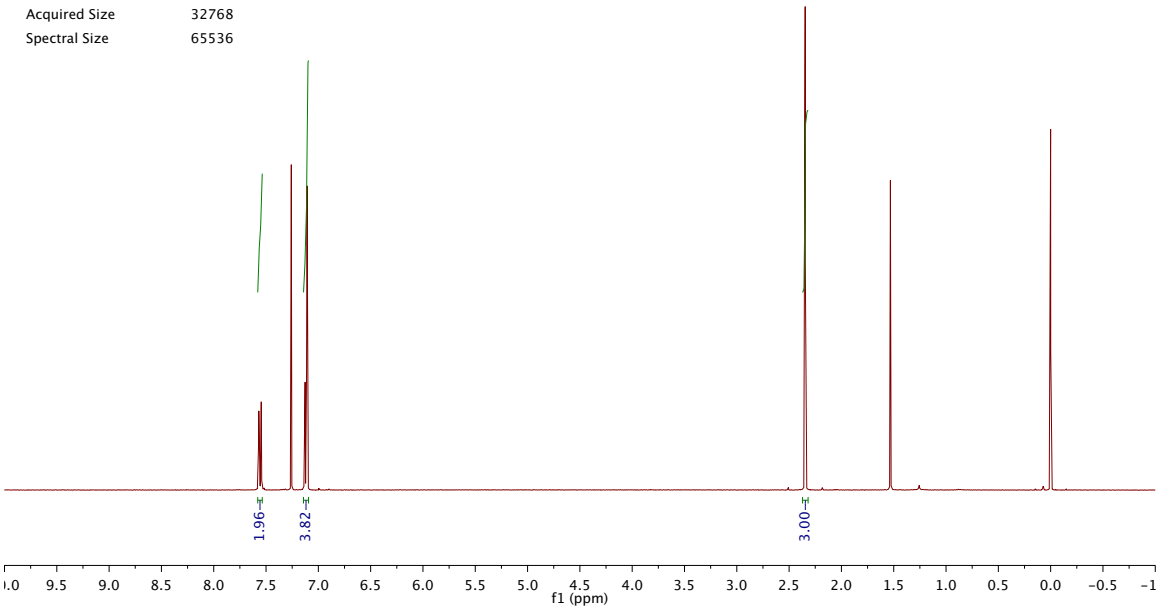

Origin	Bruker BioSpin GmbH
Solvent	CDCl3
Temperature	300.0
Pulse Sequence	zgpg30
Experiment	1D
Number of Scans	2048
Acquisition Date	2014-06-06T23:01:00
Spectrometer Frequency	100.62
Spectral Width	24038.5
Lowest Frequency	-1941.5
Nucleus	13C
Acquired Size	32768
Spectral Size	65536

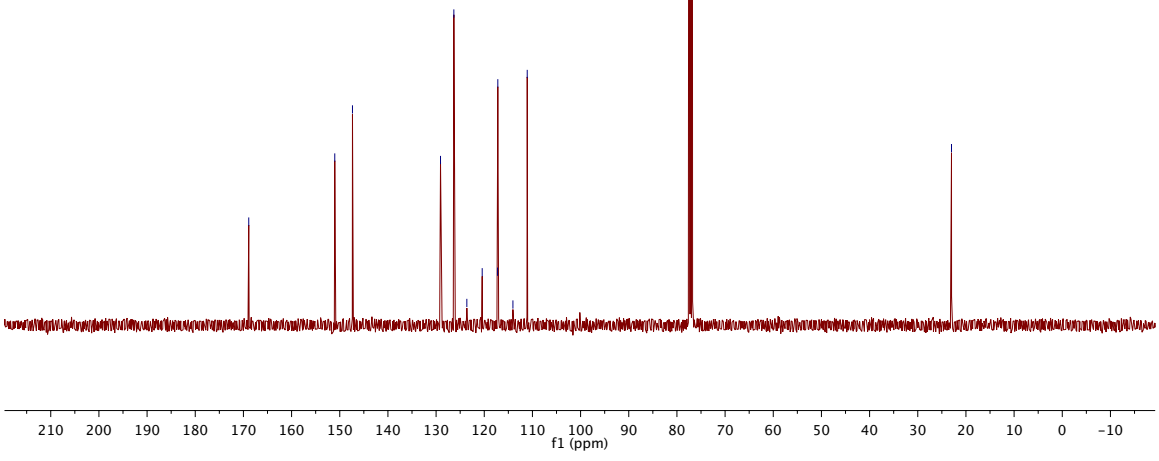

Origin	Bruker BioSpin GmbH
Solvent	MeOD
Temperature	300.0
Pulse Sequence	zg30
Experiment	1D
Number of Scans	16
Acquisition Date	2014-06-26T08:56:00
Spectrometer Frequency	400.13
Spectral Width	8223.7
Lowest Frequency	-1644.2
Nucleus	1H
Acquired Size	32768
Spectral Size	65536

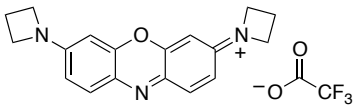

24

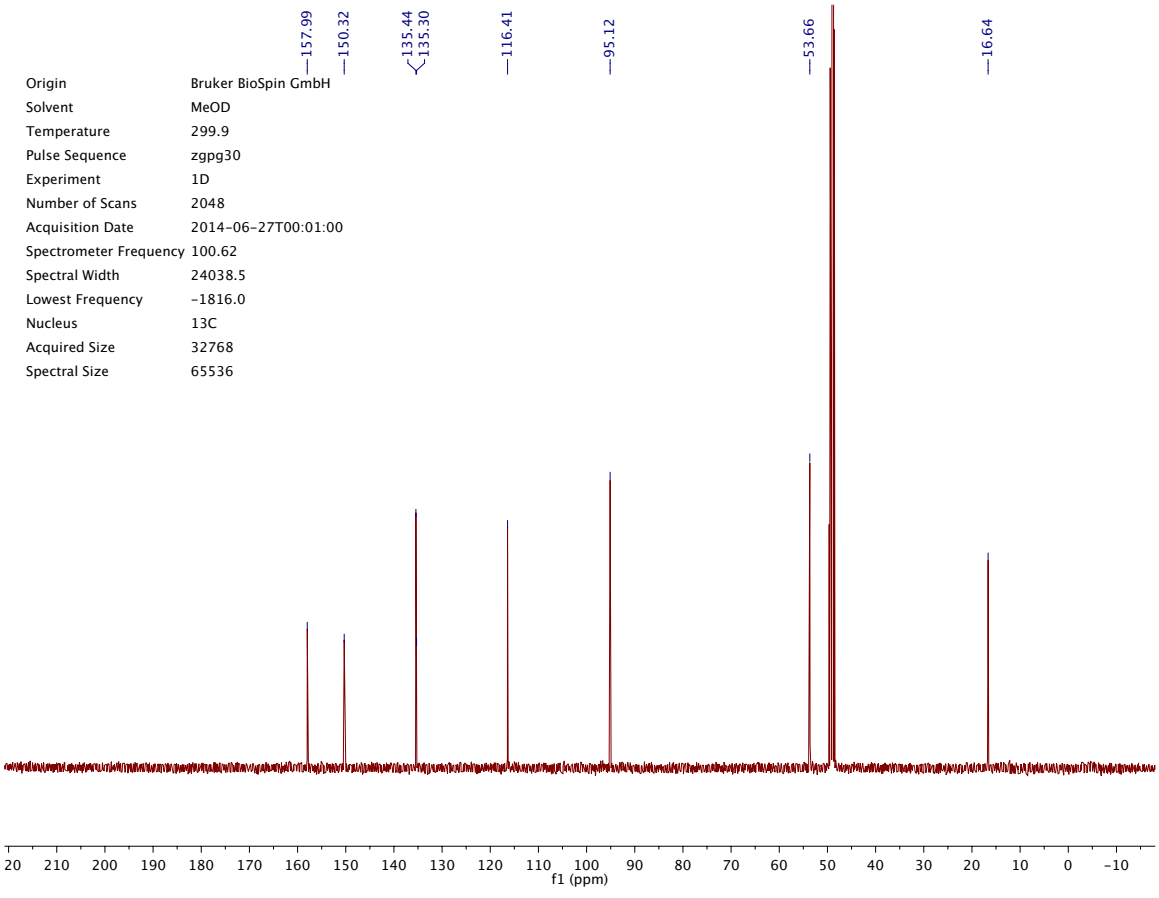

Origin	Bruker BioSpin GmbH
Solvent	MeOD
Temperature	299.9
Pulse Sequence	zgpg30
Experiment	1D
Number of Scans	2048
Acquisition Date	2014-06-27T00:01:00
Spectrometer Frequency	100.62
Spectral Width	24038.5
Lowest Frequency	-1816.0
Nucleus	13C
Acquired Size	32768
Spectral Size	65536

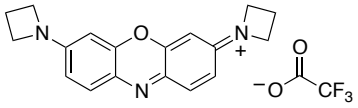

24

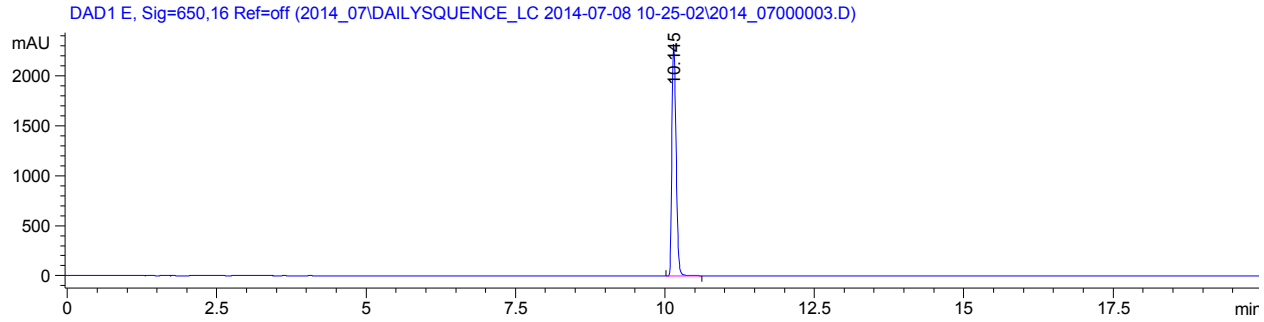
DAD1 E, Sig=650,16 Ref=off (2014_07\DAILYSQUENCE_LC 2014-07-08 10-25-02\2014_07000003.D)
mAU
2000
1500
1000
500
0
10.145
0
2.5
5
7.5
10
12.5
15
17.5
min

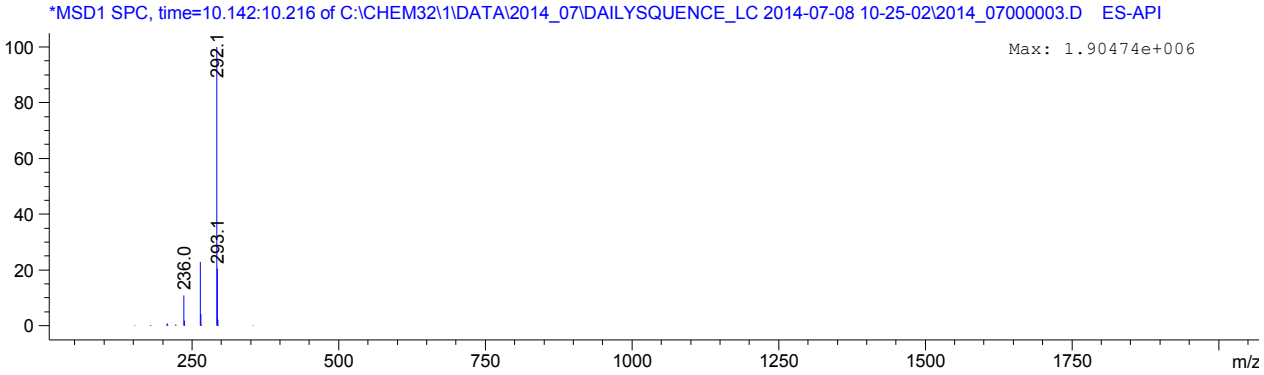
*MSD1 SPC, time=10.142:10.216 of C:\CHEM32\1\DATA\2014_07\DAILYSQUENCE_LC 2014-07-08 10-25-02\2014_07000003.D ES-API
Max: 1.90474e+006
100
80
60
40
20
0
292.1
293.1
236.0
250
500
750
1000
1250
1500
1750
m/z